Sodium Channel Loss of Function Sensitizes Conduction to Changes in Extracellular Sodium Concentration

William P. Adams

Dissertation submitted to the faculty of the Virginia Polytechnic Institute and State University in partial fulfillment of the requirements for the degree of:

Doctor of Philosophy

In

Translational Biology, Medicine, and Health

Steven Poelzing

Robert Gourdie

Sharon Swanger

Sunshine Lahmers

May 06, 2024

Roanoke, VA

Sodium Channel Loss of Function Sensitizes Conduction to Changes in Extracellular Sodium Concentration

William P. Adams

Abstract

Sudden cardiac death is largely attributable to sudden onset ventricular arrhythmias. Alterations in cardiac conduction, particularly the slowing of conduction velocity is one major factor in arrhythmogenesis. By understanding the mechanisms and factors that modulate cardiac conduction velocity, we can assess and perhaps mitigate the risk of arrhythmia in patients for whom slowed conduction is a arrhythmogenic substrate. Cardiac conduction has traditionally been described by cable theory, which predicts an inverse relationship between extracellular resistance and conduction velocity (CV). However, in studies that reduce extracellular resistance by inducing interstitial edema, there are conflicting results, with some labs showing increased CV when edema is induced with one agent, and others showing reduced CV when edema is induced with a different agent. In the first part of this dissertation, we present experimental data in support of ephaptic coupling (EpC), a theorized mechanism of conduction that resolves these apparent contradictions. In the later part of this dissertation, we address how changes in sodium concentration can alter conduction, despite conventional wisdom suggesting that it should not. We show that when sodium channels are impaired, such as by genetic mutation or pharmacologic blockade, that conduction is sensitized to changes in sodium concentrations that would not otherwise induce changes in CV. We go on to explore the mechanisms that modulate this sensitivity and present data that show it is a function of both EpC and outward potassium currents. Taken together, these data expand our understanding of the mechanics behind cardiac conduction and demonstrate that EpC has a clinically relevant impact on conduction and represents a new pathway to explore in regards to the treatment and management of arrhythmogenic and conduction disorders.

Sodium Channel Loss of Function Sensitizes Conduction to Changes in Extracellular Sodium Concentration

William P. Adams

General Public Abstract

In all large animals, life is sustained by the regular coordinated beating of the heart to pump blood throughout the body. Throughout this continuous activity, and even with minute-to-minute changes in heart rate, this electrically driven activity continues without major disruption. Until it doesn't. Major arrhythmias can occur suddenly, and without warning. Over the last century, we have begun to understand some of the reasons why heart, even an injured one, will work normally for hundreds of thousands of beats, and on the next fall into a life-threatening new pattern, and one of the most important of these reasons is the speed of conduction: the spread of electrical activation throughout the heart tissue. Understanding the mechanisms of conduction provide a way to assess and mitigate the risk of arrhythmias and may open up new avenues for treatment and prevention. This dissertation presents evidence for a previously theoretical mechanism of conduction called ephaptic coupling. We show that this electric field mediated form of conduction can be modulated with clinically used osmotic agents, and that it has a physiologically relevant impact on conduction. We also show that hyponatremia (i.e. low sodium), a condition that is traditionally thought to have minimal impact on cardiac conduction, because a significant modulator of conduction when sodium channel functions are impaired. As a great many drugs block sodium channels, this sensitization to hyponatremia and the factors that mediate it are underappreciated concerns that are relevant to a wide array of patients.

The new findings presented in this dissertation advance our collective understanding of the mechanisms of cardiac conduction and provide evidence for new avenues of exploration in the prevention and management of arrhythmias and conduction disorders.

Acknowledgements

First and foremost, I would like to thank my advisor, Steve Poelzing, for his academic and professional guidance and support over the last few years, particularly through the difficult years of 2020 and 2021. I also thank each member of the Poelzing lab past and present who have inspired me to be better each day. Tristain, Ryan, Katrina, Xiaobo, Grace, Madeline, Alec, Max, Rowan, Greg, and Chandra: you have all helped me be the scientist I am today.

I am inexpressively grateful for the love and support of my family, both by blood and by choice. To my parents who have always been there no matter what I needed, and to my Monroe family without whom my tenuous grip on sanity would have slipped long ago.

I would also like to thank four specific individuals: firstly, to my M.S. mentors, Stefano Toldo and Eleonora Mezzaroma who both taught me so many of the laboratory skills I use daily and more importantly how to fail, to step back, and to start over again. Secondly, to my dear friend Ria Fyffe-Freil, who believed in me even when I struggled to believe in myself. Finally, in memory of the late Lou De Felice, who taught me that sometimes good science means challenging the existing dogma, no matter how much push back you get. Thank you all.

Glossary of Abbreviations

AAD	Anti-Arrhythmic Drug
$BaCl_2$	Barium-Chloride salt
Ca^{2+}	Ionic Calcium
CAST	Cardiac Arrhythmia Suppression Trials
CBX	Carbenoxolone
CV	Conduction Velocity
CV_L	CV in the Longitudinal Direction
CV_T	CV in the Transverse Direction
Cx43	Connexin43
ECG	Electrocardiograph
EpC	Ephaptic Coupling
FRAP	Fluorescent Recovery After Photobleaching
GJ	Gap Junction
GJC	Gap Junction Coupling
hERG	human Ether-a-go-go Related Gene/Kv11.1 (a voltage gated potassium channel)
ID	Intercalated Disc
I_{K1}	Inwardly Rectifying Potassium Current
I_{Kr}	Rapid Delayed Rectifier Potassium Current
I_{Ks}	Slow Delayed Rectifier Potassium Current
I_{Na}	Voltage-gated Sodium Current
K^+	Ionic Potassium
LoF	Loss of Function
Na^+	Ionic Sodium
pCV43-S368	Cx43, Phosphorylated at Serine-368
SCA	Sudden Cardiac Arrest (also see (OHCA
NCX	Sarcolemmal Sodium-Calcium-Exchanger
NKA	Plasma membrane Sodium-Calcium-ATPase
OHCA	Out-of-Hospital Cardiac Arrest (also see SCA)
W_p	Width of the Perinexus

Table of Contents

Chapter 1

Sudden Cardiac Death, Arrhythmia, and Sodium Channel Loss of Function

Introduction

Cardiac conduction is defined as “the process by which electrical activation is communicated between myocytes, triggering their synchronous contraction.”[1] This process must occur regularly, in proper sequence, with minimal disruption constantly for the entirety of life. Disruptions to conduction lead to activation and contraction with improper timing or sequence, and the consequences are often fatal. This dissertation begins with an introduction that discusses the clinical impact of arrhythmia, how altered conduction can lead to arrhythmogenesis, and finally a brief overview of several mechanisms through which conduction can be modulated. After this introduction, I will present an original first author study published in Circulation Research demonstrating strong experimental evidence to support ephaptic coupling, a previously theorized mechanism of cardiac conduction. This will be followed by work demonstrating an unexpected interaction between extracellular sodium concentration ($[Na^+]$) and sodium (Na^+) channel functions. Finally, I will conclude with a discussion of the implications of these findings, what new questions they raise, and how those questions may be answered going forward.

Clinical Background

Sudden Cardiac Death

Cardiovascular disease remains the leading cause of death in the United States, accounting for nearly 700,000 deaths in 2012, and an estimated cost in excess of $200 billion annually.[2] Of these 700,000 deaths, approximately 300,000 are associated with Out of Hospital Cardiac Arrest (OHCA), or Sudden Cardiac Arrest (SCA), accounting for between 15%-20% of all deaths in the United States.[3] More than just an concern in aged and diseased hearts, SCA also occurs in children and adolescents with an estimated 20,000 incidents in patients under the age of 18.[4]

Notably, there have been two recent instances of SCA occurring in professional athletes during televised competitions: one during a 2023 NFL football game,[5] and another during the 2020 UEFA Euro Cup soccer tournament.[6] In cases like these, where medical personnel have been present at the initial collapse, the majority of patients present with ventricular tachy-arrhythmias, generally either ventricular tachycardiac or ventricular fibrillation.[7]

Although sudden and unpredictable onset ventricular arrhythmias are thought to directly precipitate collapse, a range of risk factors for SCA have been identified,[3, 8] and one of the most prominent of those risk factors is atrial fibrillation. Atrial fibrillation, which raises the risk of ventricular fibrillation by 3-fold,[9] is most commonly managed by flecainide, a “strong” sodium channel blocker, also called a Vaughn-Williams Class 1c antiarrhythmic agent.[10] Although flecainide is exceptionally effective at managing atrial arrhythmias, it is used with much more caution in the context of ventricular arrhythmias, and is specifically contraindicated in the presence of past myocardial infarction, structural heart disease, Brugada Syndrome, and Long QT Syndrome (except when associated with Na^+ channel gain of function).[11] A large part of this caution was born from the CAST trials of the late ‘80s.

The CAST Trials

The Cardiac Arrhythmia Suppression (CAST) trials have become nearly infamous among historic clinical trials. The goal of these trials was to suppress ventricular ectopy in patients following myocardial infarction. Such ectopic events, called premature ventricular contractions (PVCs), are associated with increased mortality, including sudden cardiac death.[12] Such ectopies can serve as the triggering event for life threatening ventricular arrhythmias.[13] The hypothesis of the CAST trials held that suppressing PVCs with Class 1c antiarrhythmic drugs (AADs) would improve patient mortality. Unfortunately, while the antiarrhythmic drugs did suppress asymptomatic PVCs, they resulted in a 3.6-fold increase in patient mortality (Fig. 1).[14]

This increase in mortality was attributed to an increase in lethal ventricular arrhythmic events in the treatment group, despite an equal distribution of non-lethal events between treatment and placebo groups.[15] Subsequent research into the impacts of Class 1c antiarrhythmics in infarcted hearts demonstrated that flecainide both slowed conduction and increased the risk for conduction failure in one direction (uni-directional block), thus creating a substrate that facilitated re-entrant tachyarrhythmias particularly in bentricular myocardium.[16]

Arrhythmias and Sodium Channel Blockers

Components of an Arrhythmia

Cardiac reentry occurs when a region of tissue ceases to be refractory to further electrical stimulation in a time and manner such that the electrical wavefront that has already passed through that region can re-excite or re-enter that region, and continue propagating, leading to rapid subsequent activations that are decoupled from nodal peacemaking activity.[17] At about the same time as the CAST trials Philippe Coumel began to outline a schematic of arrhythmogenic reentry that would eventually become known as “Coumel’s Triangle”.[18] Coumel proposed three factors which are necessary for an arrhythmia to occur: a triggering event, an arrhythmic substrate, and situational modulatory factors. These first two, a triggering event, and an arrhythmogenic substrate, are the keys to both the hypothesis and failure of the CAST trials. Strong Na^+ channel blockers like Class 1c AADs suppress PVCs (i.e. triggering events) by reducing the excitability of the tissue.[19] If this were the only factor at play, then the hypothesis that these drugs would reduce arrhythmias seems quite reasonable. However, 1c AADs also slow conduction velocity (CV) and slowed conduction creates a more arrhythmogenic substrate.[16] This then explains the increase in mortality seen in the CAST trials, as the CV slowing from the 1c AADs worsened the arrhythmogenic substrate created by the region of infarcted tissue.[14, 20] This meant that although the AADs did successfully reduce the number of

triggering events, when those events occurred, they were more likely to result in fatal arrhythmias, increasing mortality. Ergo, CV slowing by 1c AADs increases the risk of fatal arrhythmia.

Managing Patients on Strong Na^+ *Channel Blockers*

Many strong Na^+ channel blockers, and flecainide in particular, have narrow therapeutic windows and thus a high risk of overdose. One study on the effectiveness and risks of flecainide found that a trough plasma level of 400ng/mL resulted in only 50% of patients having a 90% suppression of ectopic depolarization, increasing to 80% of patients responding at 600ng/mL. Meanwhile 20% of patients experienced serious adverse cardiac side effects at a dose of 800ng/mL, including syncope, weakness, and bradycardia. At 1200ng/mL the risk of adverse side effects rose to 40% and included both left and right bundle branch block.[21] As little as twice the therapeutic dose, just a single extra pill at the wrong time, can result in serious adverse effects.

The primary method of treating flecainide toxicity is the administration of hypertonic sodium bicarbonate with the goal of raising serum Na^+ concentration above 150 mEq/L and pH above 7.5, and to provide circulatory support to mitigate the adverse cardiac symptoms until the drug is metabolized.[22] This course of treatment for strong Na^+ channel blockers was originally suggested by experimental work from 1959[23, 24] but the mechanism is somewhat disputed. It is often assumed that the increased pH favors a deprotonated form of the drug that binds less effectively to the channel,[25, 26] but others suggest that the increase in serum Na^+ alone is therapeutic.[27, 28] The few studies that have looked at this directly suggest that both elevated Na^+ and elevated pH may work both independently and in combination to reverse the effects of various Na^+ channel blockers.[29, 30]

Low Serum Na^+ May Exacerbate Channel LoF

Alongside the experimental evidence that elevated serum Na^+ effectively treats Na^+ channel blocker overdose, there is a growing number of case studies that show hyponatremia precipitating cardiac symptoms of overdose, most commonly syncope, bradycardia, and QRS widening — the ECG correlate of ventricular conduction. These cases include a patient on tricyclic antidepressants with renal failure,[31] a patient with paroxysmal atrial fibrillation and hypertension who developed hyponatremia from a prescribed diuretic,[32] and a patient with chronic kidney disease and paroxysmal atrial fibrillation.[33] In each of these cases, the patient's serum Na^+ dropped to between 118-128 mmol/L, and the patient's symptoms worsened as hyponatremia worsened, and subsequently improved with the resolution of hyponatremia. These are just a few examples of either hyponatremia precipitating Na^+ channel blocker overdose, or hypertonic Na^+ alone rapidly reversing the symptoms of overdose.[25, 27, 34, 35]

Hyponatremia, Conduction, and Na^+ Channel Loss of Function

Not only does hyponatremia interact with drug induced channel loss-of-function (LoF), a recent study by Blair et al. has shown that hyponatremia impairs conduction more in a haploinsufficient genetic LoF model than in wildtype animals. Hyponatremia caused significant CV slowing and often caused conduction block that was not seen in wild type controls in Scn5a/- mice, which are heterozygous/null for the main cardiac isoform of the voltage-gated Na^+ channel.[36] These data suggest that sensitivity of conduction to low serum Na^+ (which is seen in the clinical case studies as QRS widening) is not just a matter of drug/target interactions but is actually tied to Na^+ channel LoF at a more fundamental level. The two following chapters consist of original research articles exploring mechanisms of conduction and whether those mechanisms interact with the sensitization of conduction to hyponatremia that is induced by channel LoF. Before presenting those chapters, I will briefly describe here the three mechanisms we investigated:

outward potassium (K^+) currents, intracellular calcium (Ca^{2+}) accumulation, and ephaptic coupling.

Outward K^+ currents repolarize the cell, and thus directly oppose the inward depolarizing Na^+ currents (I_{Na}). Previous work from this lab has shown that agonizing I_{Ks} during sodium channel blockade with flecainide slows conduction,[37] and that blocking I_{K1} alters the dose response of CV to flecainide in the left ventricle.[38] These both suggest an interaction between conduction, sodium channel LoF, and K^+ currents.

Intracellular Ca^{2+} is known to rise during hyponatremia.[39] As a potent secondary messenger, there are many pathways through which elevated intracellular Ca^{2+} could impact conduction. Just to list a few examples, the inhibition of gap junction can occur directly from Ca^{2+} binding at micromolar concentrations,[40] or through calmodulin driven interaction in the case of nanomolar concentrations.[41, 42] Elevated Ca^{2+} can also interact with cAMP/PKA signaling[43] which can also regulate connexin activity.[44] Increased intracellular Ca^{2+} can activate PKC, which can target voltage gated Na^+ channels and reduce overall Na^+ current and cause steady-state inactivation at more hyperpolarized membrane potentials. All of these examples could further impair conduction. With so many possible pathways and targets, it is difficult to predict which ones might be the most relevant, so we instead chose to focus on modulating the intracellular Ca^{2+} accumulation itself to determine if it was a relevant factor in CV sensitization to changes in $[Na^+]$.

Finally, ephaptic coupling (EpC), which is the major focus of chapter 2, is a mechanism of electric field mediated cell-cell coupling. It was first suggested in cardiomyocytes as a way of explaining how conduction occurred in species with few or no traditional gap junction proteins.[45] The specifics will be discussed more in the next chapter, but in brief, EpC requires a situation where channel rich stretches of membrane oppose each other across an extremely narrow,

diffusion limited gap. The close proximity of channels on opposite cells allows the electric field generated by the activation of one set of channels to drive the activation of the other set of channels on the opposite cell.[46] This requires a very narrow gap between the cells because of how rapidly electric fields fall off over distance, and the modulation of this gap can impact the degree of coupling.[47] The subcellular structure that allows this is called the perinexus,[48] and the perinexal width (W_p) is a measurable parameter correlated with the degree of coupling.[49] Importantly, this mechanism of coupling would allow electrical activations to spread from cell to cell without the direct passage of current from one cell to the next.

The work presented in chapter 2 serves primarily to provide strong evidence for both the existence and the relevance of EpC, but also to contrast it with a the so-called “canonical” cable theory of conduction which is mediated in cardiomyocytes by gap junctional cell-cell coupling. Cable theory predicts that the extracellular edema will speed CV by means of reducing extracellular resistance, as demonstrated by Fleischhauer *et al.* who used dextran to increase interstitial edema, and observed an increase in CV in papillary muscles as a result.[50] This result is in apparent contrast with work by Veeraraghavan *et al.* who saw the opposite: a decrease in CV when mannitol was used to increase interstitial edema, and an increase in CV when albumin was used to decrease interstitial edema.[47] Chapter two resolves this apparent contradiction in two ways, first be demonstrating that different osmotic agents may have the same effect on edema, (and by extension extracellular resistance), but opposite effects on perinexal width, and that of these two parameters, changes in perinexal width have the larger impact on conduction velocity. Secondly it shows that the CV-W_p relationship is biphasic, that is there is a point at which further reducing W_p begins to slow CV rather than speed it.

The work presented in chapter 3 directly demonstrates that CV is more sensitive to changes of $[Na^+]$ during channel LoF than it is under normal channel function, and specifically interrogates

several mechanisms by which this sensitization may be mediated and identifies EpC and K^+ currents as modulatory targets for LoF induces CV sensitivity to changes in [Na^+].

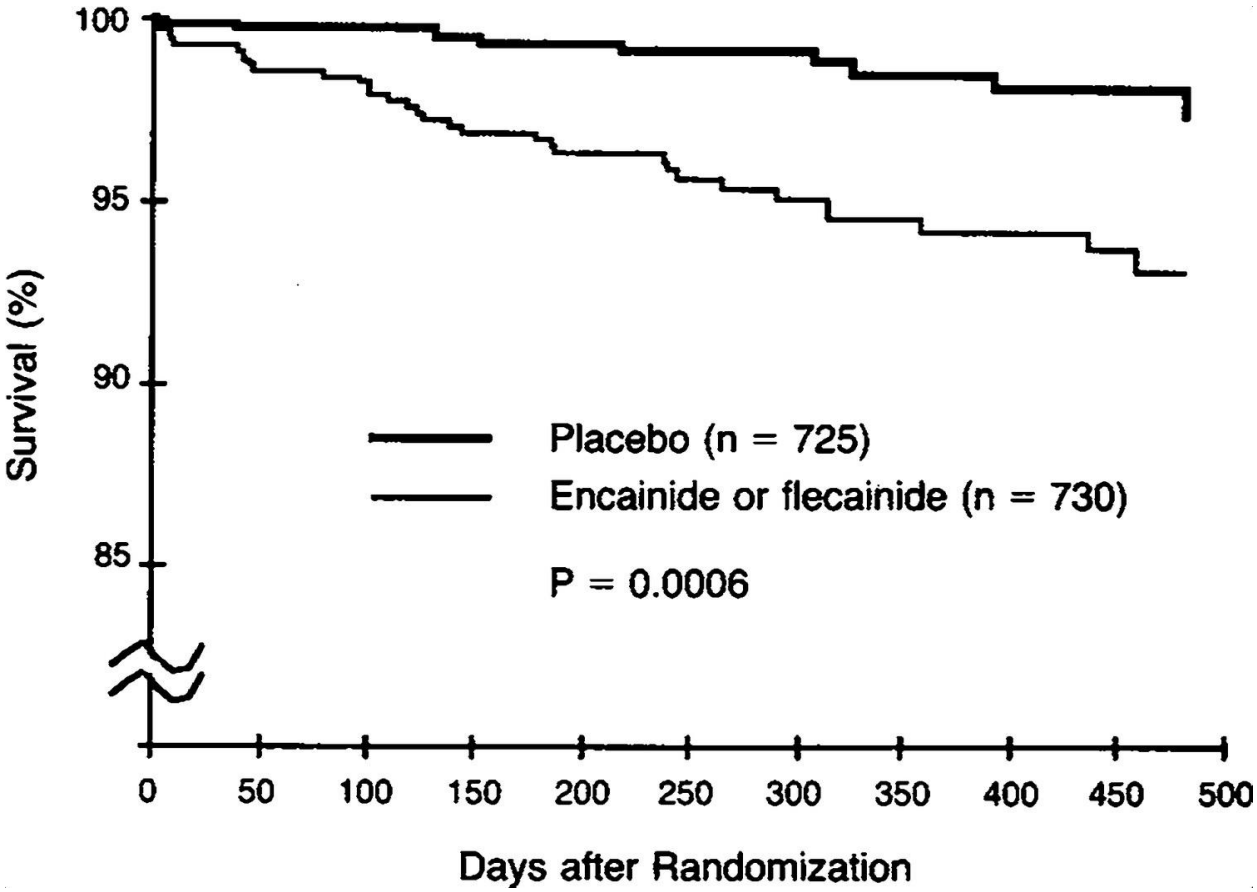

Figure 1. *Survival among 1455 Patients Randomly Assigned to Receive Encainide or Flecainide, or Matching Placebo.* Kaplan-Meier survival curve for death from arrhythmia comparing placebo against pooled flecainide or encainide treatment groups in the CAST I trial. The risk of death from arrhythmia was 3.6 times greater in the treatment group than in the placebo group. Figure reproduced from Preliminary Report: Effect of Encainide and Flecainide on Mortality in a Randomized Trial of Arrhythmia Suppression after Myocardial Infarction, NEJM 1989.[14]

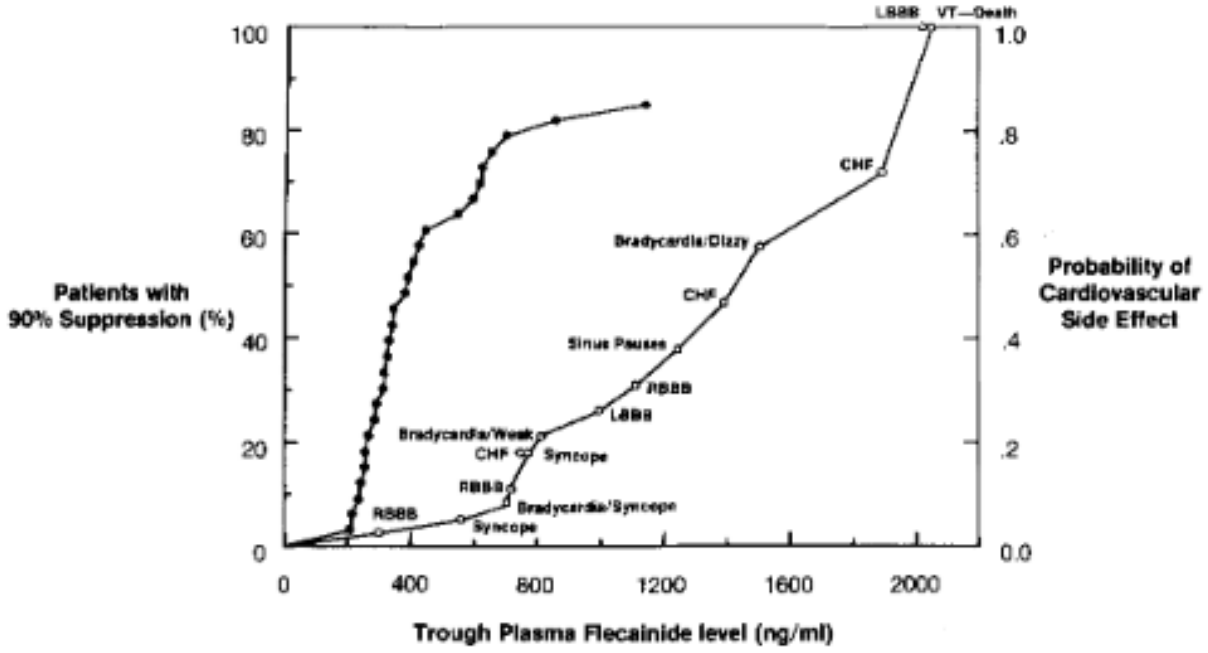

Figure 2. *Effectiveness and Probably of Adverse Side Effects as a function of Trough Plasma Flecainide Concentration.* The percentage of patients with 90% suppression of Ventricular Ectopic Depolarization is plotted on in filled circles, against the left axis. The probability of adverse cardiac events is plotted in open circles against the right axis. Abrreviations: RBBB/LBBB: Right/Left Bundle Branch Block, CHF: Congestive Heart Failure, VT; Ventricular Tachycardia. Figure reproduced from Salerno, *et al.* Clin Pharmacol Ther., 1986[21]

References

1. Veeraraghavan R, Gourdie RG, Poelzing S. Mechanisms of cardiac conduction: a history of revisions. Am J Physiol Heart Circ Physiol. 2014;306(5):H619-27. Epub 20140110. doi: 10.1152/ajpheart.00760.2013. PubMed PMID: 24414064; PMCID: PMC3949060.

2. Prevention CfDCa. Heart Disease Facts 2023. Available from: https://www.cdc.gov/heartdisease/facts.htm.

3. Hayashi M, Shimizu W, Albert CM. The spectrum of epidemiology underlying sudden cardiac death. Circ Res. 2015;116(12):1887-906. doi: 10.1161/circresaha.116.304521. PubMed PMID: 26044246; PMCID: PMC4929621.

4. Okubo M, Chan HK, Callaway CW, Mann NC, Wang HE. Characteristics of paediatric out-of-hospital cardiac arrest in the United States. Resuscitation. 2020;153:227-33. Epub 20200427. doi: 10.1016/j.resuscitation.2020.04.023. PubMed PMID: 32348794.

5. Close D. A timeline of the NFL's response after Damar Hamlin collapsed Online: CNN; 2023 [updated 1/3/2023; cited 2024 04/15].

6. Carstensen T. The day Denmark stood still: Christian Eriksen's collapse and the heroes who saved him The Guardian2021 [updated 06/20/2021; cited 2024 4/15].

7. Valenzuela TD, Roe DJ, Nichol G, Clark LL, Spaite DW, Hardman RG. Outcomes of rapid defibrillation by security officers after cardiac arrest in casinos. N Engl J Med. 2000;343(17):1206-9. doi: 10.1056/nejm200010263431701. PubMed PMID: 11071670.

8. Adabag AS, Luepker RV, Roger VL, Gersh BJ. Sudden cardiac death: epidemiology and risk factors. Nat Rev Cardiol. 2010;7(4):216-25. Epub 20100209. doi: 10.1038/nrcardio.2010.3. PubMed PMID: 20142817; PMCID: PMC5014372.

9. Bardai A, Blom MT, van Hoeijen DA, van Deutekom HW, Brouwer HJ, Tan HL. Atrial fibrillation is an independent risk factor for ventricular fibrillation: a large-scale population-based

case-control study. Circ Arrhythm Electrophysiol. 2014;7(6):1033-9. Epub 20140918. doi: 10.1161/circep.114.002094. PubMed PMID: 25236735.

10. Echt DS, Ruskin JN. Use of Flecainide for the Treatment of Atrial Fibrillation. Am J Cardiol. 2020;125(7):1123-33. Epub 20200109. doi: 10.1016/j.amjcard.2019.12.041. PubMed PMID: 32044037.

11. Zeppenfeld K, Tfelt-Hansen J, de Riva M, Winkel BG, Behr ER, Blom NA, Charron P, Corrado D, Dagres N, de Chillou C, Eckardt L, Friede T, Haugaa KH, Hocini M, Lambiase PD, Marijon E, Merino JL, Peichl P, Priori SG, Reichlin T, Schulz-Menger J, Sticherling C, Tzeis S, Verstrael A, Volterrani M. 2022 ESC Guidelines for the management of patients with ventricular arrhythmias and the prevention of sudden cardiac death. Eur Heart J. 2022;43(40):3997-4126. doi: 10.1093/eurheartj/ehac262. PubMed PMID: 36017572.

12. Ruberman W, Weinblatt E, Goldberg JD, Frank CW, Shapiro S. Ventricular premature beats and mortality after myocardial infarction. N Engl J Med. 1977;297(14):750-7. doi: 10.1056/nejm197710062971404. PubMed PMID: 70750.

13. Matto F, Parekh KR, Giudici MC, Mazur A. Recurrent idiopathic polymorphic ventricular tachycardia/ventricular fibrillation successfully treated by cardiac sympathetic denervation. HeartRhythm Case Rep. 2019;5(4):229-32. Epub 20190126. doi: 10.1016/j.hrcr.2019.01.005. PubMed PMID: 30997341; PMCID: PMC6453564.

14. Preliminary report: effect of encainide and flecainide on mortality in a randomized trial of arrhythmia suppression after myocardial infarction. N Engl J Med. 1989;321(6):406-12. doi: 10.1056/nejm198908103210629. PubMed PMID: 2473403.

15. Echt DS, Liebson PR, Mitchell LB, Peters RW, Obias-Manno D, Barker AH, Arensberg D, Baker A, Friedman L, Greene HL, et al. Mortality and morbidity in patients receiving encainide, flecainide, or placebo. The Cardiac Arrhythmia Suppression Trial. N Engl J Med. 1991;324(12):781-8. doi: 10.1056/nejm199103213241201. PubMed PMID: 1900101.

16. Coromilas J, Saltman AE, Waldecker B, Dillon SM, Wit AL. Electrophysiological effects of flecainide on anisotropic conduction and reentry in infarcted canine hearts. Circulation. 1995;91(8):2245-63. doi: 10.1161/01.cir.91.8.2245. PubMed PMID: 7697855.

17. Cluitmans MJM, Bayer J, Bear LR, Ter Bekke RMA, Heijman J, Coronel R, Volders PGA. The circle of reentry: Characteristics of trigger-substrate interaction leading to sudden cardiac arrest. Front Cardiovasc Med. 2023;10:1121517. Epub 20230417. doi: 10.3389/fcvm.2023.1121517. PubMed PMID: 37139119; PMCID: PMC10150924.

18. Coumel P. The management of clinical arrhythmias. An overview on invasive versus non-invasive electrophysiology. Eur Heart J. 1987;8(2):92-9. doi: 10.1093/oxfordjournals.eurheartj.a062259. PubMed PMID: 2436917.

19. Amarouch MY, Swan H, Leinonen J, Marjamaa A, Lahtinen AM, Kontula K, Toivonen L, Widen E, Abriel H. Antiarrhythmic Action of Flecainide in Polymorphic Ventricular Arrhythmias Caused by a Gain-of-Function Mutation in the Nav 1.5 Sodium Channel. Ann Noninvasive Electrocardiol. 2016;21(4):343-51. Epub 20151007. doi: 10.1111/anec.12312. PubMed PMID: 26965448; PMCID: PMC6931835.

20. Dobmeyer D, Muir WW, Schaal SF. Antiarrhythmic effects of flecainide against canine ventricular arrhythmias induced by two-stage coronary ligation and halothane-epinephrine. J Cardiovasc Pharmacol. 1985;7(2):238-44. doi: 10.1097/00005344-198503000-00005. PubMed PMID: 2581074.

21. Salerno DM, Granrud G, Sharkey P, Krejci J, Larson T, Erlien D, Berry D, Hodges M. Pharmacodynamics and side effects of flecainide acetate. Clin Pharmacol Ther. 1986;40(1):101-7. doi: 10.1038/clpt.1986.145. PubMed PMID: 3720173.

22. Vu NM, Hill TE, Summers MR, Vranian MN, Faulx MD. Management of life-threatening flecainide overdose: A case report and review of the literature. HeartRhythm Case Rep. 2016;2(3):228-31. Epub 20151229. doi: 10.1016/j.hrcr.2015.12.013. PubMed PMID: 28491675; PMCID: PMC5419747.

23. Bellet S, Hamdan G, Somlyo A, Lara R. A reversal of the cardiotoxic effects of procaine amide by molar sodium lactate. Am J Med Sci. 1959;237(2):177-89. doi: 10.1097/00000441-195902000-00005. PubMed PMID: 13626960.

24. Bellet S, Hamdan G, Somlyo A, Lara R. The reversal of cardiotoxic effects of quinidine by molar sodium lactate: an experimental study. Am J Med Sci. 1959;237(2):165-76 passim. doi: 10.1097/00000441-195902000-00004. PubMed PMID: 13626959.

25. Di Grande A, Giuffrida C, Narbone G, Le Moli C, Nigro F, Di Mauro A, Pirrone G, Tabita V, Alongi B. Management of sodium-channel blocker poisoning: the role of hypertonic sodium salts. Eur Rev Med Pharmacol Sci. 2010;14(1):25-30. PubMed PMID: 20184086.

26. Mirrakhimov AE, Ayach T, Barbaryan A, Talari G, Chadha R, Gray A. The Role of Sodium Bicarbonate in the Management of Some Toxic Ingestions. Int J Nephrol. 2017;2017:7831358. Epub 20170808. doi: 10.1155/2017/7831358. PubMed PMID: 28932601; PMCID: PMC5591930.

27. Chan HY, Chan YC, Lau FL. Reversal of Brugada electrocardiographic pattern with sodium bicarbonate solution after amitriptyline overdose. Clin Toxicol (Phila). 2008;46(9):892-6. doi: 10.1080/15563650802293984. PubMed PMID: 18788005.

28. Sasyniuk BI, Jhamandas V, Valois M. Experimental amitriptyline intoxication: treatment of cardiac toxicity with sodium bicarbonate. Ann Emerg Med. 1986;15(9):1052-9. doi: 10.1016/s0196-0644(86)80128-7. PubMed PMID: 3017159.

29. Bou-Abboud E, Nattel S. Relative role of alkalosis and sodium ions in reversal of class I antiarrhythmic drug-induced sodium channel blockade by sodium bicarbonate. Circulation. 1996;94(8):1954-61. doi: 10.1161/01.cir.94.8.1954. PubMed PMID: 8873674.

30. Ranger S, Sheldon R, Fermini B, Nattel S. Modulation of flecainide's cardiac sodium channel blocking actions by extracellular sodium: a possible cellular mechanism for the action of sodium salts in flecainide cardiotoxicity. J Pharmacol Exp Ther. 1993;264(3):1160-7. PubMed PMID: 8383739.

31. Subedi R, Dean RK, Chaudhary A, Szombathy T. Flecainide toxicity in renal failure. Proc (Bayl Univ Med Cent). 2018;31(3):328-30. Epub 20180509. doi: 10.1080/08998280.2018.1463042. PubMed PMID: 29904301; PMCID: PMC5997054.

32. Khavandi A, Walker PR. Flecainide cardiotoxicity precipitated by electrolyte imbalance. Caution with thiazide diuretics. Emerg Med J. 2007;24(5):e26. doi: 10.1136/emj.2006.044362. PubMed PMID: 17452686; PMCID: PMC2658510.

33. Kasia C, Henry C, Santucci P. A case of electrolyte disturbances leading to flecainide toxicity at normal serum levels and pacemaker malfunction. HeartRhythm Case Rep. 2019;5(9):448-51. Epub 20190612. doi: 10.1016/j.hrcr.2019.05.007. PubMed PMID: 31934538; PMCID: PMC6951303.

34. Ghataoura R, Patil S. Flecainide toxicity: a presentation to the emergency department with literature review. BMJ Case Rep. 2020;13(2). Epub 20200228. doi: 10.1136/bcr-2019-232691. PubMed PMID: 32114494; PMCID: PMC7050315.

35. Rognoni A, Bertolazzi M, Peron M, Macciò S, Cameroni GT, Gratarola A, Rognoni G. Electrocardiographic changes in a rare case of flecainide poisoning: a case report. Cases J. 2009;2:9137. Epub 20091203. doi: 10.1186/1757-1626-2-9137. PubMed PMID: 20062654; PMCID: PMC2803934.

36. Blair GA, Wu X, Bain C, Warren M, Hoeker GS, Poelzing S. Mannitol and hyponatremia regulate cardiac ventricular conduction in the context of sodium channel loss of function. Am J Physiol Heart Circ Physiol. 2024;326(3):H724-h34. Epub 20240112. doi: 10.1152/ajpheart.00211.2023. PubMed PMID: 38214908.

37. Veeraraghavan R, Larsen AP, Torres NS, Grunnet M, Poelzing S. Potassium channel activators differentially modulate the effect of sodium channel blockade on cardiac conduction. Acta Physiol (Oxf). 2013;207(2):280-9. Epub 20120914. doi: 10.1111/j.1748-1716.2012.02481.x. PubMed PMID: 22913299; PMCID: PMC3980511.

38. Veeraraghavan R, Poelzing S. Mechanisms underlying increased right ventricular conduction sensitivity to flecainide challenge. Cardiovasc Res. 2008;77(4):749-56. Epub 20071204. doi: 10.1093/cvr/cvm090. PubMed PMID: 18056761.

39. Luttgau HC, Niedergerke R. The antagonism between Ca and Na ions on the frog's heart. J Physiol. 1958;143(3):486-505. doi: 10.1113/jphysiol.1958.sp006073. PubMed PMID: 13588569; PMCID: PMC1356728.

40. Bennett BC, Purdy MD, Baker KA, Acharya C, McIntire WE, Stevens RC, Zhang Q, Harris AL, Abagyan R, Yeager M. An electrostatic mechanism for Ca(2+)-mediated regulation of gap junction channels. Nat Commun. 2016;7:8770. Epub 20160112. doi: 10.1038/ncomms9770. PubMed PMID: 26753910; PMCID: PMC4730032.

41. Hu Z, Riquelme MA, Gu S, Jiang JX. Regulation of Connexin Gap Junctions and Hemichannels by Calcium and Calcium Binding Protein Calmodulin. Int J Mol Sci. 2020;21(21). Epub 20201102. doi: 10.3390/ijms21218194. PubMed PMID: 33147690; PMCID: PMC7663298.

42. Peracchia C. Calmodulin-Mediated Regulation of Gap Junction Channels. Int J Mol Sci. 2020;21(2). Epub 20200112. doi: 10.3390/ijms21020485. PubMed PMID: 31940951; PMCID: PMC7014422.

43. Halls ML, Cooper DM. Regulation by Ca2+-signaling pathways of adenylyl cyclases. Cold Spring Harb Perspect Biol. 2011;3(1):a004143. Epub 20110101. doi: 10.1101/cshperspect.a004143. PubMed PMID: 21123395; PMCID: PMC3003456.

44. Zhang M, Wang ZZ, Chen NH. Connexin 43 Phosphorylation: Implications in Multiple Diseases. Molecules. 2023;28(13). Epub 20230622. doi: 10.3390/molecules28134914. PubMed PMID: 37446576; PMCID: PMC10343229.

45. Sperelakis N, Mann JE, Jr. Evaluation of electric field changes in the cleft between excitable cells. J Theor Biol. 1977;64(1):71-96. doi: 10.1016/0022-5193(77)90114-x. PubMed PMID: 836519.

46. Lin J, Keener JP. Ephaptic coupling in cardiac myocytes. IEEE Trans Biomed Eng. 2013;60(2):576-82. doi: 10.1109/tbme.2012.2226720. PubMed PMID: 23335235.

47. Veeraraghavan R, Salama ME, Poelzing S. Interstitial volume modulates the conduction velocity-gap junction relationship. Am J Physiol Heart Circ Physiol. 2012;302(1):H278-86. Epub 20111021. doi: 10.1152/ajpheart.00868.2011. PubMed PMID: 22021331; PMCID: PMC3334234.

48. Rhett JM, Veeraraghavan R, Poelzing S, Gourdie RG. The perinexus: sign-post on the path to a new model of cardiac conduction? Trends Cardiovasc Med. 2013;23(6):222-8. Epub 20130311. doi: 10.1016/j.tcm.2012.12.005. PubMed PMID: 23490883; PMCID: PMC3686992.

49. Adams WP, Raisch TB, Zhao Y, Davalos R, Barrett S, King DR, Bain CB, Colucci-Chang K, Blair GA, Hanlon A, Lozano A, Veeraraghavan R, Wan X, Deschenes I, Smyth JW, Hoeker GS, Gourdie RG, Poelzing S. Extracellular Perinexal Separation Is a Principal Determinant of Cardiac Conduction. Circ Res. 2023;133(8):658-73. Epub 20230908. doi: 10.1161/circresaha.123.322567. PubMed PMID: 37681314; PMCID: PMC10561697.

50. Fleischhauer J, Lehmann L, Kléber AG. Electrical resistances of interstitial and microvascular space as determinants of the extracellular electrical field and velocity of propagation in ventricular myocardium. Circulation. 1995;92(3):587-94. doi: 10.1161/01.cir.92.3.587. PubMed PMID: 7634473.

Chapter 2

Extracellular Perinexal Separation Is a Principal Determinant of Cardiac Conduction

Extracellular Perinexal Separation Is a Principal Determinant of Cardiac Conduction

William P. Adams, Tristan B. Raisch, Yajun Zhao, Rafael Davalos, Sarah Barrett, D. Ryan King, Chandra B. Bain, Katrina Colucci-Chang, Grace A. Blair, Alexandra Hanlon, Alicia Lozano, Rengasayee Veeraraghavan, Xiaoping Wan, Isabelle Deschenes, James W. Smyth, Gregory S. Hoeker, Robert G. Gourdie and Steven Poelzing

This manuscript has been published in Circ Research, 2023;133:658–673 and is reproduced here as part of this dissertation

ABSTRACT

Background: Cardiac conduction is understood to occur through gap junctions. Recent evidence supports ephaptic coupling as another mechanism of electrical communication in heart. Conduction via gap junctions predicts a direct relationship between conduction velocity (CV) and bulk extracellular resistance. By contrast, ephaptic theory is premised on the existence of a biphasic relationship between CV and the volume of specialized extracellular clefts within intercalated discs such as the perinexus. Our objective was to determine the relationship between ventricular CV and structural changes to micro- and nano-scale extracellular spaces.

Methods: Conduction and connexin43 (Cx43) protein expression were quantified from optically mapped guinea pig whole-heart preparations perfused with the osmotic agents albumin, mannitol, dextran 70kDa, or dextran 2MDa. Peak sodium current was quantified in isolated guinea pig ventricular myocytes. Extracellular resistance was quantified by impedance spectroscopy. Intercellular communication was assessed in a heterologous expression system with fluorescence recovery after photobleaching. Perinexal width was quantified from transmission electron micrographs.

Results: CV primarily in the transverse direction of propagation was significantly reduced by mannitol, and increased by albumin and both dextrans. The combination of albumin and dextran 70kDa decreased CV relative to albumin alone. Extracellular resistance was reduced by mannitol, unchanged by albumin, and increased by both dextrans. Cx43 expression and conductance, and peak sodium currents were not significantly altered by the osmotic agents. In response to osmotic

agents, perinexal width, in order of narrowest to widest, was: albumin with dextran 70kDa, albumin or dextran 2MDa, dextran 70kDa or no osmotic agent, and mannitol. When compared in the same order, CV was biphasically related to perinexal width.

Conclusions: Cardiac conduction does not correlate with extracellular resistance, but is biphasically related to perinexal separation, providing evidence that the relationship between CV and extracellular volume is determined by ephaptic mechanisms under conditions of normal gap junctional coupling.

Keywords: Perinexus, Intercalated Disc, Cardiac Conduction, Electrophysiology, Ephaptic Coupling

INTRODUCTION

Understanding cardiac conduction is critical to the diagnosis, treatment, and prevention of arrhythmogenic diseases of the heart. Cardiac conduction is traditionally understood to follow a cable-like model of electrical conduction.[51-54] In this paradigm, electrical current is envisaged as flowing into myocytes, through gap junction (GJ) channels at the intercalated discs (ID), back across cell membranes through outward potassium channels, and returning via the extracellular space. Importantly, experimental evidence has provided support for this long-established theoretical conception by demonstrating decreasing extracellular resistance can increase conduction velocity (CV).[50, 52, 55]

Since electrical propagation occurs in the hearts of lower vertebrate animals in which GJs are scarce,[56-58] and persists in mammalian hearts with the principal GJ protein connexin43 (Cx43) knocked out,[59] computational models of conduction were revised to propose an additional method of electrical intercellular communication.[45, 46, 60-63] In these models of ephaptic coupling (EpC: non-GJ, non-synaptic coupling), strongly depolarizing inward currents facing a 10-30 nm cleft separating adjacent cardiomoycytes significantly decrease the extracellular potential to depolarize nearby membranes. In the case of dense sodium channel localization to the ID

between cardiomyocytes, and more specifically in the GJ adjacent perinexus,[64] sodium channels self-*activate* in a positive feedback process that rapidly decreases the extracellular potential and activates more sodium channels[65] while simultaneously increasing intracellular potentials. Importantly, the rapid decrease of extracellular potentials, increase in intracellular potentials, and depletion of extracellular sodium in the cleft[61, 66] decrease the driving force during intercellular propagation in a process known as self-*attenuation*.[60] All computational models with EpC reveal that starting from a very narrow cleft, widening clefts between cardiomyocytes will first *increase* CV by reducing self-attenuation and then *decrease* CV by reducing self-activation. Importantly, the relationship between CV and cleft width is biphasic when GJ conductance is closer to experimentally measured values of gap junctional coupling (GJC).[67-74]

In order for conduction to occur, current must return to depolarizing myocytes through the bulk extracellular space, and cardiac CV should be directly proportional to extracellular volume if conduction were only dependent on cable-like propagation through GJs without EpC. However, we previously demonstrated that cardiac CV can be inversely correlated to extracellular volume.[47] Subsequent studies revealed that the osmotic agent mannitol, which increases bulk extracellular volume, also increases perinexal volume and reduces CV.[75] Since we found that ventricular conduction slowed with perinexal expansion,[76, 77] we concluded that EpC is a significant determinant of CV. However, the relative contributions of cable-like propagation through bulk interstitial volume and ephaptic-like conduction through perinexal domains remain unresolved. The purpose of this study was to determine the relationship between ventricular CV and structural changes to bulk extracellular volume and perinexal nanodomains. Results demonstrate osmotic agents alter CV primarily via an ephaptic mechanism.

METHODS

Data Availability

Data supporting the findings of this study are available from the corresponding author upon reasonable request. An expanded Materials and Methods section can be found in the Data Supplement (reproduced below).

RESULTS

Whole-Heart Electrophysiology

We quantified ventricular conduction velocity (CV) by optical mapping during perfusion with our historical lab standard solution[77] (baseline) and after 15 minutes perfusion with the addition of one of the osmotic agents. In Figure 1A, representative optical maps demonstrate how CV is affected by time and osmotic agents. After 15 minutes, CV may modestly increase in time control optical maps, is decreased with mannitol (as evidenced by crowding of isochrones), is increased by albumin (as evidenced by enhanced isochrone spacing), is modestly increased by dextran 70kDa, and increased by dextran 2MDa. Summary data in Figure 1B demonstrate the effect of the osmotic agents relative to baseline measures in the same heart, as well as a comparison of the paired change in conduction to time controls. In short, CV in the transverse direction (CV_T) was not significantly different after 15 minutes of time control perfusion (Diff: 1.1 cm/sec, 95%CI: ±1.3). Mannitol significantly decreased CV_T relative to baseline measurements (Diff: -2.7 cm/s, 95%CI: ±1.8), and the change in CV_T was significantly lower (Diff: -3.7 cm/s, 95%CI: ±3.0) than the change in CV_T observed in the 15-minute time control measurement. Albumin, on the other hand, significantly increased CV_T (Diff: 7.2 cm/s, 95%CI: ± 2.4) relative to baseline, and the change was significantly greater (Diff: 6.1 cm/s, 95%CI: ± 2.8) than the change found for the time control. Interestingly, both dextran 70kDa and dextran 2MDa increased CV_T in paired comparison (Diff: 1.0 cm/sec, 95%CI: ±0.9 and Diff: 2.7 cm/sec, 95%CI: ±1.6), but the change in CV_T was not significantly different (Diff: -0.1 cm/s, 95%CI: ±3.0 and Diff: 1.7 cm/sec, 95%CI: ±3.0) from the time control. CV in the longitudinal direction (CV_L) significantly increased after 15 minutes of time control perfusion (Diff: 4.1 cm/sec, 95%CI: ±3.9). Mannitol did not significantly change CV_L (Diff:

-2.1 cm/sec, 95%CI: ±3.5). Albumin (Diff: 8.7 cm/sec, 95%CI: ±4.1) and dextran 70kD (Diff: 4.5 cm/sec, 95%CI: ±4.4) significantly increased CV_L. Dextran 2MDa did not significantly change CV_L (Diff: 1.9 cm/sec, 95%CI: ±2.9). However, none of the magnitudes of change in CV_L were significantly different from time control. In general, CV changes induced by the osmotic agents in this study measurably changed transverse conduction. In summary, mannitol decreased, while albumin and both dextrans increased epicardial conduction measured by optical mapping relative to their paired pre-treatment baseline.

Neither APD_{90} nor maximum APD dispersion were significantly different from baseline in any treatment group (Figure S4).

Cx43 and Gap Junctions

In order to determine possible effects of osmotic agents on gap junctional coupling (GJC), levels of the principal ventricular gap junction (GJ) protein connexin43 (Cx43) were quantified by western blotting. Total Cx43 expression was not expected to change in response to 15 minute exposure to the osmotic agents, and so Cx43 phosphorylated at serine 368 (pCx43-S368) was also quantified since it has been associated with changes in GJ conductivity.[78-80] Across all conditions, neither total nor pCx43-S368 (Figure 2A,B) significantly changed in response to osmotic agent perfusion. Relative to time control tissue, total Cx43 was not significantly different in tissue perfused with mannitol (Diff: 0.1 AU, 95%CI: ±0.4), albumin (Diff: 0.3 AU, 95%CI: ±0.4), dextran 70kDa (Diff: -0.2 AU, 95%CI: ±0.4), nor dextran 2MDa (Diff: -0.02 AU, 95%CI: ±0.5). With respect to time control, pCx43-S368 was also not significantly different in tissue perfused with mannitol (Diff: 0.1 AU, 95%CI: ±0.6), albumin (Diff: -0.2 AU, 95%CI: ±0.6), dextran 70kDa (Diff: -0.1, 95%CI: ±0.6), or dextran 2MDa (Diff: -0.1 AU, 95%CI: ±0.5).

Since protein expression does not always correlate with function, functional GJC was also assessed by Fluorescence Recovery After Photobleaching (FRAP) in heterologous cells stably expressing Cx43 using an approach that we have reported previously.[81-83] Representative fluorescent images taken before photobleaching (prebleach, Figure 2C), immediately after bleaching (t=0s), and at 150 and 300s post-bleaching, demonstrate fluorescence recovers to approximately the same extent as control cells. Specifically, FRAP, as can be seen in summary data plotted in Figures 2D and E, was not significantly different for cells incubated with mannitol (Diff: 1.0%, 95%CI: ±16.2), albumin (Diff: -4.2%, 95%CI: ±20.9), dextran 70kDa (Diff: 3.8%, 95%CI: ±20.7), or dextran 2MDa (Diff: 3.6%, 95%CI: ±20.8). As a positive control, the GJ uncoupler carbenoxolone (CBX, 10 μM) decreased FRAP as expected (Diff: -23.8%, 95%CI: ±5.9). Despite a visual drop in FRAP measured in cells treated with albumin, summary data in Figure 2E reveal that only CBX significantly decreased GJC estimated by FRAP. Even if 1-hour perfusion with albumin modestly decreased GJC, that finding would be inconsistent with the observed increased CV in hearts perfused with albumin. In summary, we did not measure a change in Cx43 level or function in response to the osmotic agents employed in this study at the concentrations or incubation times noted.

Peak Sodium Current

Next, we sought to determine whether the osmotic agents affected the sodium current, which is another important determinant of cardiac conduction. Representative current traces from a single cell, the average of average current-voltage measurements from multiple cells in each heart, and summary peak current for all cells and hearts are plotted in Figure 3A-D. In summary, the osmotic agents did not significantly change peak sodium currents relative to control replicates obtained from the same hearts. Specifically, the peak sodium current relative to control was not significantly different in cells treated with mannitol (Diff: 4.1 pA/pF, 95%CI: ±11.0), albumin (Diff: -1.1 pA/pF,

95%CI: ±13.9), dextran 70kDa (Diff: -2.6 pA/pF, 95%CI: ±14.1), or dextran 2MDa (Diff: -0.7 pA/pF, 95%CI: ±14.0).

Bulk Interstitium

To test whether the volume of bulk interstitial space (VIS) correlated with changes in CV, the percentage of tissue unoccupied by cardiac cells was quantified with a positive-pixel analysis of hematoxylin and eosin (H&E)-stained tissue. Histological quantification did not reveal significant differences between tissues subjected to 15 minutes of perfusion with any osmotic agent (Figure 4). Relative to control, VIS was not significantly changed by perfusion with mannitol (Diff: 1.6%, 95%CI: ±11.4), albumin (Diff: 3.0%, 95%CI: ±11.9), dextran 70kDa (Diff: -6.1%, 95%CI: ±11.1), or dextran 2MDa (Diff: -1.0%, 95%CI: ±12.4). This was unexpected since our previous results from ventricular tissue analyzed from glutaraldehyde fixation and snap frozen samples demonstrated albumin decreases bulk extracellular volume and mannitol increases it.[47]

We therefore sought to quantify tissue impedance at baseline and after 20 minutes of treatment with the osmotic agents using a 4-electrode technique as previously described.[84-86] Extracellular tissue resistance (R_e) was measured in each heart without interventions (time control) and after serial perfusion with the osmotic agents. This permitted a pair-wise comparison to reduce errors associated with different depths of electrode penetration and orientation of electrodes relative to myocardial ultrastructure and transmural rotational anisotropy. The specific values of R_e are less important than whether the osmotic agent changed R_e and if R_e increased or decreased. Summary data in Figure 5A reveal that R_e did not significantly change over 20 minutes relative to baseline for time control measurements (Diff: 13.6 Ω, 95%CI: ±89.7), mannitol significantly reduced R_e (Diff: -4.9 Ω, 95%CI: ±5.0), albumin did not change R_e (Diff: 14.3 Ω, 95%CI: ±85.7), dextran 70kDa significantly increased R_e (Diff: 20.6 Ω, 95%CI: ±10.9), and dextran 2MDa significantly increased

R_e (Diff: 70.3 Ω, 95%CI: ±68.4). Importantly, CV changes observed above do not correlate with R_e.

Intercellular parameters, including cell membrane capacitance, cytosolic resistance and GJ resistance were modeled as a constant phase element (CPE). The distributivity of the time constant of the CPE element, the parameter η, did not significantly change relative to paired baseline measurements: time control (Diff: 0.05 AU, 95%CI: ±0.9), mannitol (Diff: 0.11AU, 95%CI: ±0.10), albumin (Diff: 0.00 AU, 95%CI: ±0.23), dextran 70kDa (Diff: -0.03AU, 95%CI: ±0.16), and dextran 2MDa (Diff: -0.03AU, 95%CI: ±0.20), as can be seen in Figure 5. These data suggest the R_e changes described above are unlikely to be the result of changes to cellular or tissue factors beyond R_e.

Molecular Exclusion from the Intercalated Disc

In order to estimate whether the different sized osmotic agents can permeate the intercalated disc (ID), the ID distribution of different sized fluorescently tagged dyes (0.5, 3, and 10kDa) was measured by laser scanning confocal microscopy. Representative images in Figure 6A reveal the presence of the 0.5kDa dye in the ID, and the exclusion of the 3 and 10kDa dyes. Figure 6B demonstrates how ID relative to bulk extracellular dye distribution was quantified by taking fluorescent intensity profiles of the dye through the Cx43 immunolabelled ID. By quantifying the intensity of dye beyond the Cx43 signal (lateral membrane) relative to the dye at the peak of the Cx43 signal, summary data on relative ID localization reveal that 0.5kDa dyes can permeate the ID with a normalized fluorescence intensity of 3.6 (95%CI: ±0.88), which is significantly greater than 1, indicating the dye accumulates in the ID. Relative normalized fluorescence intensity for 3kDa dye was 0.30 (95%CI: ±0.20) and 10kDa dye was 0.12 (95%CI: ±0.04), which are both significantly below 1, indicating these compounds were largely excluded from the ID. The data suggest that even if 66.5kDa albumin freely diffused into the bulk interstitium, it would not

penetrate the ID, nor would dextran 70kDa or 2MDa. In short, small molecular weight molecules <3kDa can penetrate the ID and cause osmotically mediated dehiscence, while larger molecules may be size restricted from the ID and prevent or reduce fluid accumulation in these nanodomains.

Ventricular Perinexus

To test the hypothesis that different sized osmotic agents differentially modulate ID volume, we quantified the width of the cardiac perinexus (W_P) with transmission electron microscopy (TEM). Representative perinexi from the LV of hearts are shown in Figure 7A at 150,000X magnification. The osmotic agents differentially modulated cell membrane separation immediately adjacent to the GJ plaque within 15 minutes of osmotic agent perfusion. Specifically, and relative to time control, mannitol significantly increased W_P by 4.3 nm (95%CI: ±3.1), albumin significantly narrowed W_P by -5.1 nm (95%CI: ±2.9), dextran 70kDa did not significantly change W_P (Diff: 0.5 nm, 95%CI: ±2.1), and dextran 2MDa significantly narrowed W_P by -3.9 nm (95%CI: ±1.8), as can be seen in Figure 7B. Importantly, perinexal quantification revealed an inverse correlation between W_P and conduction. Specifically, mannitol *widened* W_P and *decreased* CV consistent with previous reports,[47] and albumin and dextran 2MDa *narrowed* W_P and *increased* CV.

Self-Attenuation

To this point, presented data demonstrate that CV is inversely correlated to W_P. Yet, the relationship between W_P and CV is biphasic. For very narrow perinexi, CV can be directly proportional to W_P by altering sodium channel self-attenuation.[60, 87, 88] In a final set of experiments, we hypothesized that combining dextran 70kDa with albumin would further decrease W_P and slow CV relative to albumin alone, consistent with previous studies.[50] Representative perinexal images and summary data in Figure 8A demonstrate that albumin and dextran 70kDa perfused concurrently significantly decreased W_P relative to albumin alone by 2.3 nm (95%CI: ±2.0).

On average, albumin perfusion increased CV_T relative to baseline by Diff: 38% (95%CI: ±13.3). Whereas the combination of albumin and dextran 70kDa did not significantly increase CV_T (Diff: 4.8%, 95%CI: ±11.8). Therefore, albumin and dextran 70kD slowed CV_T relative to albumin alone, by Diff: 33.3% (95%CI: ±14.9). On average, albumin perfusion increased CV_L relative to baseline by Diff: 16.2% (95%CI: ±7.1). Whereas the combination of albumin and dextran 70kDa did not significantly increase CV_T (Diff: 4.5%, 95%CI: ±6.2). Therefore, albumin and dextran 70kD slowed CV_L relative to albumin alone, by Diff: 11.7% (95%CI: ±9.8). These data demonstrate that dextran 70kDa can slow conduction in the presence (Figure 8B), but not the absence of albumin.

DISCUSSION

Herein, we present two primary observations: 1) The cardiac perinexus, a specialized nanodomain of extracellular space within the intercalated disc (ID), can be osmotically expanded and collapsed on a timescale of less than 15 minutes, and 2) The regulation of cardiac epicardial conduction velocity (CV) is biphasically related with perinexal width (W_P). Among the conditions tested, we did not observe significant changes in total connexin43 (Cx43) expression or phosphorylation at serine 368 (pCx43-S368), nor did we find altered gap junction coupling (GJC) estimated by fluorescence recovery after photobleaching (FRAP). Additionally, the lack of a linear correlation between CV and altered tissue resistance argues for a minimal role in cable-like conduction mediated by gap junctions (GJ) alone. Furthermore, the osmotic agents did not significantly alter peak sodium current, although the change could have been below the resolution of detection. Our interpretation of these data is that extracellular volume changes in sodium channel-rich nanodomains such as the ID perinexus, rather than bulk extracellular resistance (R_e), play a substantial role in modulating CV by an ephaptic mechanism in the absence of GJ remodeling.

In the present study, CV measurements for both mannitol and albumin were similar to those described earlier.[47] Mannitol expanded W_P as we reported earlier.[66, 75] Albumin and dextran 2MDa both decreased W_P and increased CV. When conduction changes were noted, they were primarily observed in the transverse direction of propagation. This is consistent with electrical wavefronts encountering more ID, with associated GJs and ephapses, along the short versus the long axis of cardiomyocytes for a given unit length. More specifically, as cardiomyocytes are highly polarized and IDs are located primarily on the edges of the long-axis, transverse propagation requires the electrical wavefront to "zig-zag" through the lateral edges. Since conduction across the ID is slower than through the myocyte,[89] the increased number of junctions in the transverse, relative to the longitudinal direction will multiply the effect of modulating junctional communication on cardiac conduction. Interestingly, 40 g/L dextran 70kDa alone modestly but significantly increased CV in the whole-heart preparation, which seems to be in contrast to a previous study that found conduction slows with dextran 70kDa.[50] Unlike our study, albumin was present in the baseline perfusion solution of the previous independent study. This being said, we replicated previous findings that dextran 70kDa in the presence of albumin will prevent the conduction increase associated with albumin alone. We propose the mechanism of CV slowing with dextran 70kDa and albumin is more dependent on perinexal narrowing resulting in ephaptic self-attenuation than a decrease in bulk extracellular impedance. Self-attenuation is predicted to occur when sodium channels decrease extracellular potential or sufficiently deplete extracellular sodium such that the inward driving force of this ion is reduced in ephaptic nanodomains. The results of the experiments with concurrent perfusion of albumin and dextran 70kDa are consistent with previous demonstrations of self-attenuation,[66, 87] and reconciles conduction differences observed during osmotic stress by our group[47, 75, 77, 90] and others.[50]

Gap Junctions

Cx43-formed GJs and R_e are widely accepted as major determinants of cardiac conduction.[1, 91, 92] Since the half-life of cardiac Cx43 is on the order of 1-2 hours,[93] and we observed CV changes at 15 minutes, it is not surprising that we do not measure a significant change in overall connexin protein expression. The further absence of associated changes in pCx43-S368 level is consistent with the lack of observable change in functional GJC estimated from FRAP assays. We previously demonstrated that Cx43 expression levels were not significantly changed by the same concentrations of albumin and mannitol perfused in this study.[47] Though we cannot definitively rule out changes to GJ assembly or other Cx43 post-translational modifications, our data, combined with the short time scale of conduction changes, suggest that the primary mechanism for conduction changes may not be significantly attributed to GJC.

Most computational models of ephaptic coupling (EpC) and GJC do not demonstrate a biphasic relationship between CV and cleft width at “nominal” GJC,[46, 60-62] leading to the hypothesis that EpC is not particularly relevant during conditions of “normal” GJC. These models often reveal CV slowing secondary to widened cleft widths when GJC is reduced by more than 80%.[46, 60-62] As a result, a recurring question is whether EpC has a significant impact on cardiac conduction when GJC is nominal. In addressing this question, it is important to note that early computational models of cardiac conduction mediated by EpC and GJC often assumed normal GJ conductivity that is significantly greater[46, 60-62, 89] than has been measured experimentally between ventricular cardiomyocytes. Specifically, direct measurement of GJ conductances by dual-cell patch clamp yields estimates ranging from 3 to 2530 nS, with the majority of studies reporting an average GJC of less than 550 nS, independent of species.[67-74] Based on this consensus average, actual levels of GJC between myocytes are likely an order of magnitude smaller than the 2000nS values typically used as a nominal estimate of coupling in many computational models. Furthermore, even in models that do not incorporate EpC, GJC is often tuned to lower values than those experimentally measured for the purpose of producing *in silico* CV values consistent with

measurements made in heart.[94, 95] It is possible that unaccounted for EpC could be a reason for non-physiologic GJC tuning that is necessary to replicate experimentally measured CV in hearts. Importantly, when one retrospectively re-evaluates these key early models in the context of consensus levels of GJC experimentally reported in the literature, EpC emerges as a major determinant of CV under normal, as well as pathological conditions of GJC.

Perinexal Width

In addition to the aforementioned biphasic predictions of the CV-cleft width relationship in computational models of cardiac conduction, computational models that include both EpC and GJC also predict that CV sensitivity to GJC is reduced when intercellular separation is below approximately 20 nm and significantly enhanced at much wider cleft widths. These predictions have since been validated in mice and guinea pigs.[75, 87, 96] Additionally, expansion of the perinexus has been associated with chronic atrial fibrillation in humans.[97]

Based on the observations that CV is inversely correlated with W_P during perfusion with the individual osmotic agents, and that combining albumin and dextran 70kDa narrowed W_P more than albumin alone and prevented the albumin mediated CV increase, the data can be interpreted to support an ephaptic mechanism of osmotically regulated cardiac conduction. Specifically, very narrow perinexi are associated with relatively slow conduction (albumin and dextran 70kDa). Expanding the perinexus first increases CV (albumin or dextran 2MDa), then starts to slow CV (control or dextran 70kDa), and eventually dramatically slows CV as perinexi are dramatically disrupted (mannitol). These observations are consistent with an expected biphasic CV-W_P relationship predicted by models which include both EpC and GJC.[45, 60-62, 98]

While we frequently report W_P near 20 nm, we also have demonstrated that the absolute value is dependent on the blinded experimentalist who traces the boundary of the perinexus in

transmission electron microscopy images.[97] Additionally, estimating a 3-dimensional volume from 2-dimensional images limits the precision of estimating perinexal volume, and therefore correlation between CV and W_P. Even so, the relationship between CV and W_P is biphasic and therefore non-linear. Regardless, modelling and experimental data should be compared cautiously when attempting to establish numerical relationships between something as simple as channel conductance, whole-cell electrophysiology, and tissue level responses. For example, models often assume a cylindrical geometry of myocytes with a surface area that significantly underestimates the tortuosity of the ID. Incorporating ion tracking[61] or simple structural detail into the model such as interdigitation or the known disposition of larger GJs to encircle the ID[46] modulates the response and range of CV observed with altered cleft width. The estimated CV values in EpC models are also dependent on sodium channel density in the ID,[46] and the location of sodium channel clusters and their relative apposition within the ID.[65] While it is tempting to infer a nominal starting point for any parameter on a predicted curve and speculate if CV should increase or decrease with a specific change in W_P, this approach is likely premature. New studies utilizing models with enhanced structural detail, biophysics of spatial interactions, and ion channel clustering will likely yield important new insights into the effect of EpC on electrophysiology.[88, 99]

Extracellular Impedance

The electrochemical impedance experiments revealed significant R_e changes at a similar time scale when conduction changes, as reported previously.[47] Further, the data were collected on a similar temporal scale to the measurements of previous studies that carefully quantified tissue resistance at each point when conduction was measured.[50] The physics of cable-like conduction through GJs alone is not compatible with our results, as R_e did not directly correlate with conduction. Notably, whereas both the 70kDa and 2MDa dextrans increased R_e and should have slowed conduction, they did not: Specifically, 70kDa and 2MDa dextran significantly increased CV. Furthermore, mannitol decreased R_e while simultaneously slowing CV as reported

previously,[47] but according to models only including GJC alone, mannitol should have increased CV.

Importantly, dextran 70kDa increased R_e by 21% in guinea pig whole-heart, similar to what was reported by others in isolated rabbit papillary muscle (a change of roughly 45%).[50] To address the possibility that one or more osmotic agents altered GJC, cell size, membrane capacitance or any additional intercellular electrical parameters, we modeled the cellular pathway using a constant phase element (CPE). Tissue is composed of various cell types with different shapes and membrane properties, resulting in a distributed cell membrane time constant – the response speed of the cell membrane to electrical stimulation. This distributivity is what we quantified in the parameter, η. Since this parameter did not significantly change with time control, or with the addition of any of our osmotic agents, we conclude that the cell membrane time constant distribution on the tissue level was not substantially affected by our interventions. Therefore, the changes to R_e described above are likely a result of changes to the extracellular compartment, i.e. interstitial space. The lack of change in η is also consistent with non-significant changes induced by the osmotic agents in Cx43 expression or FRAP coupling assays. Importantly, macroscopic impedance measurement and its relationship to the cable theory is at best complicated and requires additional study.

Sodium Channels

Despite the non-significant change in peak sodium current (I_{Na}) with osmotic agents, it is possible that conduction changes reported in this and previous studies[47, 76] could be attributed to a change in peak sodium current below our resolution of detection. It should be noted here that the statistical approach may play a role in the ability to report a significant change in peak conductance. Specifically, if each current obtained from a cell is considered an independent measurement, regardless of which heart it was obtained from, a simple non-paired Student's t-test would suggest

that mannitol modestly decreases peak I_{Na} on the order of 20%. If mannitol does significantly decrease peak I_{Na}, this and previous studies may over-associate conduction slowing with perinexal widening. It is possible that a relatively small sodium channel inhibitory effect of mannitol exacerbates conduction slowing under these conditions as well. Yet, perinexal expansion associated with a peptide developed to disrupt sodium channel beta subunit trans-adhesion did not affect peak sodium current density and also slowed conduction in the same isolated guinea pig whole-heart preparation.[77]

The computationally predicted relationship of CV to W_P is also non-symmetric in the self-attenuation (positive correlation) and self-activation (negative correlation) phases of conduction. It is therefore difficult to know where the "normal" heart may reside on the CV-W_P curve because this relationship is also modulated by factors such as sodium and potassium channel localization to the ID, channel unitary conductances, channel availability, cell size, and extracellular sodium and potassium.[46, 60-62, 66, 100-103] Importantly, we provide experimental evidence that the degree of perinexal narrowing or expansion is associated with different magnitudes of CV increase or decrease, respectively. Thus, at present, it is difficult to state to what degree the different osmotic agents should change CV for a given change in W_P. We can say with confidence that the change in CV with narrower and wider W_P is not uniform. Regardless, evidence continues to support the conclusion that cardiac conduction is well-described by models including both EpC and GJC.

Membrane and Intracellular Pathways

The 4-electrode distributivity measurement, a metric of cell membrane capacitance, cytosolic resistance and GJ resistance, does not significantly differ between controls and cells or tissue incubated with the osmotic agents. This inconclusive result does not support nor exclude the possibility that osmotically induced changes in cellular parameters are significant determinants of CV. The lack of distributivity change is inconsistent with previous results when cell volume was

measured by cell morphometry, for example. Specifically, we and others reported that mannitol can decrease *isolated* ventricular myocyte volume by approximately 7% to 25% for concentrations of mannitol between 50 mM and 143 mM.[47, 104, 105] The discrepancy and lack of significant differences in metrics of intracellular impedance in this study could therefore be a result of: a change that is below the detection resolution of the technique, intra- and interventricular heterogeneity,[38] inter-animal variability, and/or variability secondary to cellular isolation.[106] Importantly, a previous computational model of conduction found that the relationship between cell size and CV is complexly dependent on both forms of electrical coupling.[63, 103] Specifically, with relatively high GJC (2500 nS), decreasing cell size can slow conduction, and EpC can modestly steepen that relationship. In contrast, with relatively nominal but closer to normal GJC (100 nS), decreasing cell size can increase CV, but once again EpC modestly increases the steepness of this relationship.[103] Since GJC has been measured over a large range of values, and the average value in literature is closer to 550 nS,[67-74] we do not know which result to expect. Therefore, the effect of parameters such as cell volume on the observed changes in CV still requires significantly more independent investigation for a number of reasons including: 1) Morphometric changes in myocyte geometry are likely different in an isolated, unloaded cell relative to cells in intact myocardium, 2) The osmotic agents will partition differently between vascular, extracellular, and ID compartments based on osmolyte permeability and size, and 3) The molarity of the osmotic agents used in this study are not identical.

Limitations

No intervention can be applied without experimental consequence. Osmotic agents employed in this study have well-established effects in addition to changing oncotic pressure, and some are used clinically for these and other reasons.

Albumin, for example, has been used to regulate blood pressure due to its binding affinity to the vascular endothelium, leaving vessels at a rate of approximately 5% per hour. Albumin furthermore regulates vascular function and can bind to a number of cations, fatty acids and hormones, in addition to acting as an antioxidant.[107]

Mannitol, a sugar alcohol, has been used as a hyperosmotic agent to treat high intracranial pressure.[108, 109] With appropriate dosing and time courses of treatment, mannitol will decrease interstitial edema by drawing fluid out of the cerebral parenchyma; though at higher doses and over long time courses, mannitol will also cross the blood-brain barrier. Once across the blood-brain barrier, mannitol will then have the opposite intended effect, more similar to what we observe in cardiac tissue: drawing fluid into tissue and exacerbating edema.

Dextrans of various sizes have been used, like albumin, as a blood volume expander, with larger dextrans having a more pronounced effect on blood viscosity. Dextran 70kDa has antithrombotic properties and reduces the inflammatory response and troponin-I release after cardiac surgery.[110, 111] It remains unknown, however, whether the other non-osmotic properties affected our results over the much more acute time frame of less than 15 minutes studied here.

Despite our efforts to select osmotic agents with minimal binding or metabolic effects, we cannot definitively exclude any such effects and advise the reader to cautiously interpret our results about any implications for clinical treatment.

As mentioned previously, experiments were conducted in excised, isolated, male retired breeder, guinea pig ventricles that were perfused with di-4-ANEPPS and preserved for hematoxylin and eosin staining and electron microscopy with formalin and glutaraldehyde, respectively. As such, all values of structural dimensions presented – e.g. W_P and interstitial volume, should be

interpreted without implication of explicit *in vivo* values. Additionally, while our CV results are similar to those published previously,[47] we observed no significant differences in interstitial volumes between interventions, though all of our values were similar to the controls reported previously. It is worth noting that the reported interstitial volume differences may be attributed to a shorter protocol (15 minutes in this study vs 60 minutes in previous studies), different fixatives (formalin vs glutaraldehyde), different analysis programs (positive-pixel vs color deconvolution), and the statistical approach. Interestingly, previous work suggests that 30 minutes of perfusion is required for changes in R_e to reach steady-state.[50]

Furthermore, albumin is difficult to work with in optical mapping experiments because signal quality degrades quickly, as demonstrated previously[76] and in Figure S2A. The reasons for this are not entirely understood since the absorption peak of albumin is approximately 280 nm[112, 113] and peak excitation for di-4-ANNEPS is near 480 nm.

Optical mapping also provides fluorescent signals from a volume of tissue that includes intramural cells, and volume averaging may “blur” the upstrokes of optical action potentials and capture transmural propagation patterns.[114-118] The values of conduction between the left and right ventricle may also be affected by transmural rotational anisotropy given the difference in myocardial thickness.[119] Additionally, our CV measures represent an average across the anterior epicardial surface, and the averages contain an indeterminate ratio of points from the left and right ventricles, as well as points that are more apical or basal relative to the pacing electrode. Regional heterogeneities in tissue response and which regions of tissue are quantified in a given image may have unanticipated effects on the magnitude of the observed effects, particularly as our measurement field of view and pacing site is biased towards the left ventricle. Therefore, caution should be taken when considering the absolute CV values presented herein. However, our group is careful about conducting positive and time control measurements with optical

mapping under a variety of conditions previously reported to affect conduction: sodium channel inhibitors,[37, 75] GJ inhibition and Cx43 genetic loss of function[87, 102] mannitol or albumin,[47, 76] and changes in extracellular potassium.[102]

With regards to whether edema confounds epicardial measures of CV due to volume averaging, we currently discount this hypothesis for a few reasons. First, dehydrating tissues should bring more cells into the field of view epicardially and transmurally. Epicardial recruitment of cells into an imaging volume should decrease the speed of conduction by increasing the number of IDs in each pixel, even if the dimmer mid-myocardium would increase conduction. The epicardial recruitment effect is inconsistent with our finding that solutions associated with increased or decreased R_e, a metric of bulk hydration, do not correlate with the directional change in conduction. Furthermore, we provide confirmatory evidence that dextran 70kDa in the presence of albumin is associated with slower conduction when compared to hearts perfused only with albumin, and this is consistent with studies using microelectrodes, the same osmotic agents, and papillary muscles that lack rotational anisotropy.[50]

Finally, within our tissue impedance experiments, electrode array orientation was visually aligned with local fiber orientation. However, as fiber orientation changes in 3-dimensional myocardial tissue, we cannot compare tissue impedance changes between experiments, only between interventions in the same heart. As a result, only the finding that R_e changed has practical meaning, but the absolute values of R_e and magnitude of change do not have direct physiologic relevance. Additionally, the measurement of R_e does not distinguish between bulk extracellular volume expansion or changes to conductivity in the ID. Both volume changes could change R_e in the same direction.[120, 121] However, our observations that CV does not change proportionally in response to R_e argues against bulk extracellular volume expansion as the principal determinant of CV in these experiments.

CONCLUSIONS

Clinically relevant osmotic agents may impact cardiac conduction by a previously unappreciated mechanism of modulating nanodomain separation between cardiomyocytes in the perinexi of ID. Specifically, this study demonstrates that expanding ID nanodomains densely expressing ion handling proteins can both increase and decrease cardiac conduction consistent with computational predictions of cardiac conduction dependent on both EpC and GJC. While we cannot definitively exclude the possibility of off-target effects from the experimental interventions studied, our data suggest that EpC modulation of one type of ID nanodomain, the perinexus, is a major determinant of cardiac conduction. The perinexus therefore continues to emerge as a therapeutic target for managing cardiac arrhythmias, and further research is needed to better understand the conditions under which perinexal expansion represents a beneficial adaptation or pathologic remodeling.

SUPPLEMENTAL MATERIALS

Expanded Materials and Methods Section

All animal research for this study was carried out in accordance with the principles of the Basel Declaration and recommendations of the Guide for the Care and Use of Laboratory Animals, National Research Council. The protocol was approved by the Institutional Animal Care and Use Committee (IACUC) at Virginia Polytechnic Institute and State University (Protocol #21-091)

Data Availability

Raw data are available upon request. Details of all statistical methods and experimental materials are available in the accompanying Supplement and Major Resource Table, respectively.

Guinea Pig Langendorff Preparations

Adult male Hartley guinea pigs from Hilltop Lab Animals, Inc. (13-15 months; 900-1200 grams) were chosen for these experiments in order to compare positive controls to previous ephaptic studies using the same age, sex and species.[28,29] Animals were anesthetized by isoflurane inhalation. Hearts were excised and quickly (<5 minutes) cannulated in a Langendorff preparation using an oxygenated perfusion solution containing, as previously described,[28] (in mmol/L): 1.25 CaCl2•2H2O, 140 NaCl, 4.5 KCl, 10 Dextrose, 1 MgCl2•6H2O, 10 HEPES, 5.5 mL/L of 1N NaOH and the electro-mechanical uncoupler 2,3-butanedionemonoxime to reduce motion. The perfusate was equilibrated to a pH of 7.41 at 37°C using NaOH or HCl, as necessary. Hearts were immersed in a 3D printed poly(lactic acid) bath containing the perfusion solution maintained at 37°C. 32 In all experiments, control solution was perfused for 30 minutes, followed by the same solution with either mannitol (Sigma-Aldrich M4125, D-mannitol, 26.1 g/L), albumin (Sigma-Aldrich A9647, bovine serum albumin, 4 g/L), dextran 70kDa (Sigma-Aldrich 31390, dextran from Leuconostoc pp. Mr ~70,000, 40 g/L) or dextran 2MDa (Sigma-Aldrich D5376, dextran from Leuconostoc mesenteroides average mol wt 1,500,000-2,800,000, 40 g/L) for 15 minutes. In preparing the osmotic agent solutions, dextran 2MDa was shaken to dissolve into solution. Mannitol, albumin, and dextran 70kDa concentrations were chosen for comparisons to previous studies, 6,28 and dextran 2MDa was selected for its preferential restriction to vasculature. 33

Statistical Analysis

The total number of animals or plates used (N) and replicate measures (n) were determined to detect 20% effect size based on means and averages obtained in previous studies with similar techniques to achieve an alpha of 0.05 and power of 0.8. Differences among experimental groups were determined through ordinary one-way ANOVA, nested-ANOVA to account for experimental replicates within hearts or plates in heterologous culture experiments, and

Student's t-test, or with non-parametric tests when appropriate (Kruskal-Wallis test or Wilcox test). Corrections for multiple comparisons were applied within but not across experiment types, and all tests were carried out in GraphPad/Prism v9.0 or later. As the distribution of perinexal width (WP) has an elongated right tail, a generalized linear mixed effects model specifying a gamma distribution and identity link was performed using the lme4 package in R version 4.2.2 to compare test groups to time control. Applied statistical tests are noted in figure legends and details are provided in the supplement (Supplementary Statistics). Reported values are compared to baseline and time control experiments. A p< 0.0 0.05 was considered statistically significant. Data in the text are presented as mean difference with 95% confidence interval using the following notation (Diff: X units, 95%CI: ±Y). Figures include individual data points, median, and 25 to 75 percentiles with whiskers representing the range, unless otherwise noted in the legends. Representative images were chosen from the complete data set with the three following subjective criteria: 1) The image provided a clear visual example of the type of data being collected. 2) The difference shown between treatment conditions represented the average change in the data as supported by statistical analysis. 3) The data represented the general quality of imaging collected.

Optical Mapping

Conduction velocity (CV) was quantified by optical voltage mapping using di-4-ANEPPS (15 μM, Biotium #61010) as previously described.[28] Briefly, the preparation was stained with di-4-ANEPPS by direct coronary perfusion for approximately 10 minutes after an initial 15-minute stabilization period following cannulation. Following a 20-minute dye wash-out period, the tissue was excited by 510 nm light, and the emitted light, filtered by a 610 nm filter, was captured by a Micam Ultima L-type CMOS camera with 100x100 pixels and a magnification of 0.63X, covering an area of 15.9 mm by 15.9 mm. Hearts were stimulated at a basic cycle length of 300ms with a 5ms wide cathodal pulse at 1.5X the minimum current required to excite the tissue through a

monopolar Ag-Ag/Cl electrode. The pacing electrode was placed near the center of the anterior epicardial surface of the heart, beside the left anterior descending (LAD) coronary artery, on the side proximal to the left ventricle (LV) so as to map epicardial propagation into both left and right ventricular tissue. Hearts were then positioned such that the electrode was near the center of the imaging field of view. Neither the electrode, heart, nor field of view were moved after this initial placement. Optical data were analyzed to quantify transverse and longitudinal CV (CVT and CVL, respectively), action potential duration (APD),[34-36] and maximum dispersion of repolarization – the greatest time difference in repolarization between the left, right, base, and apex quadrants of the imaging field.[37,38] Figure S1 demonstrates how CVT and CVL are measured from optical maps. As albumin degrades optical signals,[30] six consecutive paced beats were signal-averaged prior to analysis for hearts perfused with albumin. APD was quantified as the time between activation and 90% repolarization. Half of the experiments were performed by a second blinded experimentalist and conditions were randomized for the purpose of rigor and reproducibility. In these experiments, test solutions were prepared by one experimentalist who knew the conditions being tested and were provided to a second experimentalist with non-identifying markers (1&2, A&B, or similar) while the second experimentalist selected the animal to be used, and carried out the isolation, perfusion, and mapping with no knowledge of the condition being tested. Experimentalists were unblinded only after CV measurements were made.

Western Blots

LV tissue samples were snap frozen at specific time points in the protocol and western blotting was performed as previously described.[39] Briefly, the samples were homogenized in RIPA lysis buffer (containing 50mM Tris pH 7.4, 150mM NaCl, 1mM EDTA, 1% Triton X-100, 1% sodium deoxycholate, 0.1% sodium dodecyl sulphate, 2mM NaF, 200μM Na3VO34) supplemented with Roche Protease Inhibitor Cocktail (4693159001, Sigma-Aldrich). Protein concentration was

determined by a BioRad DC protein assay and concentrations were normalized prior to analysis. Electrophoresis was performed to separate proteins which were then transferred to a PVDF membrane, blocked with 5% bovine serum albumin for 1 hour at room temperature and incubated overnight with a primary antibody against the principal ventricular GJ protein connexin43 (Cx43) phosphorylated at Ser368 (pCx43-S368, 1:1000, #3511S, Cell Signaling Technologies), at 4°C. The membranes were then washed and incubated with secondary antibody (1:5000, Goat Anti-Rabbit HRP, ab6721, abcam) at room temperature for 1 hour. After washing, bound antibody was detected using West Pico Plus chemiluminescent substrate (Thermo Scientific #34579) and imaged using the Licor Odyssey Fc system. Membranes were stripped with ReBlot Plus according to manufacturer's instructions, blocked in Odyssey Blocking Buffer (Licor #927-50000) at room temperature for 1 hour and incubated with primary antibodies against total Cx43 (1:5000, C6219 rabbit, Sigma Aldrich) and GAPDH (1:5000, 101983-284 mouse, VWR). Membranes were then washed and incubated with secondary antibodies for 1 hour (both 1:10,000, goat anti-rabbit IRDye 800CW and goat anti-mouse IRDye 680RD) and washed again. Membranes were again imaged using the Licor Odyssey Fc system to determine protein expression, which includes an internal background subtraction algorithm that accounts for residual florescence and a specific secondary antibody binding. Total Cx43 was normalized to GAPDH and pCx43-S368 was normalized to total Cx43. Primary antibodies for total Cx43 and pCx43-S368 are widely used commercially available antibodies that have been validated previously.[40,41] The full uncropped immunoblots and ladders of representative data are presented in Figure S2.

Fluorescence Recovery After Photobleaching (FRAP)

Rat glioma C6 cells (ATCC® CCL-107TM) transfected to stably overexpress Cx4342 were plated at ~1.5e5 cells on a 35 mm dish with 20 mm glass bottom inset (Cellvis D35-20-1.5-N) and cultured for 48 hours in DMEM/F12 media mixture with 10% FBS as previously

described.[43,44] After 48 hours growth, cells were rinsed with Ca2+ and Mg2+ free DPBS and then incubated for 1 hour in a CO2-free incubator with Invitrogen Opti-MEM with 5% FBS and all treatments but the GJ inhibitor carbenoxolone (CBX). CBX was added after dye loading to avoid interference with dye loading. After a 60-minute equilibration period, cells were rinsed and loaded with 2.5 μM calcein-AM, dissolved in serum-free OptiMEM, and incubated for 15 minutes without any treatment. Cells were then rinsed and returned to OptiMEM with 5% FBS and the appropriate treatment, and incubated for 5-10 minutes before imaging. The cells were imaged on a Leica TCS SP8 confocal microscope using a 488 nm laser at 0.5% power, 256x265 pixel resolution, 700Hz scan speed, and a 7.0 Airy unit pinhole. Pre-bleach images (n=5) were collected, then cells were bleached at 100% laser intensity for 50 cycles (377ms cycle duration). Postbleaching, one image was collected every 0.5 seconds for 300 seconds. During the imaging procedure, cells were maintained near 37oC through use of a heated stage. FRAP was measured for 15-25 cells per plate as replicates. The minimum fluorescence value was subtracted from each cell, so recovery is calculated from zero and normalized to a percent recovery, where the pre-bleach intensity is 1. Recovery was then fit to the following function: $I(t) = Iinf * (1 - e^{-t*k})$. 44 Coefficients Iinf and k were calculated for each cell using the Matlab fit function with the nonlinear least squares method. Total number of plates per condition are as follows: Control (N=13), CBX (N=6), mannitol (N=7), albumin (N=4), dextran 70kDa (N=4), and dextran 2MDa (N=4). All cells (replicates) were averaged, and the averages for each plate are treated and presented graphically as individual data points for each intervention. Relative recoveries (Iinf) were statistically compared with GraphPad/Prism's nested ANOVA function. The Nested parameter was the plate.

Whole Cell Patch-Clamp Recording

Myocytes were isolated from LV free wall of guinea pig hearts using enzymatic dispersion technique as described previously[45] and were re-suspended in 10 mL of Dulbecco modified

Eagle medium, stored at room temperature, and used within 24 hours of isolation. Sodium currents (INa) were recorded by ruptured-patch whole cell voltage clamp at room temperature. Microelectrodes were filled with a solution of (in mmol/L): CsF 120, MgCl2 2, HEPES 10, EGTA 11 and brought to a pH of 7.3. Isolated myocytes were placed in the solution containing NaCl 25, N-methyl Dglucamine 120, CsCl 5, MgCl2 1, NiCl2 1, glucose 10, HEPES 10, pH 7.3. Sodium currents were elicited from a holding potential of -80 mV with depolarizing voltage pulses from -60 to 45 mV for 16 ms. Ionic current density (pA/pF) was calculated from the ratio of current amplitude to cell capacitance. Command and data acquisition were operated with an Axopatch 200B patch clamp amplifier controlled by a personal computer using a Digidata 1200 acquisition board driven by pCLAMP 7.0 software (Axon Instruments, Foster City, CA).

Histology

A positive-pixel analysis of hematoxylin and eosin (H&E)-stained LV tissue, which had been fixed in 10% formalin for at least 24 hours, was performed to quantify interstitial volume (VIS), similar to what we have described previously.[28] All measurements were made from the subepicardium, defined as the region from the epicardial surface to a depth of no more than 500 μm. Images of 5 μm-thick slices of stained tissue were analyzed by an Aperio positive-pixel analysis program which quantified interstitial space as a percentage of the entire array which was devoid of stained pixels.

Extracellular Resistance

In a separate group of experiments, hearts were cannulated with the same perfusion solutions described above, but were not perfused with di-4-ANNEPS. Instead, after a similar stabilization period, a four-probe stainless steel electrode array, with the electrodes 2 mm apart and extending to a depth of 2 mm, was placed on the anterior surface of the LV, approximately parallel to the LAD, and connected to a Gamry Interface 1000 Potentiostat. Using the Gamry

Framework electrochemical impedance program, tissue impedance was measured with the following parameters: Frequency sweep: 1-1E10 Hz; points/decade: 10; ACV: 0.2 mV; DVC: 0; Area: 1 cm2 ; Estimated Z: 100 Ω. The data were then fit to an electrical circuit model of a resistor in parallel with a constant phase element (CPE) and intracellular resistance (Figure S3). Values for the impedance were measured over the frequency band of 200 Hz~1E6 Hz to estimate extracellular resistance (Re) and CPE.[46,47] Impedance of CPE is expressed by:

$$Z_{CPE} = \frac{1}{P(jw)^{\eta}}$$

where P and η are the parameters of CPE. At the tissue level, the cell membrane time constant is spatially distributed because of the variety of cells within the tissue. The distributivity of the time constant is described by the parameter η in CPE, which we can use as an index of the response of cell membrane electrical parameters to the addition of osmotic agents. After a baseline measurement, an osmotic agent was perfused for 20 minutes, followed by a final measurement. This 20-minute time point was selected to ensure we captured the impedance effects of osmotic agent perfusion observed in a previous study.[6]

Fixable Dye Perfusion

In order to assess how different sized osmotic agents partition between the bulk interstitial volume and the intercalated disc (ID), hearts were perfused with fixable dyes of different molecular weights: Alexa 488 hydrazide (0.5kDa; ThermoFisher Scientific #A10436) and biotin-dextran (3 or 10kDa; ThermoFisher Scientific, #D7135 and #D1956). After 30 minutes of dye perfusion, tissue samples collected from the anterior LV free wall were fixed in paraformaldehyde (2%) for 3 hours at 4°C, equilibrated sequentially in 15 and 20% solutions of sucrose, and frozen for cryosectioning. Sections were cut (5 μm) and immunolabeled as described above using a rabbit polyclonal anti-Cx43 antibody (Sigma-Aldrich C6219, St. Louis, MO) followed by goat anti-rabbit Alexa 568 (1:4000) and Streptavidinconjugated Alexa 647

(1:4000) (ThermoFisher Scientific, #S21374) for biotin binding. Confocal imaging was performed using a TCS SP8 confocal microscope as previously described.[31] Regions of interest were selected from confocal images surrounding IDs, which were identified based on Cx43 immunosignal. Fluorescence intensity of the green (0.5kDa Alexa 488), red (3 or 10kDa biotin-dextran), and magenta (Cx43) signals were averaged along an axis perpendicular to the ID to generate intensity profiles. The intensities of green and red signals at the maxima of the magenta (Cx43) signal were normalized to their respective median values on either side of the ID to yield an ID accumulation / depletion index. Values greater than 1 indicate accumulation within the ID while values close to 0 indicate exclusion from the ID.

Electron Microscopy

Anterior epicardial tissue from the base of the LV was collected from hearts after the conclusion of the optical mapping experiments. LV tissue was cut into 1 mm3 chunks which were fixed in 2.5% glutaraldehyde for at least 24 hours at 4°C before being washed and stored in phosphate-buffered saline (PBS) at 4°C. Samples were then prepared for transmission electron microscopy (TEM) and imaged as previously described using a JEM JEOL 1400 Electron Microscope at 150,000X magnification.[48] To quantify perinexal width (W_p), 15 images were analyzed per sample using a previously-described custom Matlab program.[48] The average intermembrane distance between 30-105 nm from the edge of the GJ plaque is reported as WP. Previous work measuring this parameter indicates that 10 to 15 images taken from a minimum of 4 hearts is sufficient to detect changes in WP more than 2 nm.[49]

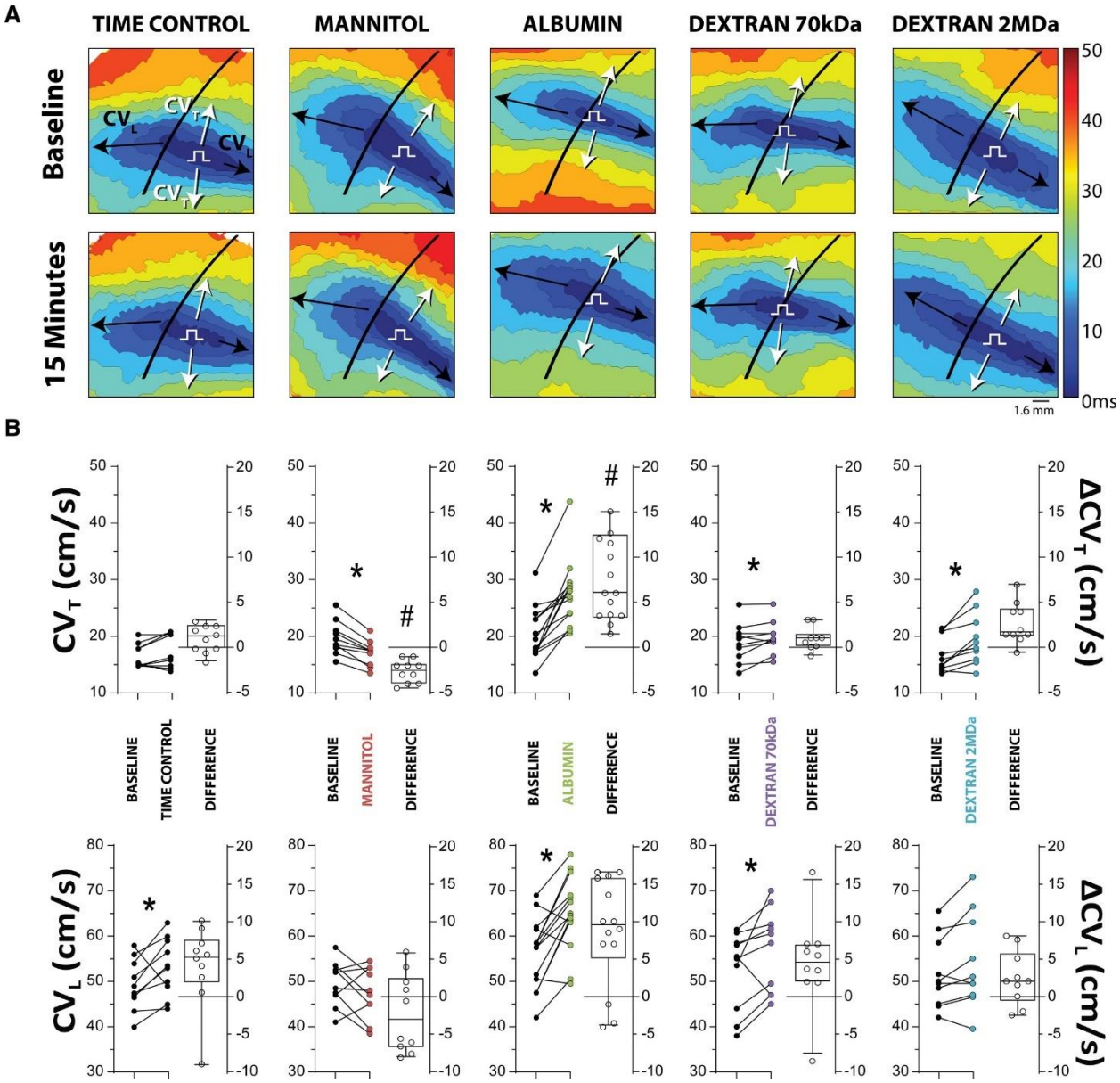
A
TIME CONTROL
MANNITOL
ALBUMIN
DEXTRAN 70kDa
DEXTRAN 2MDa
Baseline
15 Minutes
CV_L
CV_T
50
40
30
20
10
0ms
1.6 mm
B
CV_T (cm/s)
ΔCV_T (cm/s)
BASELINE
TIME CONTROL
DIFFERENCE
MANNITOL
ALBUMIN
DEXTRAN 70kDa
DEXTRAN 2MDa
CV_L (cm/s)
ΔCV_L (cm/s)

Figure 1. *Osmotic agents modulate transverse conduction velocity (CV).* **A.** Representative 3 ms activation time isochrones demonstrate the effect of various osmotic agents on the spread of activation. A detailed explanation can be found in the methods supplement **B.** CV plotted as individual points (*left* axis) and the change in CV (*right* axis) from paired baseline experiments demonstrates mannitol (N=10) significantly decreases, albumin (N=14) significantly increases, dextran 70kDa (N=10) increases, and dextran 2MDa (N=10) increases CV preferentially in the transverse direction *p<0.05 relative to paired baseline measurement, paired Student's t-test. #p<0.05 relative to time control, ΔCV across groups compared with ordinary one-way ANOVA applying Dunnett's correction.

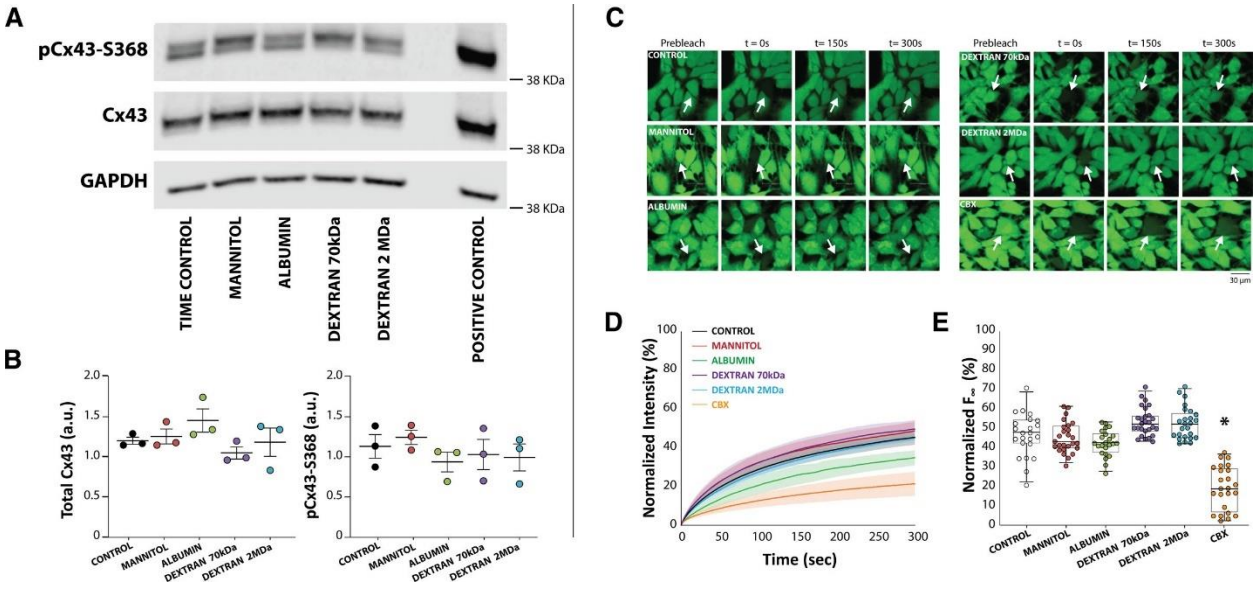

Figure 2. *Osmotic agents do not significantly alter Cx43 protein expression or function.* **A.** Representative western blots suggest that neither total connexin43 (Cx43) nor Cx43 phosphorylated at serine-368 (pCx43-S368) significantly change in response to acute exposure to osmotic agents. Lane 7 contains a positive control using hearts exposed to 60 min of room temperature ischemia, a condition shown to upregulate pCx43-S368.[91] **B.** Summary data do not reveal significant differences in either total or pCx43-S368 for all conditions (N=3 hearts per condition. p=n.s. via ordinary one-way ANOVA applying Dunnett's correction. Center is the mean and whiskers are standard deviation). **C.** Representative fluorescent images of calcein-AM fluorescence in Control cultures (N=13 plates, n=220 cells) and cultures exposed to Mannitol (N=7 plates, n=116 cells), Albumin (N=4 plates, n=77 cells), Dextran 70kDa (N=4 plates, n=102 cells), Dextran 2MDa (N=4 plates, n=95 cells), and Carbenoxolone (CBX, N=6 plates, n=110 cells). **D.** Fluorescence recovery after photobleaching (FRAP) plot of bleached cells during 300s post-bleaching. Solid lines denotes the average and shaded areas the standard error of the mean. **E.** Only CBX significantly decreased FRAP relative to control. *p<0.05, nested ANOVA applying Dunnett's correction with culture plate nested under treatment type.

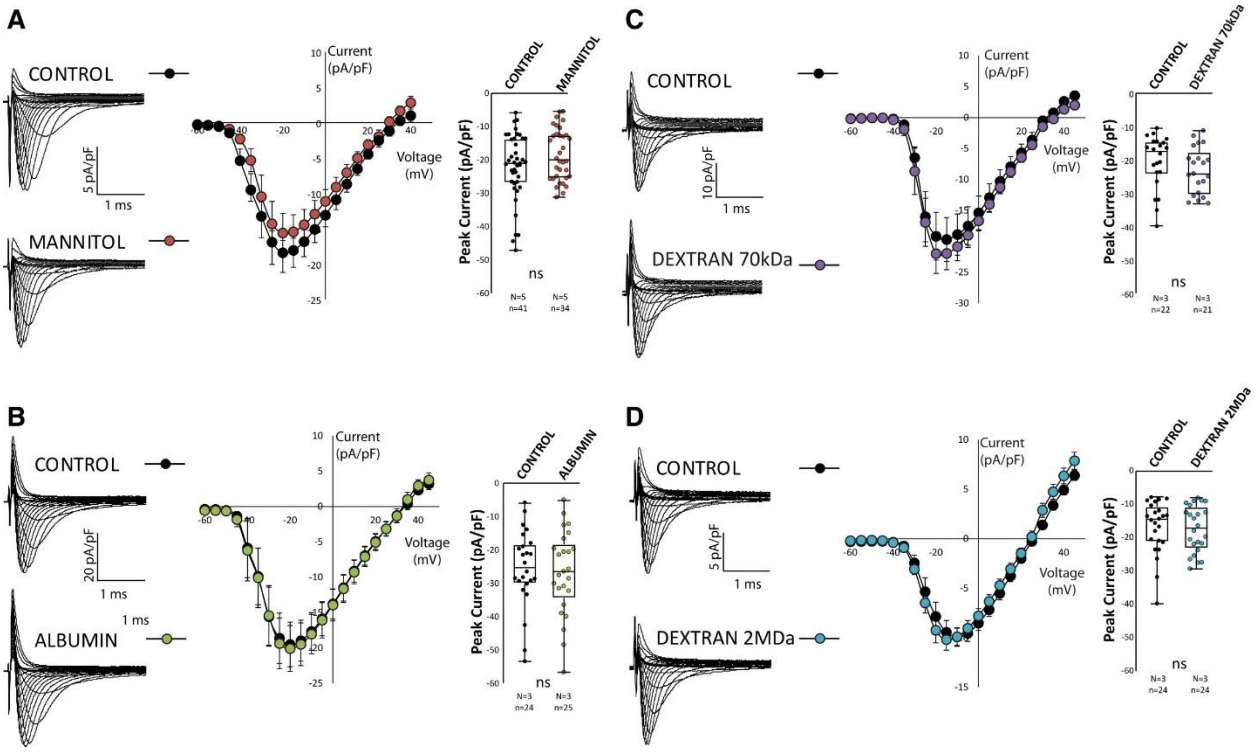

Figure 3. *Osmotic agents do not significantly alter peak sodium current.* Representative currents from a single cell, current-voltage curves averaged from a single heart, and peak current at -20 mV step potential for all hearts and cells reveal none of the test agents significantly decrease sodium currents relative to Control **A.** Mmannitol (N=5 hearts, n=34 cells, red) **B.** Albumin (N=3 hearts, n=25 cells, green) **C.** Dextran 70kDa (N=3 heart, n=21 cells, purple**D.** Dextran 2MDa (N=3 hearts, n=24 cells, blue) All treatment groups were compared to same day measurements from control group cells using a nested ANOVA applying Šidák's correction, where the heart is the nested variable.

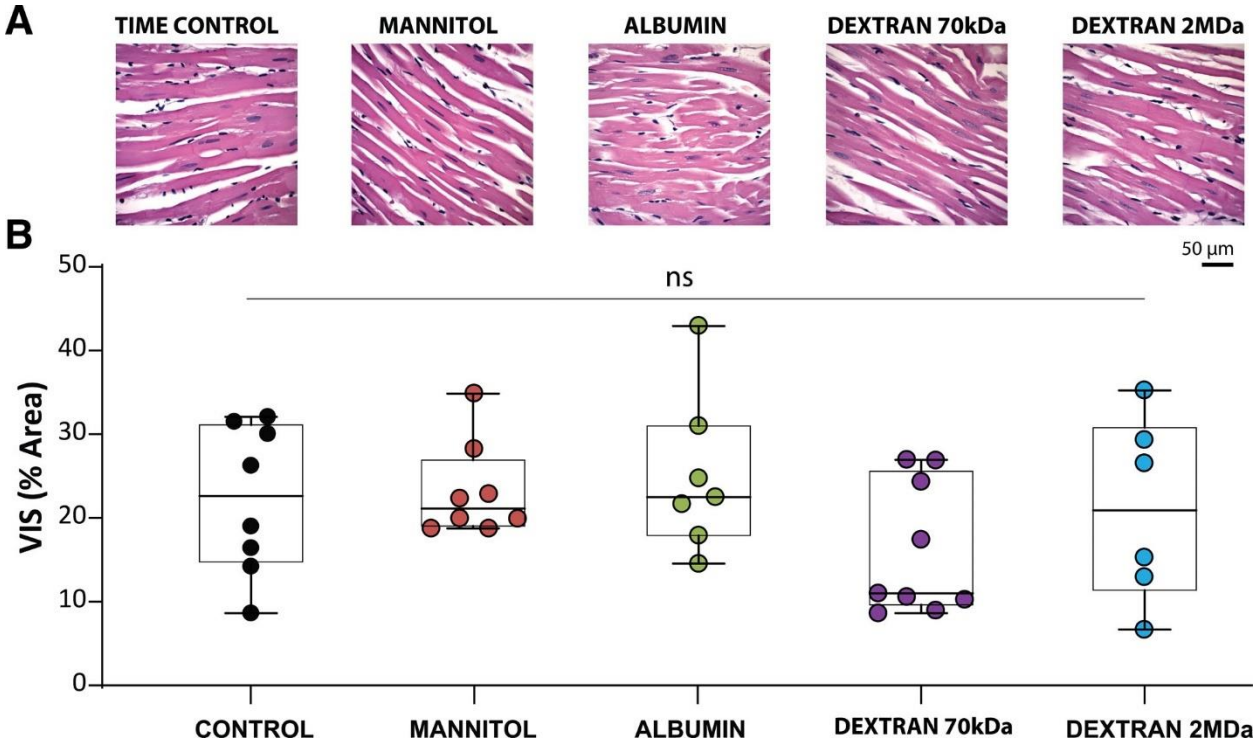

Figure 4. *Osmotic agents do not significantly interstitial space analyzed from hemotoxalin and eosin (H&E) stained ventricular tissue.* **A.** Representative images of H&E-stained tissue **B.** Volume of bulk interstitial space (VIS) as quantified by a positive-pixel algorithm for Control (N=8 hearts, n=84 images), Mannitol (N=8 hearts, n=73 images), Albumin (N=7 hearts, n=71 images), Dextran 70kDa (N=9 hearts, n=91 images), Dextran 2MDa (N=6, n=62 images). p=n.s. nested one-way ANOVA applying Šidák's correction, with heart nested under treatment type.

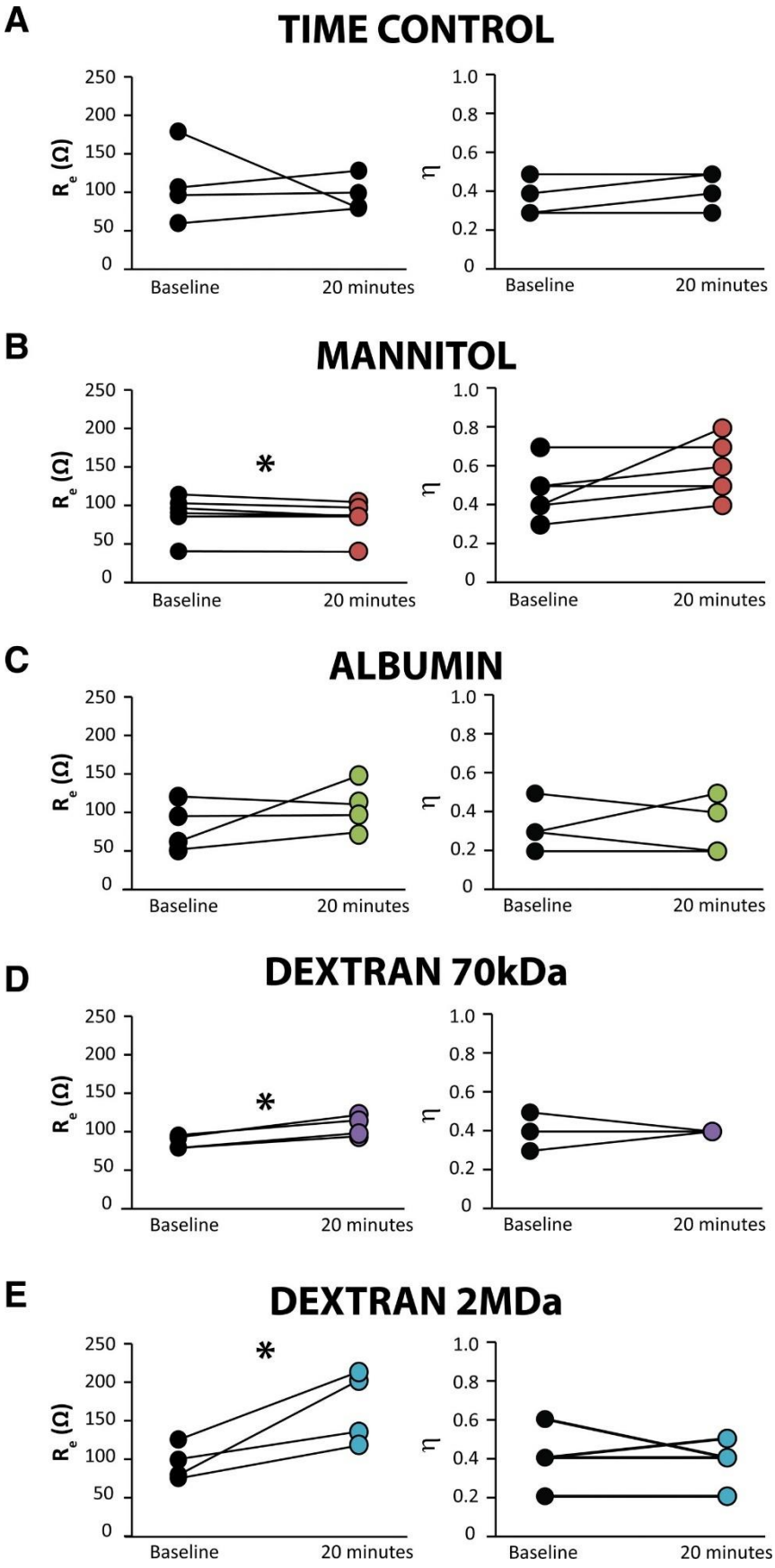
A
TIME CONTROL
B
MANNITOL
C
ALBUMIN
D
DEXTRAN 70kDa
E
DEXTRAN 2MDa
R_e (Ω)
η
250
200
150
100
50
0
1.0
0.8
0.6
0.4
0.2
0
Baseline
20 minutes
*

Figure 5. *Osmotic agents modulate extracellular resistance.* **A.** Neither extracellular resistance (R_e), nor the constant-phase element (CPE) parameter η varied during Time Control (N=4). **B.** Mannitol decreased R_e but did not change η (N=7). **C.** Albumin did not affect either R_e or η (N=4). **D.** However, Dextran 70kDa significantly increased R_e but not η (N=4). **E.** Similarly, Dextran 2MDa increased R_e but not η (N=4). *$p<0.05$, paired 2-tailed Student's t-test, relative to baseline.

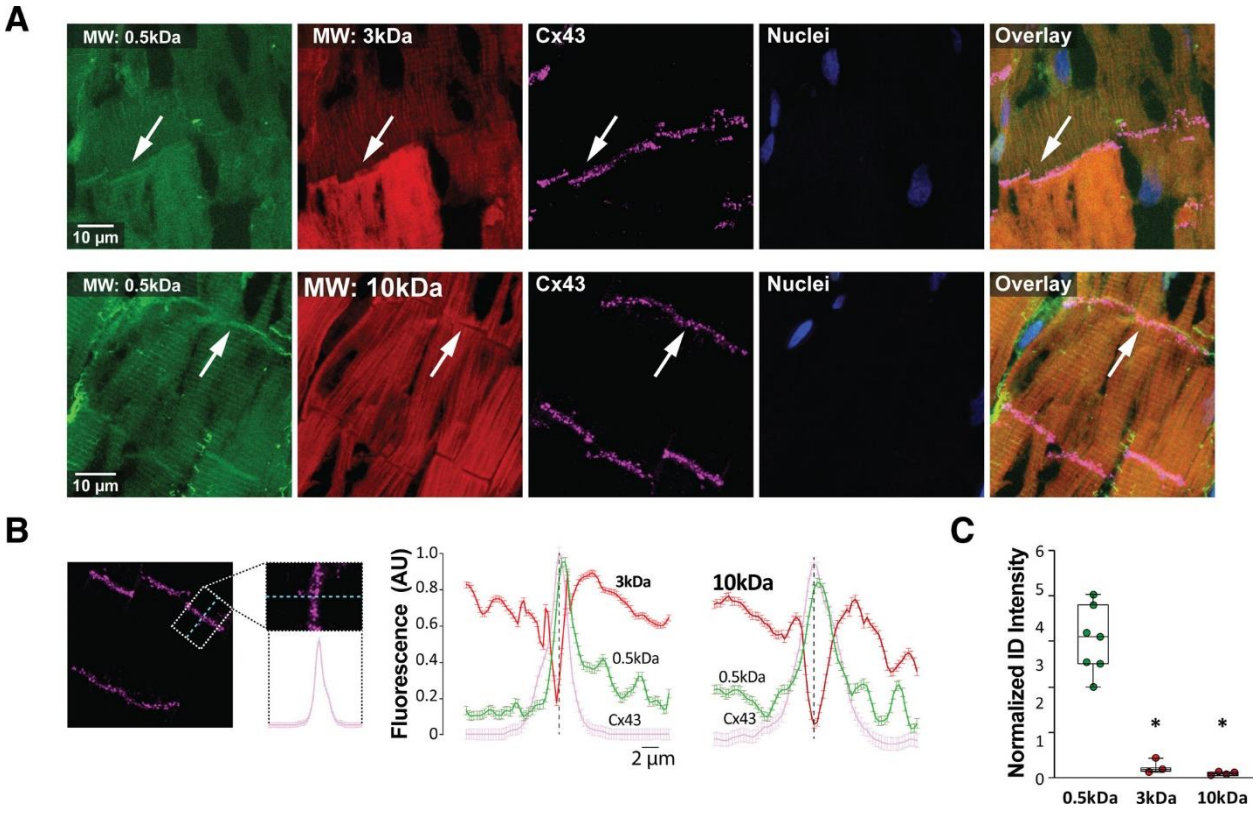

Figure 6. *Molecules smaller than 0.5kDa can permeate the intercalated disc.* **A.** Representative images of ventricular tissue slices perfused with 0.5, 3, and 10kDa fluorescent dyes. Panels demonstrate extracellular diffusion. Cx43 signal is used to identify the intercalated disc (ID), and nuclei are shown alone and with overlay of all signals. **B.** A region of interest is identified around the Cx43 ID signal and intensity of signal is averaged to identify the peak of the Cx43 signal. The same spatial averaging with 0.5, 3, and 10kDa signals demonstrates a dip in 3kDa and 10kDa signals with a peak in the 0.5kDa dye signal demonstrating the 0.5kDa dye permeates the ID, but the other two do not. **C.** The intensity of the dye fluorescent signal at the peak of the Cx43 signal is normalized to the intensity of signal beyond the ID to reveal that fluorescent signal intensities for 3kDa (n=3 images) and 10kDa (n=4 images) are significantly lower than for 0.5kDa (n=7 images) signal intensity. *p<0.05 relative to 0.5kDa, one way ANOVA with Dunnett's correction.

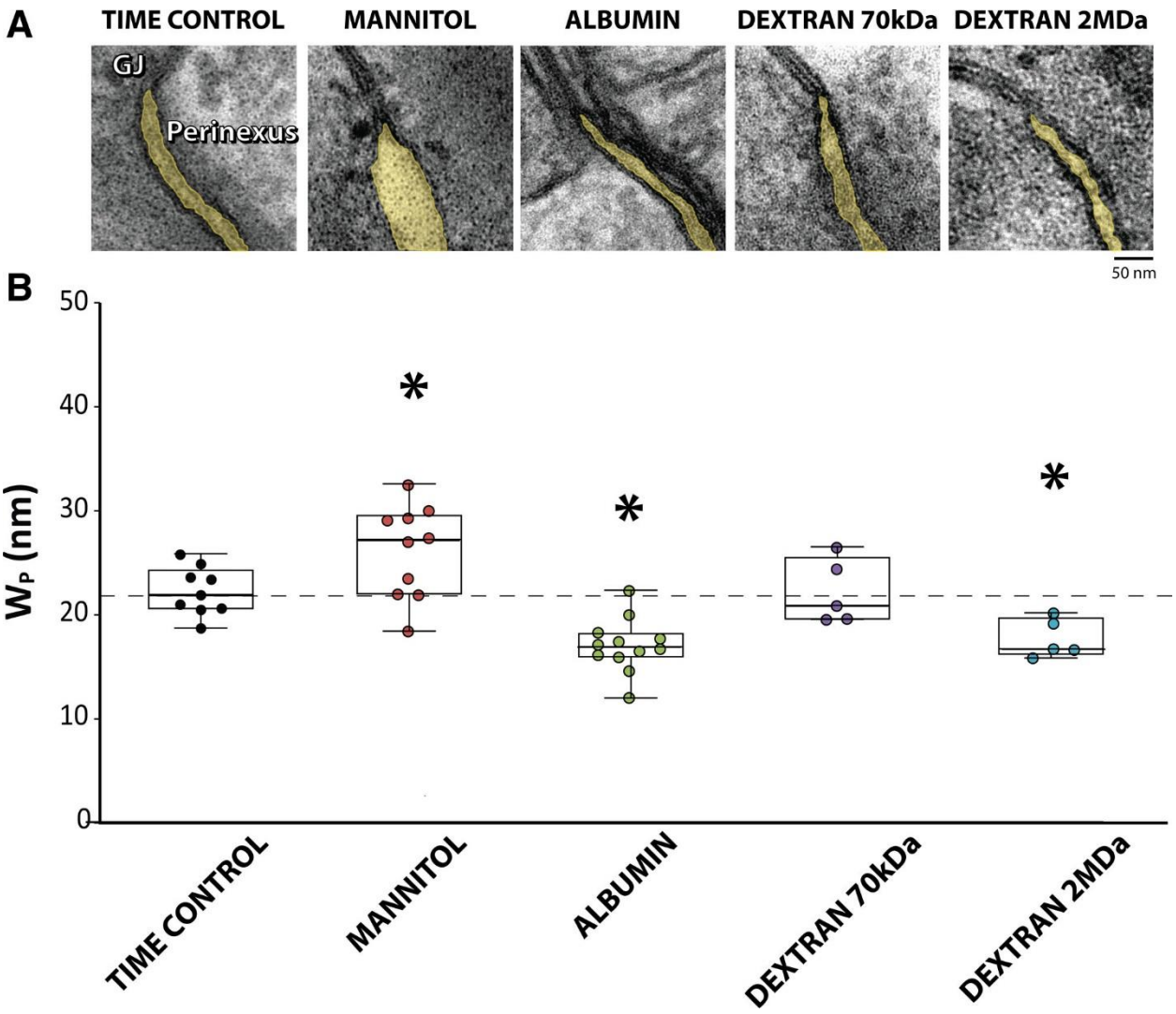

Figure 7. C*ardiac perinexal width inversely correlates with CV.* **A.** Representative TEM images of ventricular perinexi (shaded yellow) suggest osmotic agents differentially modulate perinexal width (W_P). **B.** Summary data reveal that relative to Time Control (N=9 hearts, n=140 images), Mannitol significantly increases (N=10 hearts, n=170 images), Albumin significantly decreases (N=12 hearts, n=135 images), Dextran 70k Da does not change (N=5 hearts, n=74 images), and Dextran 2MDa significantly decreases (N=5 hearts, n=75 images) W_P. Dashed line represents mean W_P for time control. *$p<0.05$, as evaluated with a generalized linear mixed effects model specifying a gamma distribution and identity link between samples collected from the same heart.

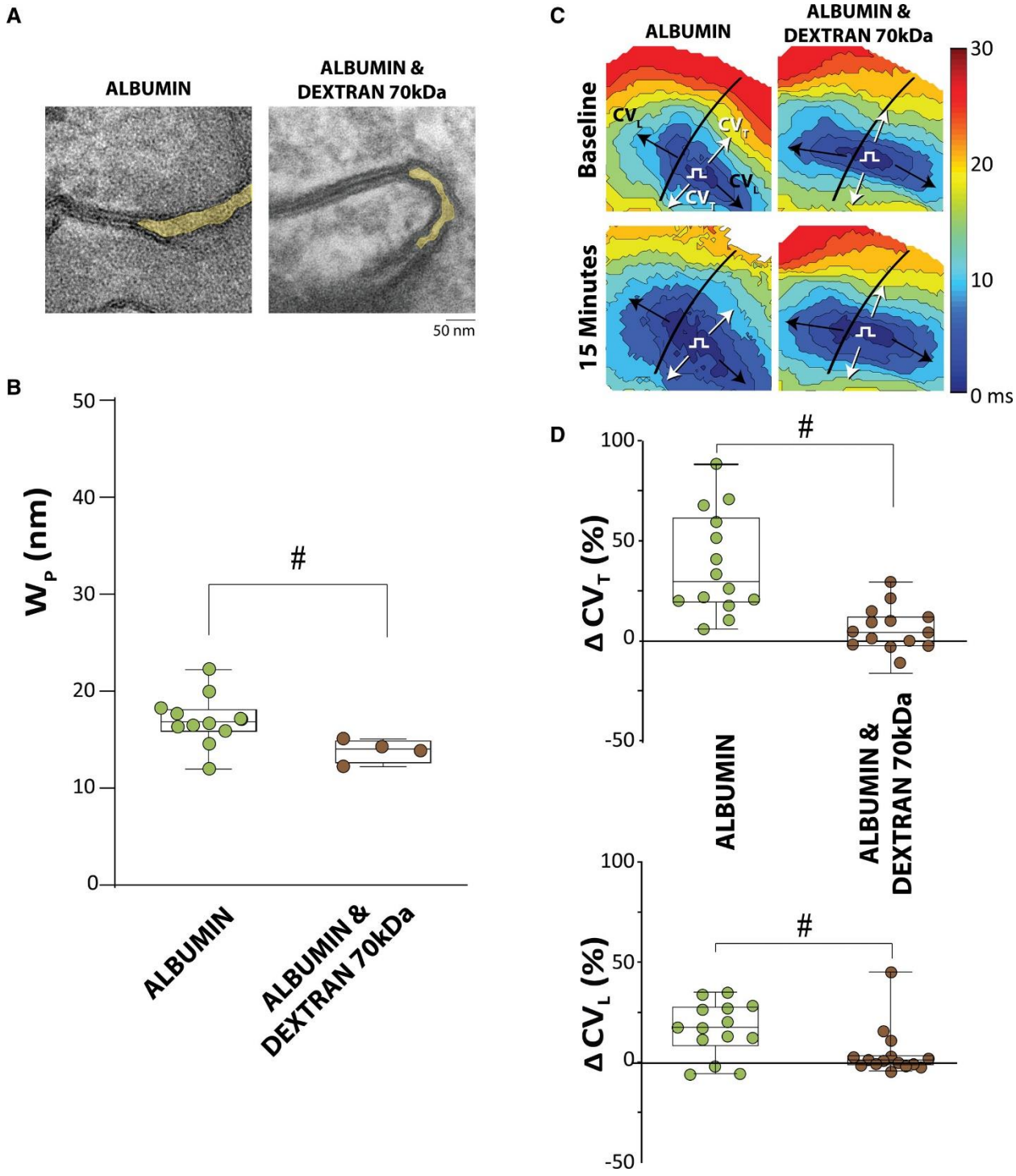
A
ALBUMIN
ALBUMIN &
DEXTRAN 70kDa
50 nm
B
W_P (nm)
50
40
30
20
10
0
#
ALBUMIN
ALBUMIN &
DEXTRAN 70kDa
C
ALBUMIN
ALBUMIN &
DEXTRAN 70kDa
Baseline
15 Minutes
CV_L
CV_T
30
20
10
0 ms
D
ΔCV_T (%)
100
50
0
-50
#
ALBUMIN
ALBUMIN &
DEXTRAN 70kDa
ΔCV_L (%)
100
50
0
-50
#

Figure 8. *Dextran 70kDa in the presence of albumin can narrow perinexal width and slow conduction relative to albumin alone.* **A.** Representative TEM images of ventricular perinexi (shaded yellow) and **B.** summary data reveal that simultaneous perfusion of Albumin and Dextran 70kDa (N=4 hearts, n=60 images) significantly narrows perinexal width (W_P) relative to Albumin alone (N=10 hearts, n=150 images), #p<0.05 relative to albumin, as evaluated with a generalized linear mixed effects model specifying a gamma distribution and identity link between samples collected from the same heart. **C.** Representative activation time isochrones. **D.** Summary data reveal that cardiac conduction is significantly slower in hearts treated with both Albumin and Dextran 70kDa (N=15 hearts) relative to albumin alone (N=14 hearts). #p<0.05, unpaired two-tailed t-test. Note CV and Wp data for albumin alone is replicated from figures 1 and 7 for comparison.

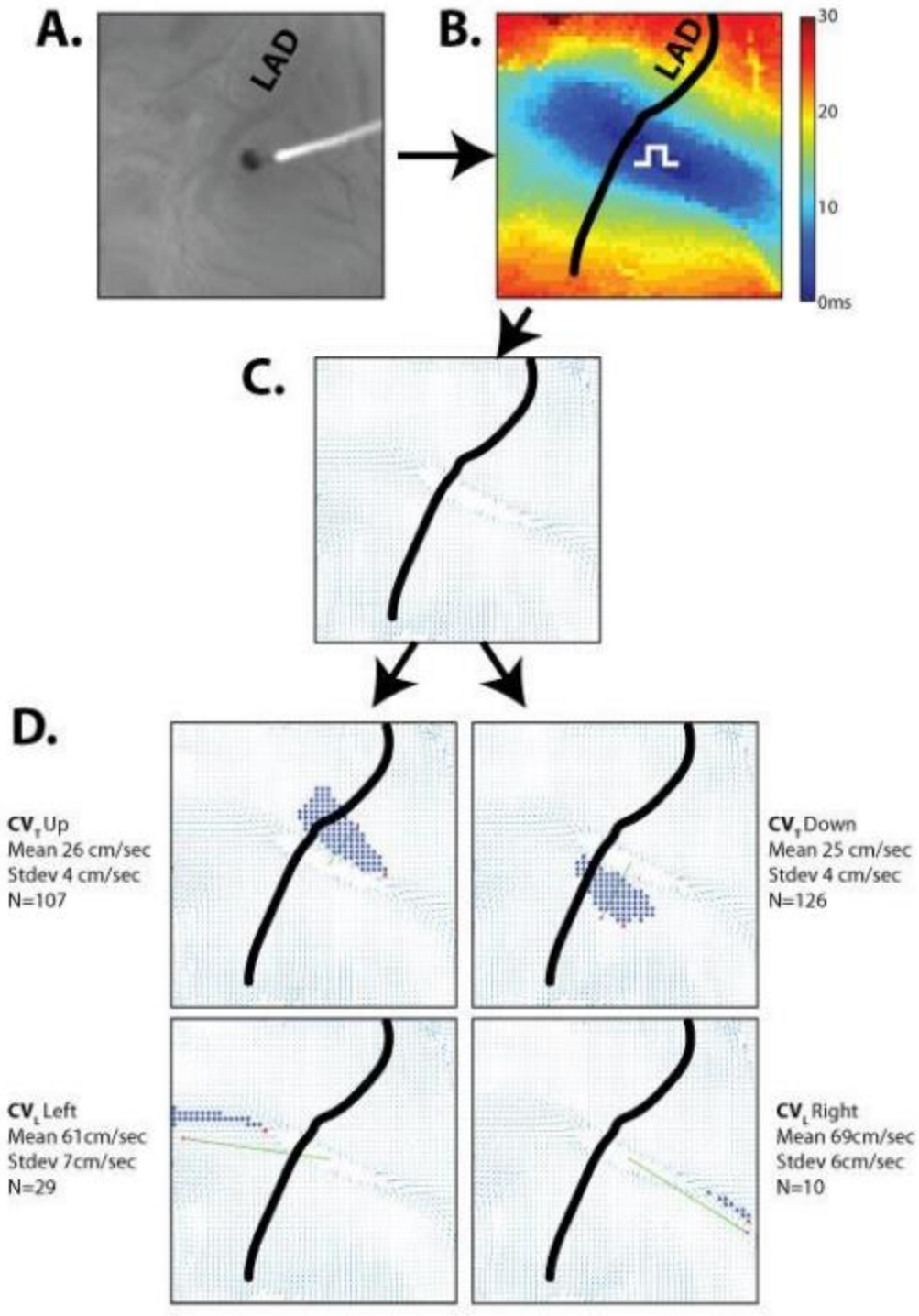

E.

Experiment	CV_T	CV_L
20230601b	25.5 cm/sec	65 cm/sec

Supplemental Figure S1. Conduction velocity from epicardial optical maps were analyzed as previously described in Entz, et. al, Frontiers in Physiology 2016. A. An image showing the placement of the pacing electrode and underlying anatomy in the imaging field. B. The maximum rate of optical action potential rise was calculated for each pixel to generate an Activation Time map. The black line represents the LAD and the approximate pacing electrode location is indicated by the white marker. C. Conduction velocity vectors were generated using an algorithm by Bayly, et. al, IEEETrans.Biomed.Eng 1998. A parabolic surface was fit to activation times with the following parameters: vectors were calculated over a 5x5 pixel area, activation times greater than 200ms past the time of stimulation were excluded, each vector required activation times from 12 of the 25 surrounding pixels, and vectors with CV values below 1 cm/sec and greater than 100 cm/sec were excluded. D. A user defined vector, shown as a green line, was drawn by selecting a starting point at the center of the pacing site and an end vector no more than 10 pixels away from the start point in the transverse direction. In the main text figures, these vectors are represented as black (longitudinal) or white (transverse) arrows. All vectors within 5 pixels of the user defined line with an angle within $\pm$ 16° were selected. If the average angle of the selected vectors was within 5°, then the first pixels immediately adjacent to the site of pacing were removed. The average transverse conduction velocity (CVT) (upper panels) from the selected vectors were calculated from CV in the transverse direction above the site of pacing (CVT Up) and below the site of pacing (CVT Down). The same approach was used to measure longitudinal conduction velocity (CVL) (lower panels) for the largest vectors to the left (CVL Left) and to the right of pacing (CVL Right). E. For a single optical map, CVT Up and Down were averaged to obtain a single CVT for a heart. CVL Left and Right were averaged to obtain a single CVL for a heart. Statistics were performed on these averaged values.

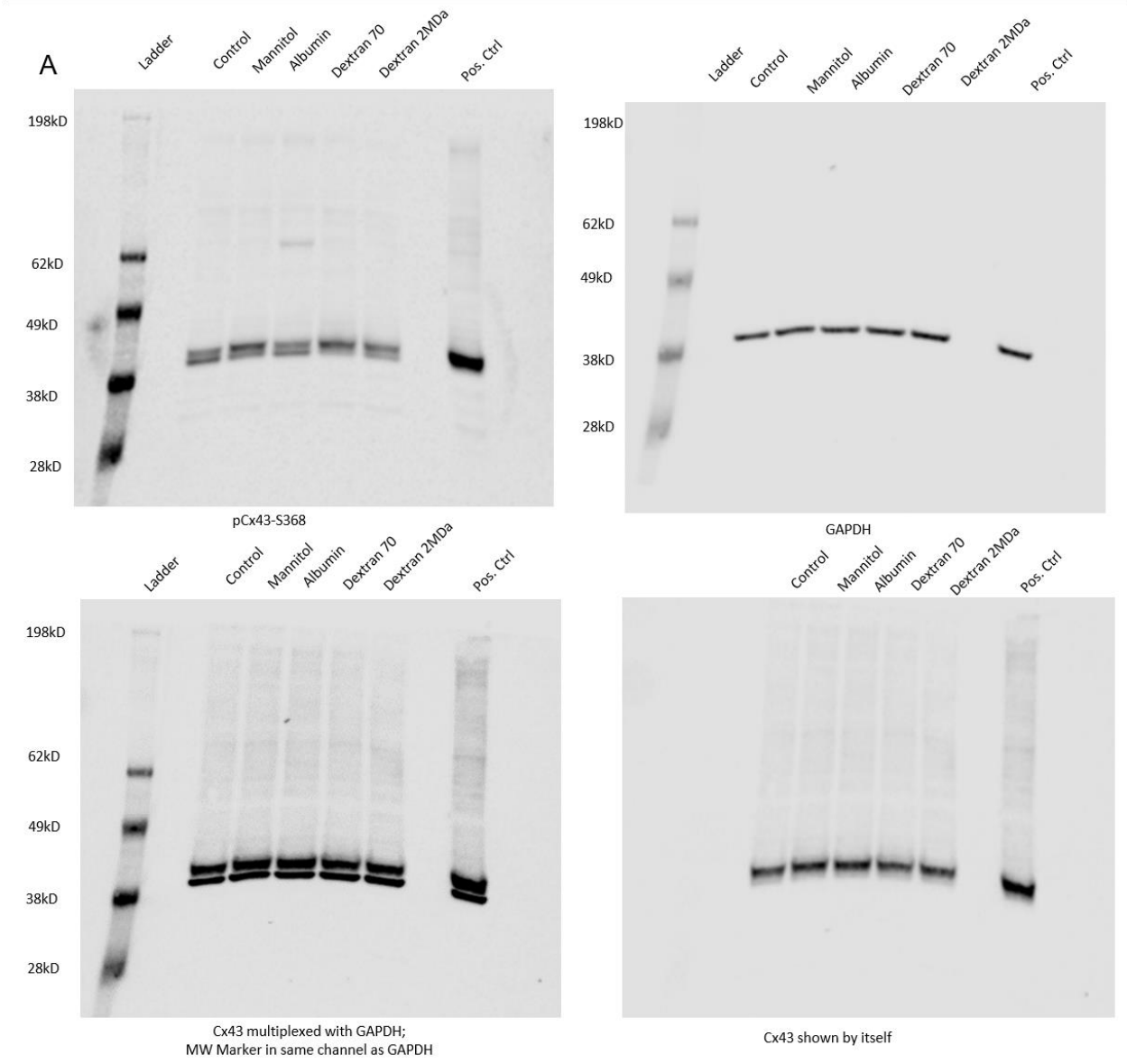
A
Ladder
Control
Mannitol
Albumin
Dextran 70
Dextran 2MDa
Pos. Ctrl
198kD
62kD
49kD
38kD
28kD
pCx43-S368
GAPDH
Cx43 multiplexed with GAPDH;
MW Marker in same channel as GAPDH
Cx43 shown by itself

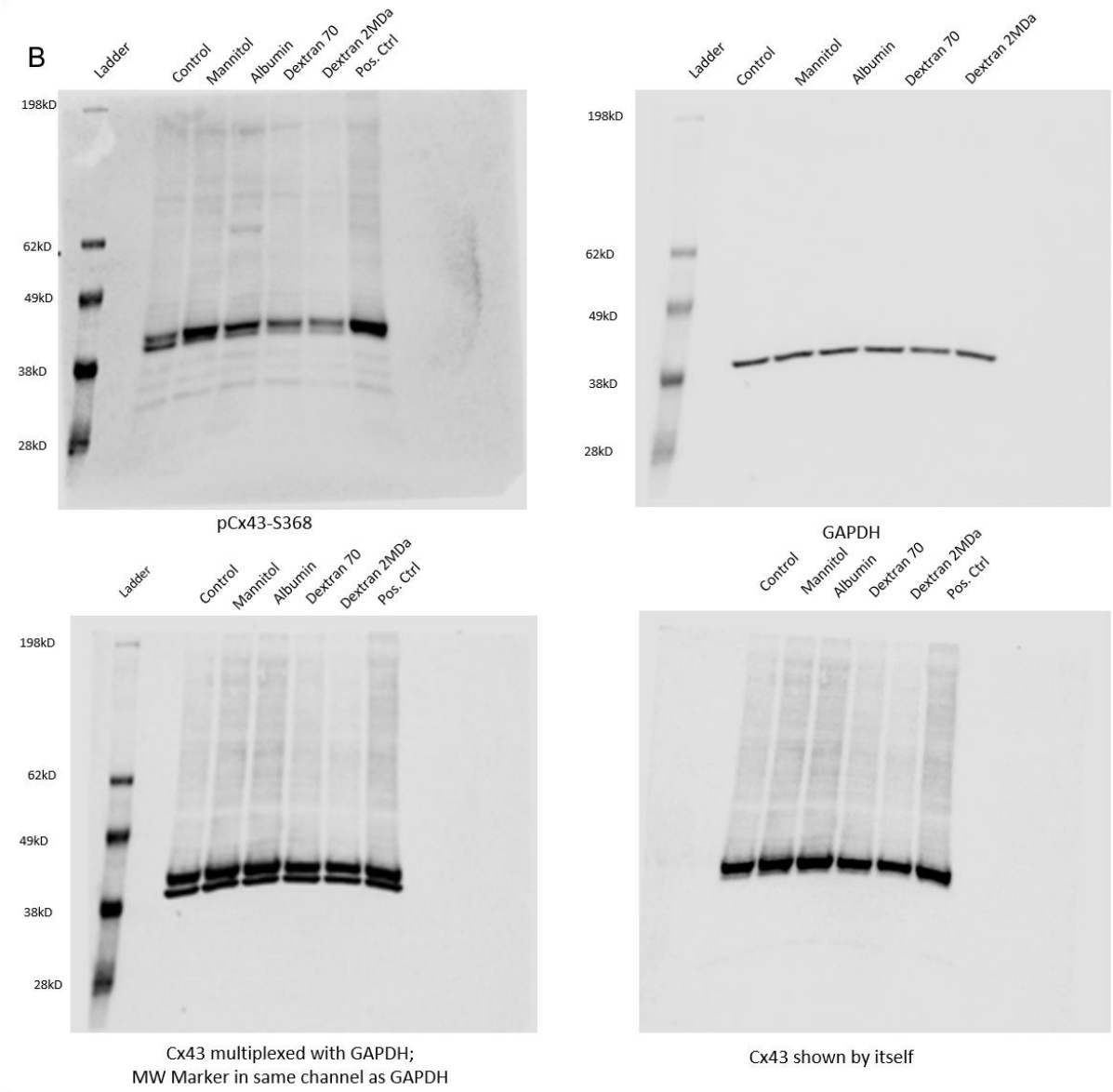
B
Ladder
Control
Mannitol
Albumin
Dextran 70
Dextran 2MDa
Pos. Ctrl
198kD
62kD
49kD
38kD
28kD
pCx43-S368
GAPDH
Cx43 multiplexed with GAPDH;
MW Marker in same channel as GAPDH
Cx43 shown by itself

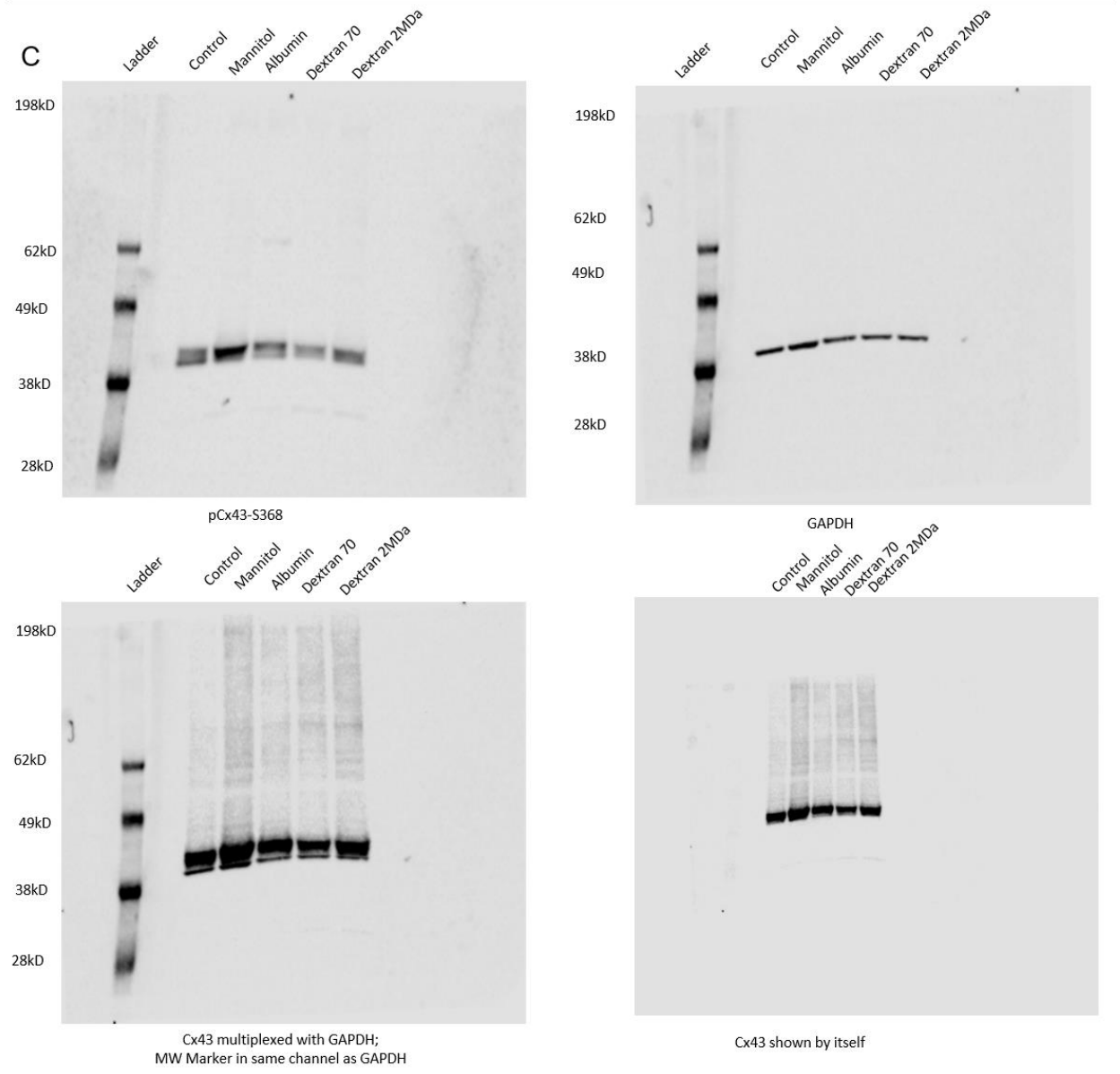

Supplemental Figure S2. Full unedited Western blot images. Blot A is used as the representative image for figure 3. Note that GAPDH and total Cx43 were multiplexed using different host species for the primary antibody and different fluorescent channels for the secondary antibodies. As such, the kDa markers are only visible in the GAPDH channel and the total florescence overlay. It does not appear when viewing the total Cx43 channel alone.

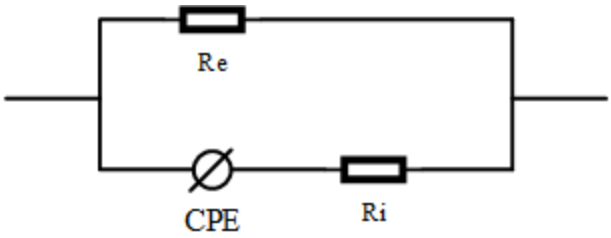

Supplemental Figure S3. Electrical model for Impedance Spectroscopy and the estimation of the extracellular resistance (R_e), a constant phase element (CPE) and an intracellular resistance (R_i). Values for impedance were measured over the frequency band of 200 Hz~1E6 Hz to estimate Re and CPE with units Ω and η respectively. The CPE reflects changes in transmembrane capacitance and resistance, as well as any changes in intercellular electrotonic coupling.

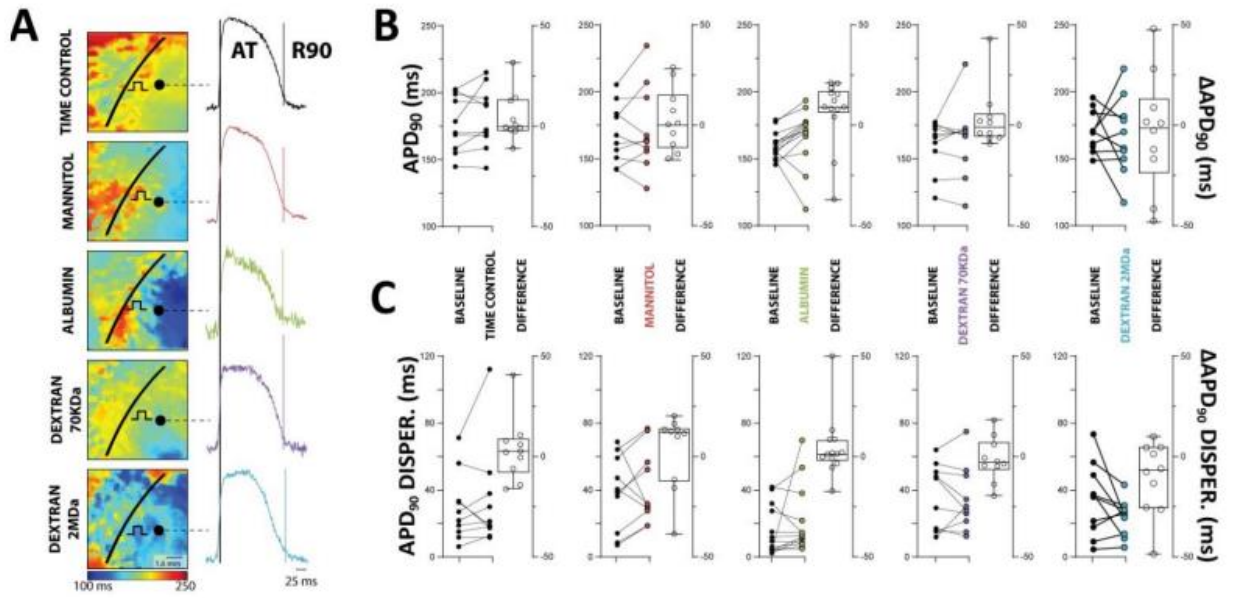

Supplemental Figure S4. Osmotic agents do not change epicardial action potential duration (APD) in whole-heart. A. Representative optical action potential duration (APD) maps and action potentials recorded from the anterior left ventricular epicardium. Π notes the approximate site of pacing in the field of view. APD90 is the difference of Repolarization at 90% (R90) and Activation Time (AT). B. Summary APD90 data reveal that APD90 is not significantly affected by the osmotic agents utilized in this study. P is not significant relative to pretreatment paired control, paired Student's t-test, nor are the magnitudes of the change different from that of the time control, p=n.s. ANOVA with multiple comparisons and Dunnett's multiple comparisons test and Kruskal-Wallis test with Dunn's multiple comparisons test. C. Furthermore, the maximum APD dispersion between quadrants of the imaging field are not significantly different from time control (Time Control N=10, Mannitol N=10, Albumin N=13, Dextran 70kDa N=10, Dextran 2MDa N=10. p=n.s. relative to Time Control, ordinary one-way ANOVA with Šídák's multiple comparisons test and Kruskal-Wallis test with Dunn's multiple comparisons test.

REFERENCES

1. Keener JP. The effects of gap junctions on propagation in myocardium: a modified cable theory. *Annals of the New York Academy of Sciences*. 1990;591:257-277. doi: 10.1111/j.1749-6632.1990.tb15094.x
2. Henriquez CS. Simulating the electrical behavior of cardiac tissue using the bidomain model. *Crit Rev Biomed Eng*. 1993;21:1-77.
3. Nadim F, Golowasch J. Signal transmission between gap-junctionally coupled passive cables is most effective at an optimal diameter. *J Neurophysiol*. 2006;95:3831-3843. doi: 10.1152/jn.00033.2006
4. Johnston BM, Coveney S, Chang ETY, Johnston PR, Clayton RH. Quantifying the effect of uncertainty in input parameters in a simplified bidomain model of partial thickness ischaemia. *Med Biol Eng Comput*. 2018;56:761-780. doi: 10.1007/s11517-017-1714-y
5. Kleber AG, Riegger CB. Electrical constants of arterially perfused rabbit papillary muscle. *The Journal of physiology*. 1987;385:307-324.
6. Fleischhauer J, Lehmann L, Kleber AG. Electrical resistances of interstitial and microvascular space as determinants of the extracellular electrical field and velocity of propagation in ventricular myocardium. *Circulation*. 1995;92:587-594.
7. Sperelakis N, McConnell K. Electric field interactions between closely abutting excitable cells. *IEEE engineering in medicine and biology magazine : the quarterly magazine of the Engineering in Medicine & Biology Society*. 2002;21:77-89.

8. Shibata Y, Yamamoto T. Freeze-fractrue studies of gap junctions in vertebrate cardiac muscle cells. *J Ultrastruct Res*. 1979;67:79-88. doi: 10.1016/s0022-5320(79)80020-9

9. Akester AR. Intercalated discs, nexuses, sarcoplasmic reticulum and transitional cells in the heart of the adult domestic fowl (Gallus gallus domesticus). *J Anat*. 1981;133:161-179.

10. Gutstein DE, Morley GE, Tamaddon H, Vaidya D, Schneider MD, Chen J, Chien KR, Stuhlmann H, Fishman GI. Conduction slowing and sudden arrhythmic death in mice with cardiac-restricted inactivation of connexin43. *Circulation research*. 2001;88:333-339.

11. Sperelakis N, Mann JE, Jr. Evaluation of electric field changes in the cleft between excitable cells. *J Theor Biol*. 1977;64:71-96. doi: 10.1016/0022-5193(77)90114-x

12. Kucera JP, Rohr S, Rudy Y. Localization of sodium channels in intercalated disks modulates cardiac conduction. *Circulation research*. 2002;91:1176-1182.

13. Mori Y, Fishman GI, Peskin CS. Ephaptic conduction in a cardiac strand model with 3D electrodiffusion. *Proceedings of the National Academy of Sciences of the United States of America*. 2008;105:6463-6468. doi: 10.1073/pnas.0801089105

14. Tsumoto K, Ashihara T, Haraguchi R, Nakazawa K, Kurachi Y. Roles of subcellular Na+ channel distributions in the mechanism of cardiac conduction. *Biophysical journal*. 2011;100:554-563. doi: 10.1016/j.bpj.2010.12.3716

15. Lin J, Keener JP. Ephaptic coupling in cardiac myocytes. *IEEE transactions on bio-medical engineering*. 2013;60:576-582. doi: 10.1109/TBME.2012.2226720

16. Weinberg SH. Ephaptic coupling rescues conduction failure in weakly coupled cardiac tissue with voltage-gated gap junctions. *Chaos*. 2017;27:093908. doi: 10.1063/1.4999602

17. Rhett JM, Ongstad EL, Jourdan J, Gourdie RG. Cx43 associates with Na(v)1.5 in the cardiomyocyte perinexus. *The Journal of membrane biology*. 2012;245:411-422. doi: 10.1007/s00232-012-9465-z

18. Hichri E, Abriel H, Kucera JP. Distribution of cardiac sodium channels in clusters potentiates ephaptic interactions in the intercalated disc. *The Journal of physiology*. 2018;596:563-589. doi: 10.1113/JP275351

19. Greer-Short A, George SA, Poelzing S, Weinberg SH. Revealing the Concealed Nature of Long-QT Type 3 Syndrome. *Circulation Arrhythmia and electrophysiology*. 2017;10:e004400. doi: 10.1161/CIRCEP.116.004400

20. Yao JA, Hussain W, Patel P, Peters NS, Boyden PA, Wit AL. Remodeling of gap junctional channel function in epicardial border zone of healing canine infarcts. *Circulation research*. 2003;92:437-443. doi: 10.1161/01.RES.0000059301.81035.06

21. Xing D, Kjolbye AL, Nielsen MS, Petersen JS, Harlow KW, Holstein-Rathlou NH, Martins JB. ZP123 increases gap junctional conductance and prevents reentrant ventricular tachycardia during myocardial ischemia in open chest dogs. *Journal of cardiovascular electrophysiology*. 2003;14:510-520. doi: 10.1046/j.1540-8167.2003.02329.x

22. Yao JA, Gutstein DE, Liu F, Fishman GI, Wit AL. Cell coupling between ventricular myocyte pairs from connexin43-deficient murine hearts. *Circulation research*. 2003;93:736-743. doi: 10.1161/01.RES.0000095977.66660.86

23. White RL, Spray DC, Campos de Carvalho AC, Wittenberg BA, Bennett MV. Some electrical and pharmacological properties of gap junctions between adult ventricular myocytes. *The American journal of physiology*. 1985;249:C447-455. doi: 10.1152/ajpcell.1985.249.5.C447

24. Weng S, Lauven M, Schaefer T, Polontchouk L, Grover R, Dhein S. Pharmacological modification of gap junction coupling by an antiarrhythmic peptide via protein kinase C activation. *FASEB journal : official publication of the Federation of American Societies for Experimental Biology*. 2002;16:1114-1116. doi: 10.1096/fj.01-0918fje

25. Kameyama M. Electrical coupling between ventricular paired cells isolated from guinea-pig heart. *The Journal of physiology*. 1983;336:345-357. doi: 10.1113/jphysiol.1983.sp014585

26. Noma A, Tsuboi N. Dependence of junctional conductance on proton, calcium and magnesium ions in cardiac paired cells of guinea-pig. *The Journal of physiology*. 1987;382:193-211.

27. Verheule S, van Kempen MJ, te Welscher PH, Kwak BR, Jongsma HJ. Characterization of gap junction channels in adult rabbit atrial and ventricular myocardium. *Circulation research*. 1997;80:673-681. doi: 10.1161/01.res.80.5.673

28. Veeraraghavan R, Salama ME, Poelzing S. Interstitial volume modulates the conduction velocity-gap junction relationship. *American journal of physiology Heart and circulatory physiology*. 2012;302:H278-286. doi: 10.1152/ajpheart.00868.2011

29. Veeraraghavan R, Lin J, Hoeker GS, Keener JP, Gourdie RG, Poelzing S. Sodium channels in the Cx43 gap junction perinexus may constitute a cardiac ephapse: an experimental and modeling study. *Pflugers Archiv : European journal of physiology*. 2015;467:2093-2105. doi: 10.1007/s00424-014-1675-z

30. George SA, Hoeker G, Calhoun PJ, Entz M, 2nd, Raisch TB, King DR, Khan M, Baker C, Gourdie RG, Smyth JW, et al. Modulating cardiac conduction during metabolic ischemia with perfusate sodium and calcium in guinea pig hearts. *American journal of physiology Heart and circulatory physiology*. 2019;316:H849-H861. doi: 10.1152/ajpheart.00083.2018

31. Veeraraghavan R, Hoeker GS, Alvarez-Laviada A, Hoagland D, Wan X, King DR, Sanchez-Alonso J, Chen C, Jourdan J, Isom LL, et al. The adhesion function of the sodium channel beta subunit (beta1) contributes to cardiac action potential propagation. *Elife*. 2018;7. doi: 10.7554/eLife.37610

32. Entz M, 2nd, King DR, Poelzing S. Design and validation of a tissue bath 3-D printed with PLA for optically mapping suspended whole heart preparations. *American journal of physiology Heart and circulatory physiology*. 2017;313:H1190-H1198. doi: 10.1152/ajpheart.00150.2017

33. Dreher MR, Liu W, Michelich CR, Dewhirst MW, Yuan F, Chilkoti A. Tumor vascular permeability, accumulation, and penetration of macromolecular drug carriers. *J Natl Cancer Inst*. 2006;98:335-344. doi: 10.1093/jnci/djj070

34. George SA, Poelzing S. Cardiac conduction in isolated hearts of genetically modified mice - Connexin43 and salts. *Progress in biophysics and molecular biology*. 2015. doi: 10.1016/j.pbiomolbio.2015.11.004

35. George SA, Bonakdar M, Zeitz M, Davalos R, Smyth JW, Poelzing S. Extracellular Sodium Dependence of the Conduction Velocity-Calcium Relationship: Evidence of Ephaptic Self-Attenuation. *American journal of physiology Heart and circulatory physiology*. 2016:ajpheart 00857 02015. doi: 10.1152/ajpheart.00857.2015

36. Entz M, 2nd, George SA, Zeitz MJ, Raisch T, Smyth JW, Poelzing S. Heart Rate and Extracellular Sodium and Potassium Modulation of Gap Junction Mediated Conduction in Guinea Pigs. *Frontiers in physiology*. 2016;7:16. doi: 10.3389/fphys.2016.00016

37. Veeraraghavan R, Lin J, Keener JP, Gourdie R, Poelzing S. Potassium channels in the Cx43 gap junction perinexus modulate ephaptic coupling: an experimental and modeling study. *Pflugers Archiv : European journal of physiology*. 2016;468:1651-1661. doi: 10.1007/s00424-016-1861-2

38. Burton FL, Cobbe SM. Dispersion of ventricular repolarization and refractory period. *Cardiovascular research*. 2001;50:10-23. doi: 10.1016/s0008-6363(01)00197-3

39. Smyth JW, Hong TT, Gao D, Vogan JM, Jensen BC, Fong TS, Simpson PC, Stainier DY, Chi NC, Shaw RM. Limited forward trafficking of connexin 43 reduces cell-cell coupling in stressed human and mouse myocardium. *The Journal of clinical investigation*. 2010;120:266-279. doi: 10.1172/JCI39740

40. Solan JL, Fry MD, TenBroek EM, Lampe PD. Connexin43 phosphorylation at S368 is acute during S and G2/M and in response to protein kinase C activation. *J Cell Sci*. 2003;116:2203-2211. doi: 10.1242/jcs.00428

41. Bohuslavova R, Kolar F, Sedmera D, Skvorova L, Papousek F, Neckar J, Pavlinkova G. Partial deficiency of HIF-1alpha stimulates pathological cardiac changes in streptozotocin-induced diabetic mice. *BMC Endocr Disord*. 2014;14:11. doi: 10.1186/1472-6823-14-11

42. Decrock E, De Vuyst E, Vinken M, Van Moorhem M, Vranckx K, Wang N, Van Laeken L, De Bock M, D'Herde K, Lai CP, et al. Connexin 43 hemichannels contribute to the propagation of apoptotic cell death in a rat C6 glioma cell model. *Cell Death Differ*. 2009;16:151-163. doi: 10.1038/cdd.2008.138

43. Yum SW, Zhang J, Valiunas V, Kanaporis G, Brink PR, White TW, Scherer SS. Human connexin26 and connexin30 form functional heteromeric and heterotypic channels. *American journal of physiology Cell physiology*. 2007;293:C1032-1048. doi: 10.1152/ajpcell.00011.2007

44. Rhett JM, Jourdan J, Gourdie RG. Connexin 43 connexon to gap junction transition is regulated by zonula occludens-1. *Molecular biology of the cell*. 2011;22:1516-1528. doi: 10.1091/mbc.E10-06-0548

45. Wan X, Laurita KR, Pruvot EJ, Rosenbaum DS. Molecular correlates of repolarization alternans in cardiac myocytes. *Journal of molecular and cellular cardiology*. 2005;39:419-428. doi: 10.1016/j.yjmcc.2005.06.004

46. Zhao Y, Liu H, Bhonsle SP, Wang Y, Davalos RV, Yao C. Ablation outcome of irreversible electroporation on potato monitored by impedance spectrum under multi-electrode system. *Biomed Eng Online*. 2018;17:126. doi: 10.1186/s12938-018-0562-9

47. Bonakdar M, Latouche EL, Mahajan RL, Davalos RV. The Feasibility of a Smart Surgical Probe for Verification of IRE Treatments Using Electrical Impedance Spectroscopy. *IEEE transactions on bio-medical engineering*. 2015;62:2674-2684. doi: 10.1109/TBME.2015.2441636

48. Raisch T, Khan M, Poelzing S. Quantifying Intermembrane Distances with Serial Image Dilations. *Journal of visualized experiments : JoVE*. 2018. doi: 10.3791/58311

49. Raisch TB, Yanoff MS, Larsen TR, Farooqui MA, King DR, Veeraraghavan R, Gourdie RG, Baker JW, Arnold WS, AlMahameed ST, et al. Intercalated Disk Extracellular Nanodomain Expansion in Patients With Atrial Fibrillation. *Frontiers in physiology*. 2018;9:398. doi: 10.3389/fphys.2018.00398

50. Lampe PD, TenBroek EM, Burt JM, Kurata WE, Johnson RG, Lau AF. Phosphorylation of connexin43 on serine368 by protein kinase C regulates gap junctional communication. *The Journal of cell biology*. 2000;149:1503-1512. doi: 10.1083/jcb.149.7.1503

51. Ek-Vitorin JF, King TJ, Heyman NS, Lampe PD, Burt JM. Selectivity of connexin 43 channels is regulated through protein kinase C-dependent phosphorylation. *Circulation research*. 2006;98:1498-1505. doi: 10.1161/01.RES.0000227572.45891.2c

52. Solan JL, Lampe PD. Connexin43 phosphorylation: structural changes and biological effects. *The Biochemical journal*. 2009;419:261-272. doi: 10.1042/BJ20082319

53. De Vuyst E, De Bock M, Decrock E, Van Moorhem M, Naus C, Mabilde C, Leybaert L. In situ bipolar electroporation for localized cell loading with reporter dyes and investigating gap junctional coupling. *Biophysical journal*. 2008;94:469-479. doi: 10.1529/biophysj.107.109470

54. Stiles DK, Oakley BA. Four-point electrode measurement of impedance in the vicinity of bovine aorta for quasi-static frequencies. *Bioelectromagnetics*. 2005;26:54-58. doi: 10.1002/bem.20074

55. Ivanovic E, Kucera JP. Localization of Na(+) channel clusters in narrowed perinexi of gap junctions enhances cardiac impulse transmission via ephaptic coupling: a model study. *The Journal of physiology*. 2021;599:4779-4811. doi: 10.1113/JP282105

56. Shaw RM, Rudy Y. Ionic mechanisms of propagation in cardiac tissue. Roles of the sodium and L-type calcium currents during reduced excitability and decreased gap junction coupling. *Circulation research*. 1997;81:727-741.

57. de Groot JR, Veenstra T, Verkerk AO, Wilders R, Smits JP, Wilms-Schopman FJ, Wiegerinck RF, Bourier J, Belterman CN, Coronel R, et al. Conduction

slowing by the gap junctional uncoupler carbenoxolone. *Cardiovascular research*. 2003;60:288-297.

58. Veeraraghavan R, Gourdie RG, Poelzing S. Mechanisms of cardiac conduction: a history of revisions. *American journal of physiology Heart and circulatory physiology*. 2014;306:H619-627. doi: 10.1152/ajpheart.00760.2013

59. Kleber AG, Saffitz JE. Role of the intercalated disc in cardiac propagation and arrhythmogenesis. *Frontiers in physiology*. 2014;5:404. doi: 10.3389/fphys.2014.00404

60. Shaw RM, Fay AJ, Puthenveedu MA, von Zastrow M, Jan YN, Jan LY. Microtubule plus-end-tracking proteins target gap junctions directly from the cell interior to adherens junctions. *Cell*. 2007;128:547-560. doi: 10.1016/j.cell.2006.12.037

61. Neu JC, Krassowska W. Homogenization of syncytial tissues. *Crit Rev Biomed Eng*. 1993;21:137-199.

62. Pourtaheri N, Ying W, Kim J, Henriquez C. Thresholds for Transverse Stimulation: Fiber Bundles in a Uniform Field. *IEEE transactions on neural systems and rehabilitation engineering : a publication of the IEEE Engineering in Medicine and Biology Society*. 2021;PP. doi: 10.1109/TNSRE.2009.2039600

63. George SA, Calhoun PJ, Gourdie RG, Smyth JW, Poelzing S. TNFalpha Modulates Cardiac Conduction by Altering Electrical Coupling between Myocytes. *Frontiers in physiology*. 2017;8:334. doi: 10.3389/fphys.2017.00334

64. Lin J, Keener JP. Modeling electrical activity of myocardial cells incorporating the effects of ephaptic coupling. *Proceedings of the National Academy of Sciences of*

the United States of America. 2010;107:20935-20940. doi: 10.1073/pnas.1010154107

65. Moise N, Struckman HL, Dagher C, Veeraraghavan R, Weinberg SH. Intercalated disk nanoscale structure regulates cardiac conduction. *The Journal of general physiology*. 2021;153. doi: 10.1085/jgp.202112897

66. Nowak MB, Greer-Short A, Wan X, Wu X, Deschenes I, Weinberg SH, Poelzing S. Intercellular Sodium Regulates Repolarization in Cardiac Tissue with Sodium Channel Gain of Function. *Biophysical journal*. 2020;118:2829-2843. doi: 10.1016/j.bpj.2020.04.014

67. Nowak MB, Poelzing S, Weinberg SH. Mechanisms underlying age-associated manifestation of cardiac sodium channel gain-of-function. *Journal of molecular and cellular cardiology*. 2020;153:60-71. doi: 10.1016/j.yjmcc.2020.12.008

68. King DR, Entz M, 2nd, Blair GA, Crandell I, Hanlon AL, Lin J, Hoeker GS, Poelzing S. The conduction velocity-potassium relationship in the heart is modulated by sodium and calcium. *Pflugers Archiv : European journal of physiology*. 2021;473:557-571. doi: 10.1007/s00424-021-02537-y

69. Nowak MB, Veeraraghavan R, Poelzing S, Weinberg SH. Cellular Size, Gap Junctions, and Sodium Channel Properties Govern Developmental Changes in Cardiac Conduction. *Frontiers in physiology*. 2021;12:731025. doi: 10.3389/fphys.2021.731025

70. Boyett MR, Frampton JE, Kirby MS. The length, width and volume of isolated rat and ferret ventricular myocytes during twitch contractions and changes in

osmotic strength. *Exp Physiol*. 1991;76:259-270. doi: 10.1113/expphysiol.1991.sp003492

71. Morell M, Burgos JI, Gonano LA, Vila Petroff M. AMPK-dependent nitric oxide release provides contractile support during hyperosmotic stress. *Basic research in cardiology*. 2018;113:7. doi: 10.1007/s00395-017-0665-7

72. Veeraraghavan R, Poelzing S. Mechanisms underlying increased right ventricular conduction sensitivity to flecainide challenge. *Cardiovascular research*. 2008;77:749-756. doi: 10.1093/cvr/cvm090

73. Burton RAB, Rog-Zielinska EA, Corbett AD, Peyronnet R, Bodi I, Fink M, Sheldon J, Hoenger A, Calaghan SC, Bub G, et al. Caveolae in Rabbit Ventricular Myocytes: Distribution and Dynamic Diminution after Cell Isolation. *Biophysical journal*. 2017;113:1047-1059. doi: 10.1016/j.bpj.2017.07.026

74. Quinlan GJ, Martin GS, Evans TW. Albumin: biochemical properties and therapeutic potential. *Hepatology*. 2005;41:1211-1219. doi: 10.1002/hep.20720

75. Muizelaar JP, Lutz HA, 3rd, Becker DP. Effect of mannitol on ICP and CBF and correlation with pressure autoregulation in severely head-injured patients. *J Neurosurg*. 1984;61:700-706. doi: 10.3171/jns.1984.61.4.0700

76. Knapp JM. Hyperosmolar therapy in the treatment of severe head injury in children: mannitol and hypertonic saline. *AACN Clin Issues*. 2005;16:199-211. doi: 10.1097/00044067-200504000-00011

77. Gombocz K, Beledi A, Alotti N, Kecskes G, Gabor V, Bogar L, Koszegi T, Garai J. Influence of dextran-70 on systemic inflammatory response and myocardial

ischaemia-reperfusion following cardiac operations. *Crit Care*. 2007;11:R87. doi: 10.1186/cc6095

78. Zhang B, Wieslander JB. Dextran's antithrombotic properties in small arteries are not altered by low-molecular-weight heparin or the fibrinolytic inhibitor tranexamic acid: an experimental study. *Microsurgery*. 1993;14:289-295. doi: 10.1002/micr.1920140415

79. Togashi D, Ryder A, Mc Mahon D, Dunne P, McManus J. *Fluorescence study of bovine serum albumin and Ti and Sn oxide nanoparticles interactions*. SPIE; 2007.

80. Gautam S, Gupta MN. Solid state fluorescence of proteins in high throughput mode and its applications. *F1000Res*. 2013;2:82. doi: 10.12688/f1000research.2-82.v2

81. Hyatt CJ, Mironov SF, Wellner M, Berenfeld O, Popp AK, Weitz DA, Jalife J, Pertsov AM. Synthesis of voltage-sensitive fluorescence signals from three-dimensional myocardial activation patterns. *Biophysical journal*. 2003;85:2673-2683. doi: 10.1016/S0006-3495(03)74690-6

82. Bray MA, Wikswo JP. Examination of optical depth effects on fluorescence imaging of cardiac propagation. *Biophysical journal*. 2003;85:4134-4145. doi: 10.1016/S0006-3495(03)74825-5

83. Hyatt CJ, Mironov SF, Vetter FJ, Zemlin CW, Pertsov AM. Optical action potential upstroke morphology reveals near-surface transmural propagation direction. *Circulation research*. 2005;97:277-284. doi: 10.1161/01.RES.0000176022.74579.47

84. Bishop MJ, Rodriguez B, Eason J, Whiteley JP, Trayanova N, Gavaghan DJ. Synthesis of voltage-sensitive optical signals: application to panoramic optical mapping. *Biophysical journal*. 2006;90:2938-2945. doi: 10.1529/biophysj.105.076505

85. Taccardi B, Macchi E, Lux RL, Ershler PR, Spaggiari S, Baruffi S, Vyhmeister Y. Effect of myocardial fiber direction on epicardial potentials. *Circulation*. 1994;90:3076-3090. doi: 10.1161/01.cir.90.6.3076

86. Vetter FJ, Simons SB, Mironov S, Hyatt CJ, Pertsov AM. Epicardial fiber organization in swine right ventricle and its impact on propagation. *Circulation research*. 2005;96:244-251. doi: 10.1161/01.RES.0000153979.71859.e7

87. Veeraraghavan R, Larsen AP, Torres NS, Grunnet M, Poelzing S. Potassium channel activators differentially modulate the effect of sodium channel blockade on cardiac conduction. *Acta Physiol (Oxf)*. 2013;207:280-289. doi: 10.1111/j.1748-1716.2012.02481.x

88. Ebihara L, Mathias RT. Linear impedance studies of voltage-dependent conductances in tissue cultured chick heart cells. *Biophysical journal*. 1985;48:449-460. doi: 10.1016/S0006-3495(85)83800-5

89. Mathias RT. Effect of tortuous extracellular pathways on resistance measurements. *Biophysical journal*. 1983;42:55-59. doi: 10.1016/S0006-3495(83)84368-9

90. Xue J, Yan X, Yang Y, Chen M, Wu L, Gou Z, Sun Z, Talabieke S, Zheng Y, Luo D. Connexin 43 dephosphorylation contributes to arrhythmias and cardiomyocyte

apoptosis in ischemia/reperfusion hearts. *Basic research in cardiology*. 2019;114:40. doi: 10.1007/s00395-019-0748-8

Chapter 3

Sudden Cardiac Death, Arrhythmia, and Sodium Channel Loss of Function

Flecainide Sensitizes Conduction to Hyponatremia Through an Ephaptic Mechanism

William Adams & Steven Poelzing

This manuscript is being prepared for submission for review & publication

ABSTRACT

Background: There is both clinical and basic science data which suggest that channel loss of function (LoF), often through the use of ubiquitous sodium channel inhibitors such as tricyclic anti-depressants, some recreational drugs, and importantly, class 1c anti-arrhythmics, will sensitize conduction to distribution by hyponatremia, but the mechanism driving this sensitivity is unknown.. A recent study from our lab demonstrated that conduction is more impaired in the sodium channel haploinsufficient Scn5a/- mouse at low perfusate sodium concentrations ($[Na^+]$) than in wildtype mice and that reducing ephaptic coupling (EpC) rescues this impairment. We tested the hypotheses that changes in EpC, intracellular calcium accumulation, and outward potassium currents would modulate this CV sensitivity to $[Na^+]$.

Methods: Optical maps were made from Langendorff-perfused guinea pig hearts, and conduction velocity (CV) was measured at either 145 mM or 120 mM $[Na^+]$, under conditions of nominal channel function, with flecainide alone, and with the combination of flecainide and one of the following: EpC uncouplers mannitol or LQLEED peptide, NCX inhibitor SEA0400, NKA inhibitor ouabain, I_{Kr} blocker E4031, or I_{K1} blocker $BaCl_2$. The percentage change caused by lowering sodium was compared across all treatment groups.

Results: Flecainide induced channel LoF resulted in increased CV sensitivity to low $[Na^+]$. EpC uncoupling with mannitol or LQLEED significantly attenuated [Na+] sensitivity. Altering intracellular calcium handling with SEA0400 or ouabain had no significant effect on the $[Na^+]$ sensitivity. Blocking I_{Kr} with E4031, or I_{K1} with $BaCl_2$ both attenuated [Na+] sensitivity.

Conclusions: Sodium channel LoF sensitizes CV to changes in $[Na^+]$, through an EpC mediated mechanism, and this sensitivity is modulated by changes in potassium currents.

INTRODUCTION

Sodium channel blockers encompass a wide range of drug, including anti-epileptics, tricyclic anti-depressants, class 1c anti-arrhythmic, certain recreationally used drugs such as cocaine, and even some topic anesthetic such as lidocaine. These drugs can often have cardiac side effects at high doses. In one case report a patient presented with the characteristic ECG of Bragada syndrome, a cardiac disorder frequently associated with genetic sodium (Na^+) channel loss of function (LoF), from a tricyclic antidepressant overdose.[1] Ironically, special care must be taken to monitor patients on class 1c anti-arrhythmics, such as flecainide, for adverse cardiac side effects.[2]

Although flecainide is used as an anti-arrhythmic to reduce atrial excitability, it is used with caution due to its potentially pro-arrhythmic slowing of ventricular conduction velocity (CV).[2] This CV slowing has been shown to likely underlie the increase in mortality observed in the CAST Trials.[3, 4] Further, it is a drug with a narrow therapeutic window. As little as twice the minimum therapeutic dose in some patients can be enough to cause serious adverse cardiac side effects in others, including syncope, weakness, bradycardia, and in more serious cases bundle branch block and sinus pause.[5] As a result, it is important to carefully monitor patients being treated with this anti-arrhythmic drug to ensure both safe and effective treatment.

Exploring the clinical literature surrounding reports of flecainide overdose reveals an interesting pattern. Interspersed among typical case reports of both accidental and intentional overdoses are a number of cases where flecainide toxicity is precipitated by electrolyte imbalances, notably, hyponatremia. One example is the 2007 case of a 78 year old woman on a very low dose of flecainide (50 mg 2x/day) who developed symptomatic bradycardia and severe QRS widening, both classic symptoms of flecainide toxicity, that progressively worsened in combination with worsening hyponatremia (126 mmol/L), which was driven by chronic kidney disease and treatment with hydrochlorothiazide. Resolving the hyponatremia with sodium

bicarbonate treatment alone resolved the cardiac symptoms.[6] Another example is the 2019 case of a patient who, after two months on a well tolerated 100 mg 2/day dose of flecainide presented with syncope and notable QRS widening. It was determined that this episode was likely precipitated by bendroflumethiazide treatment for hypertension, resulting in hyponatremic serum Na^+ (118 mmol/L) and hypokalemic serum potassium (K^+) (2.7 mmol/L).[7] These and other studies[8-11] suggest that serum Na^+ levels play an important role in the impact of strong Na^+ channel blockers. Using buffered hypertonic saline solutions to treat overdose of strong Na^+ channel blockers, like flecainide, is the standard of care[9, 12] dating back to early experimental work in 1959,[13, 14] and further experimental work suggests that some portion of the benefit comes directly from the elevation of Na^+ levels.[15, 16] Despite this combination of clinical and experimental evidence, it remains poorly understood exactly how hyponatremia interacts with channel LoF, such as from strong Na^+ channel blockers, and what impact that has on functional parameters such as CV.

Recent work in an Scn5a/- mouse, a Brugada Syndrome model that is haploinsufficient for the main cardiac voltage gated Na^+ channel, showed that lowering perfusate sodium concentration ($[Na^+]_)$ disrupts conduction more in the Na^+ channel LoF mice than it does in their wild type counterparts. Further, that same study suggests that mannitol treatment may rescue some of this conduction impairment in the LoF mutants.[17] That this occurs in a genetic model suggests that this sensitization of conduction to hyponatremia may be a more fundamental aspect of reduced Na^+ channel function than just a drug-channel interaction. Three major pathways that modulate CV are ephaptic coupling, calcium accumulation, and repolarizing K^+ currents. This study aims to determine how these pathways may modulate conduction sensitivity to hyponatremia as induced by flecainide treatment.

MATERIALS AND METHODS

All animal research for this study was carried out in accordance with the principles of the Basel Declaration and recommendations of the Guide for the Care and Use of Laboratory Animals, National Research Council. The protocol was approved by the Institutional Animal Care and Use Committee (IACUC) at Virginia Polytechnic Institute and State University (Protocol #21-09

Guinea Pig Langendorff Preparation

Adult Hartley guinea pigs of both sexes were acquired from Hilltop Lab Animals, Inc. (13-15 months; 900-1200 grams). Animals were anesthetized by isoflurane inhalation and isoflurane was maintained until the completion of the thoracotomy. Hearts were removed and cannulated in oxygenated constant flow Langendorff preparation as previously described[18] in solution containing either 145 mM or 120 mM [Na^+]. The composition of the 145 mM [Na^+] perfusion solution was based off of previously published solution, and in brief contained (in mmol/L): 1.25 CaCl2•2H2O, 140 NaCl, 4.5 KCl, 10 Dextrose, 1 MgCl2•6H2O, 10 HEPES, 5.5 mL/L of 1N NaOH. The 120 mM [Na^+] solution was identical except that a reduced 114 mmol/L NaCl was used. Both solutions were equilibrated to a pH of 7.40 at 37°C using 1N NaOH or 1N HCl to titrate pH. Hearts were given at least 15 minutes perfusion to stabilize before being loaded with 7.5 μM di-4-ANEPPS, followed by a 15-minute washout period during which the hearts were electromechanically uncoupled with 10 μM blebbistatin. At the end of this washout period the stimulation threshold was determined, and the first optical mapping image taken. A full list of treatment compounds, suppliers, concentrations, and preparations can be found in Supplemental Table 1. Treatments included the sodium channel blocker flecainide, the NCX inhibitor SEA0400, the NKA inhibitor ouabain, the hERG inhibitor E4031, $BaCl_2$ salt to inhibit I_{K1}, the osmotic agent and ephaptic uncoupler mannitol, and the peptide LQLEED. LQLEED is a smaller derivative of the peptide BADP1 which has previously been shown to slow conduction and widen the perinexus in a dose dependent manner.[19]

Optical Mapping

The tissue was epicardially stimulated with a 5 ms pulse of direct anodal current at 2x the minimum current necessary trigger a propagated excitation using a monopolar Ag-Ag/Cl electrode at a 300 ms cycle length. The electrode was placed to the left of the anterior descending (LAD) coronary artery approximately midway between apex and base. The electrode was centered in the middle of the field of view of a Micam Ultima L-type CMOS camera (100x100 pixel array). Using a tandem lens system with a net magnification of 0.63X, the imaging field of view was 15.9 by 15.9 mm. Florence was excited by a green LED light source passed through a 520/35 nm band pass filter, and the emitted light was passed through a 610 nm long pass filter. After dye loading and washout, treatment compounds were washed in for an additional 15 minutes before mapping images were taken. After the image was taken, a new solution with the same treatment compound, but a different [Na^+] was washed in for 10 minutes before the next image was taken.

Optical data were analyzed using a custom MatLab software (available at https://github.com/spoelzing/OMAnalysis). Activation times were assigned to each channel as the peak rate of change of florescence. Conduction velocities were calculated in transverse direction (perpendicular to epicardial fiber orientation) based on activations times and the calculated interpixel distance. Action potential duration was calculated as the global average of the time between activation time and time when fluorescence had recovered to 90% the pre-action potential value.

Statistical Analysis

All statistical analyses were performed in GraphPad Prism V10.2.0 or later. The total number of animals used was calculated based off of preliminary data to detect an effect size of [effect] at 0.8 power and 0.05 alpha. Direct comparisons of paired conditions were done using a paired two-tailed Student’s T-test. Comparisons across all groups were done using a one-way ANOVA, with Dunnett's multiple comparisons test.

Results

Sequential Treatment of Flecainide and Mannitol

We initially investigated how both flecainide and mannitol modulate CV in guinea pig ventricular myocardium at two different perfusate sodium concentrations ([Na^+]). Relative to paired baseline measurements at 145 mM [Na^+], flecainide alone slowed conduction velocity (CV) from 22.7±1.9 cm/s to 19.1±1.5 cm/s ($p<0.001$). At 120 mM [Na^+] flecainide slowed CV from 26.8±3.0 cm/s to 19.3±2.2 cm/s ($p<0.001$, Fig. 1B). Notably, the percent slowing at 120 mM [Na^+] (-27.4±6.3%) was significantly greater than the percent slowing at 145 mM [Na^+] (-15.7±3.3%, $p=0.004$) (Fig. 1B).

Relative to paired baseline at 145 mM [Na^+], the ephaptic uncoupler mannitol alone slowed CV from 23.3±3.3 cm/s to 19.3±3.4 cm/s ($p<0.001$). At 120 mM [Na^+] flecainide slowed CV from 22.3±1.8 cm/s to 18.1±2.3 cm/s ($p<0.001$, Fig. 1B). The percent slowing at 120 mM [Na^+] (-17.4±3.1%) was not significantly greater than the percent slowing at 145 mM [Na^+] (-17.4±5.8%, $p=0.63$) (Fig. 1D).

Relative to paired baseline at 145 mM [Na^+], flecainide+mannitol together slowed CV from 22.9±1.7 cm/s to 16.3±1.1 cm/s ($p<0.001$). At 120 mM [Na^+] flecainide slowed CV from 24.9±2.3 cm/s to 17.8±1.5 cm/s ($p<0.001$, Fig. 1B). The percent slowing at 120 mM [Na^+] (-28.4±4.3%) was not significantly greater than the percent slowing at 145 mM [Na^+] (-27.4±2.9%, $p=0.68$) (Fig. 2). Taken together, these data demonstrate that CV slowing from flecainide is sensitive to [Na^+], and that concurrent treatment with flecainide+mannitol abolishes that sensitivity.

Changing [Na^+] with or without Flecainide

Since flecainide appeared to cause greater CV slowing at low [Na^+], we chose to explore the effects of changing [Na^+] in a direct paired fashion by measuring CV in the same heart before and after changing [Na^+]. In approximately half of these experiments, [Na^+] was lowered from

145 mM to 120 mM, and in the other half [Na^+] was raised from 120 mM to 145 mM to control for time and order dependent effects, but data were pooled and analyzed together when no difference was seen between treatment order. Under baseline conditions, lowering [Na^+] resulted in a non-significant change in CV (+0.7±0.7 cm/s, p=0.08) (Fig. 3B). In contrast, lowering [Na^+] resulted in significant CV slowing with 0.5 μM flecainide (-2.7±1.3 cm/s, p<0.001) (Fig. 3C). This is consistent with the prior unpaired experiments that show flecainide slows CV to greater degree at 120 mM [Na^+] than at 145 mM [Na^+]. We then compared the magnitude of the CV change induced by lowering [Na^+] across all tested conditions via ANOVA to quantify the extent to which flecainide sensitized CV to changes in [Na^+]. The magnitude of the CV change at baseline condition (2.7±2.8%) was significantly different from the magnitude of change with flecainide (-14.6±4.0%, p<0.001) (Fig. 3C).

Changing [Na^+] with Flecainide and Ephaptic Uncoupling

Although the combination of flecainide and mannitol did not rescue conduction as it appeared to do in the mouse model used by Blair *et al.*, the CV slowing from this combination was similar at both [Na^+], unlike what was seen with flecainide alone. To test the hypothesis that the flecainide induced CV sensitivity to changes in [Na^+] is a function of intercalated disc width, we once again changed [Na^+] in a paired fashion during treatment with the combination of flecainide+mannitol, or flecainide+LQLEED (50 μM), a small peptide designed to competitively inhibit an intercalated disc binding domain. With flecainide+mannitol, lowering [Na^+] resulted in a non-significant change in CV (0.1±0.5 cm/s, p=0.84) (Fig. 4B). However, with flecainide+LQLEED, lowering [Na^+] resulted in significant CV slowing (-1.2±0.4 cm/s, p<0.001) (Fig. 4C). Importantly, the magnitude of the CV change with flecainide+mannitol (+0.4±3.0%) and with flecainide+LQLEED (-6.9±2.0%) were significantly different from the magnitude of change with flecainide alone (p<0.001 and p=0.008) (Fig. 4B&C).

Changing [Na^+] with Flecainide and Altered Intracellular Calcium (Ca^{2+}) Accumulation

The flux of Na^+ and Ca^{2+} ions are tightly linked in cardiomyocytes such that lowering extracellular Na^+ usually raises intracellular Ca^{2+}.[20] Furthermore, Ca^{2+} serves as an important secondary messenger in many cellular processes. Thus, we tested the hypothesis that flecainide induced CV sensitivity to changes in $[Na^+]$ is driven by a downstream change in intracellular Ca^{2+}. We changed $[Na^+]$ in a paired fashion during treatment with the combination of flecainide+SEA0400 (1 μM), an inhibitor of the Na^+-Ca^{2+}-exchanger (NCX), or flecainide+ouabain (1 μM), an inhibitor of the Na^+-K^+-ATPase (NKA). With both flecainide+SEA0400 and flecainide+ouabain, lowering $[Na^+]$ resulted in significant CV slowing (-2.6±1.1 cm/s, $p<0.001$ and -1.9±1.0 cm/s, $p=0.001$) (Fig. 5B&C). The magnitude of the CV change with flecainide+SEA0400 (-13.8±3.5%) and with flecainide+ouabain (-8.1±3.8%) were not significantly different from the magnitude of change with flecainide alone ($p=0.99$ and $p=0.16$) (Fig. 5B&C).

Changing $[Na^+]$ with Flecainide and Potassium (K^+) Channel Inhibition

One known effect of mannitol is the inhibition of the I_{kr} and early activating K^+ current[21]. Since mannitol showed the most dramatic effect on flecainide induced CV sensitivity to changes in $[Na^+]$, we tested the hypothesis that this sensitivity was driven by K^+ currents. Once again, $[Na^+]$ was changed in a paired fashion during treatment with the combination of flecainide+E4031 (1 μM), an inhibitor of the channel KV11.1 also called hERG, or flecainide+$BaCl_2$ (10 μM), to inhibit Ba^{2+} sensitive K^+ channels, namely $K_{ir}2.1$. With both flecainide+E4031 and flecainide+ $BaCl_2$, lowering $[Na^+]$ resulted in significant CV slowing (-1.1±0.5 cm/s, $p<0.001$ and -1.3±0.4 cm/s, $p<0.001$) (Fig. 6B&C). Notably, the magnitude of the CV changes with both flecainide+ E4031 (-7.2±2.9%) and with flecainide+ $BaCl_2$ (-7.1±1.8%) was significantly different from the magnitude of change with flecainide alone ($p=0.004$ and $p=0.007$) (Fig. 6B&C).

Discussion

The above results present direct evidence that conduction velocity (CV) is relatively insensitive to changes in extracellular Na^+ concentration under baseline conditions with normal levels of Na^+ channel function, which matches the conventional wisdom that modest hyponatremia rarely has a significant impact on conduction.[22] However, this study also demonstrates that flecainide treatment sensitizes conduction to clinically relevant changes in Na^+ concentration, which is in agreement with the case studies where hyponatremia precipitates flecainide toxicity.[6, 7]

In our initial series of experiments, we held perfusate sodium concentration ($[Na^+]$) constant and applied different treatments to determine if there was a qualitatively different response to those treatments at hyponatremia. Consistent with our hypothesis that flecainide sensitizes conduction to $[Na^+]$, flecainide treatment slowed conduction to a significantly greater degree at 120 mM $[Na^+]$ than at 145 mM $[Na^+]$ (Fig. 1A&B). We saw no difference between the two Na^+ concentrations for mannitol or the combination of mannitol and flecainide Fig. 1C&D, Fig. 2). This last is noteworthy, as it suggests that the combination of mannitol and flecainide attenuates the sensitivity to $[Na^+]$ induced by flecainide alone (Fig. 2). Because this initial set of experiments was paired within a single $[Na^+]$ rather than between different $[Na^+]$s, it is more difficult to detect smaller effects. Therefore, in our second set of experiments we shifted the experimental paradigm to test a consistent combination of treatments at our two different $[Na^+]$s. Consistent with the previous data, lower $[Na^+]$ at baseline did not significantly alter CV, but lowering $[Na^+]$ in the presence of flecainide resulted in significant slowing.

Ephaptic Coupling

One of the effects of mannitol is that is reduces ephaptic coupling. Ephaptic coupling is a non-gap junction mediate form of conduction that is highly dependent on the volume of an intercellular nano-domain called the perinexus.[18] The perinexus is a Na^+ and K^+ channel rich

nano-domain of the intercalated disc and is dramatically expanded by mannitol treatment.[23] When combined with mannitol, flecainide did not sensitize CV to changes in [Na^+]. This suggests ephaptics may play a role in this sensitization.

In our paired experiments, we explored two different means of reducing ephaptic coupling. First mannitol, and second the peptide LQLEED, a sequence designed to comparatively interfere with the trans-interaction of cellular adhesion molecules in the perinexus.[23] With combined flecainide and mannitol treatment, CV did not significantly change with lowered [Na^+]. With combined flecainide and mannitol treatment, CV did slow with lowered [Na^+], but this slowing was to a significantly smaller degree than what was seen with flecainide alone (Fig. 3). These data together suggest that this induced CV sensitivity to [Na^+] is ephaptically mediated.

Calcium (Ca^{2+}) Accumulation

It is well established that lowering extracellular Na^+ leads to intracellular Ca^{2+} accumulation in cardiomyocytes,[20] and that this effect is largely mediated through the Na^+-Ca^{2+}-Exchanger (NCX).[24] Ionic Ca^{2+} is a potent secondary messenger that impacts many cellular processes. It is possible that that the Ca^{2+} accumulation driven by low [Na^+] could exacerbate the conduction slowing caused by flecainide. In our paired experiments, we blocked NCX with SEA0400, which would attenuate Ca^{2+} accumulation, and alternatively blocked the Na^+-K^+-ATPase (NKA) with ouabain, which would exacerbate Ca^{2+} accumulation.[25] If intracellular Ca^{2+} accumulation is the mechanism of CV sensitization to [Na^+], the sensitivity should be modulated in the same direction as the Ca^{2+} accumulation. However, our data showed no significant difference in the degree of CV slowing when lowering [Na^+] with flecainide or with the combination of flecainide and SEA0400, or flecainide and ouabain. These data suggest that both exacerbating and attenuating intracellular Ca^{2+} accumulation do not impact flecainide induced CV sensitivity to [Na^+], which leads us to conclude that this phenomenon is not a function of Ca^{2+} accumulation.

Potassium (K^+) Channel Inhibition

In addition to widening the perinexus, mannitol has been demonstrated to inhibit the hERG mediated K^+ current I_{Kr}.[21] Since mannitol showed a greater reduction in the CV sensitivity to $[Na^+]$ than LQLEED, we investigated whether the magnitude of repolarizing K^+ currents might play a role in this sensitivity, and if the CV sensitization to $[Na^+]$ could be reduced by blocking these currents. Our data demonstrate that blocking either I_{Kr} with E4031, or I_{K1} with $BaCl_2$ both attenuate the CV sensitivity to lowered $[Na^+]$ to a similar degree as LQLEED. These data suggest that outward K^+ currents can modulate flecainide induced CV sensitivity to $[Na^+]$. Interestingly, $K_{ir}2.1$, the protein primarily responsible for carrying I_{K1} has been demonstrated to localize to the perinexal region[26] and may even co-traffic as part of a macromolecular complex with cardiac voltage gated Na^+ channels.[27] Whether hERG, the protein primarily responsible for carrying I_{Kr} localizes to the intercalated disc in general or the perinexus specifically has not yet been investigated, but if it does, then this may suggest that flecainide induced CV sensitivity to $[Na^+]$ is a K^+ mediated ephaptic phenomenon, but further study would be needed to confirm that hypothesis.

Conclusion

This study provides clear experimental evidence to support the small but growing body of literature demonstrating that conduction is markedly more sensitive to hyponatremia when Na^+ channel function is impaired than it is under conditions of normal channel function. Furthermore, we herein demonstrate several mechanisms by which this sensitivity is modulated, including through the regulation of multiple outward K^+ currents and changes in perinexal width, a key determinant of conduction through ephaptic coupling. As blocking K^+ channels poses its own arrhythmogenic risk, this paper adds to the body of evidence that the modulation of ephaptic coupling represents a clinically significant mechanism in conduction diseases.

Table S1			
Intervention	Target Effect	Dosage	Preparation
Flecainide	Na-channel blocker	0.5 μM	1 mM stock solution prepared in DMSO
Mannitol	Osmotic Agent	26.1g/L	Dissolved in perfusion buffer
LQLEED	Ephaptic Uncoupler	50 μM	50 mM stock solution prepared in DMSO
SEA0400	NCX Inhibitor	1 μM	5 mM stock solution prepared in DMSO
Ouabain	NKA Inhibitor	1 μM	5 mM stock solution prepared in DMSO
E4031	hERG Inhibitor	1 μM	2 mM stock solution prepared in DMSO
$BaCl_2$	Ik1 Inhibitor	10 μM	Dissolved in perfusion buffer
Blebbistatin	Electromechanical uncoupler	10 μM	10 mM stock solution prepared in DMSO
Di-4-ANEPPS	Voltage Sensitive Dye	7.5 μM	8 mM stock solution prepared in 100% ethanol

Table 1. A list of drugs and chemical interventions used, their target, the dosage, and the medium and stock concentration they were prepared in.

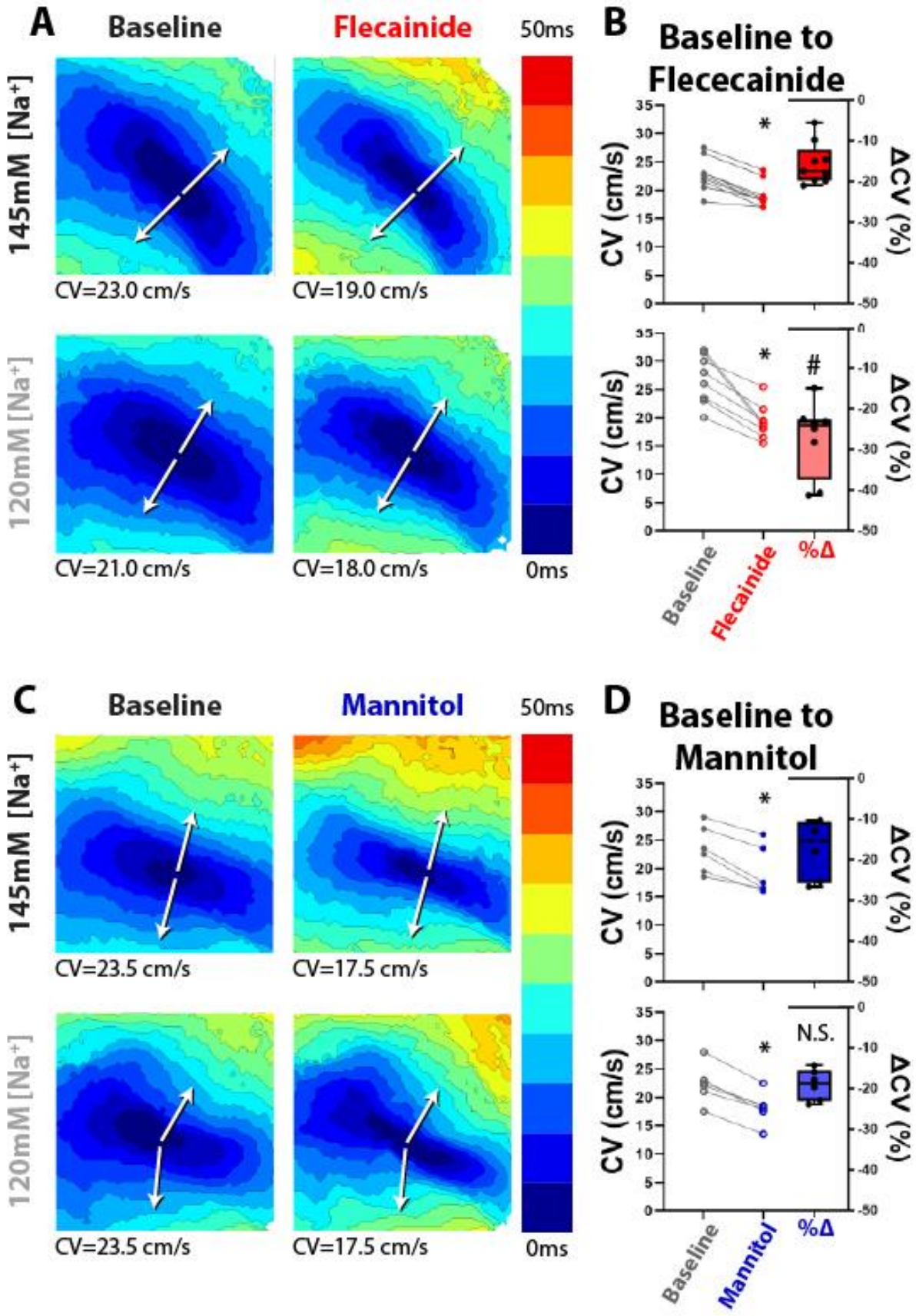
A
Baseline
Flecainide
50ms
145mM [Na+]
120mM [Na+]
CV=23.0 cm/s
CV=19.0 cm/s
CV=21.0 cm/s
CV=18.0 cm/s
0ms
B
Baseline to Flececainide
CV (cm/s)
ΔCV (%)
*
#
Baseline
Flecainide
%Δ
C
Baseline
Mannitol
50ms
145mM [Na+]
120mM [Na+]
CV=23.5 cm/s
CV=17.5 cm/s
CV=23.5 cm/s
CV=17.5 cm/s
0ms
D
Baseline to Mannitol
CV (cm/s)
ΔCV (%)
*
N.S.
Baseline
Mannitol
%Δ

Figure 1. *Flecainide slows conduction velocity (CV) more at low [*Na^+*] than at normal [*Na^+*].* A) Isochrones showing the change in CV from baseline (left) to 0.5 μM flecainide (right) at either 145 mM [Na^+] (top) or 120 mM [Na^+] (bottom). B) Quantification of those changes. Raw CV values are plotted as paired data points on the left axis, and percent change is plotted as a bar graph on the right. The upper graph shows data collected at 145 mM [Na^+] (n=9) and the lower graph shows data collected at 120 mM [Na^+] (n=8). C) & D) show are the same as A & B respectively except hearts were treated with 261g/L mannitol at 145 mM [Na^+] (top, n=6) 120 mM [Na^+] (bottom, n=6). *p<0.05 paired T-test, #p<0.05 unpaired T-test

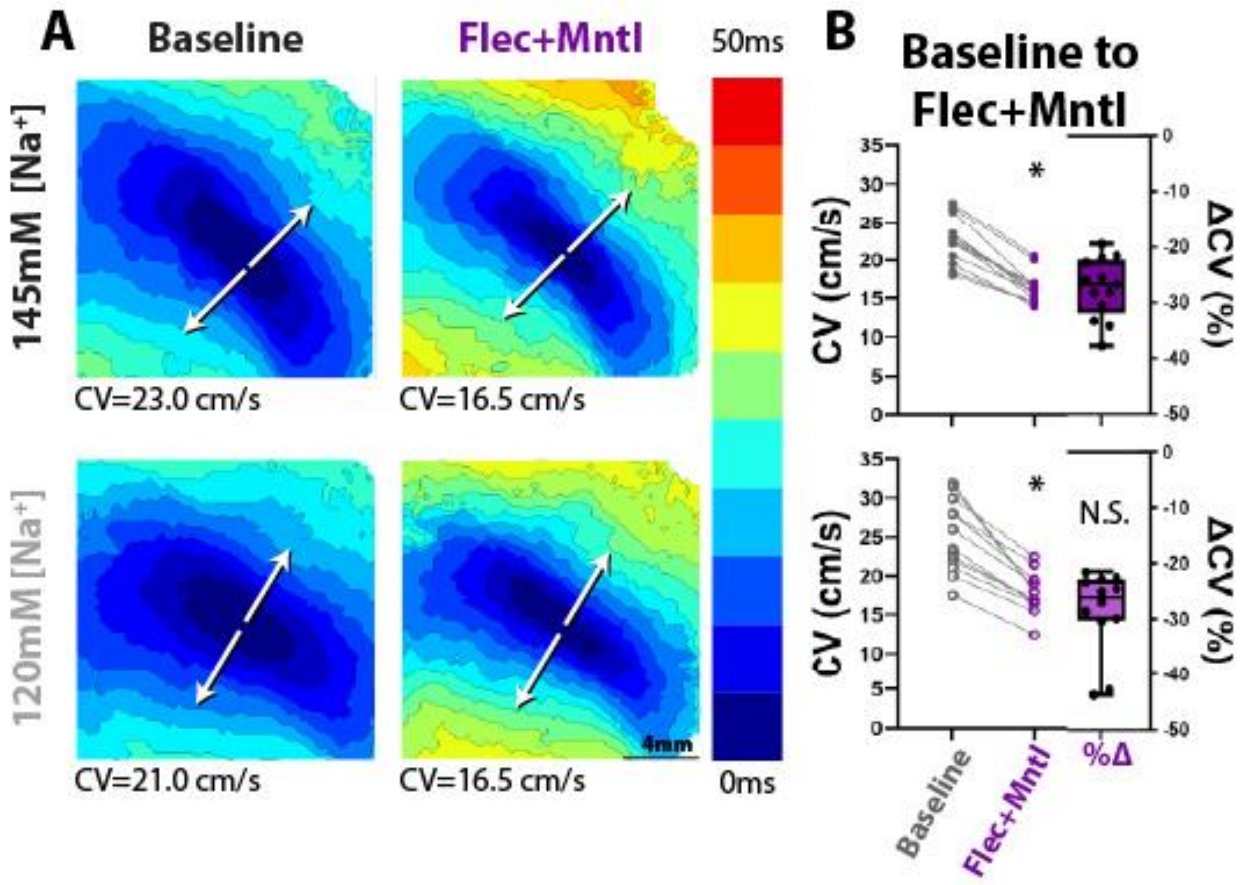

Figure 2. *The combination of flecainide+mannitol slows CV to the same degree at low [*Na^+*] and at normal [*Na^+*].* A) Isochrones showing the change in CV from baseline (left) to the combination of 0.5 μM flecainide +26.1g/L Mannitol (right) at either 145 mM [Na^+] (top) or 120 mM [Na^+] (bottom). B) Quantification of those changes. Raw CV values are plotted as paired data points on the left axis, and percent change is plotted as a bar graph on the right. The upper graph shows data collected at 145 mM [Na^+] (n=15) and the lower graph shows data collected at 120 mM [Na^+] (n=14). *p<0.05 paired T-test

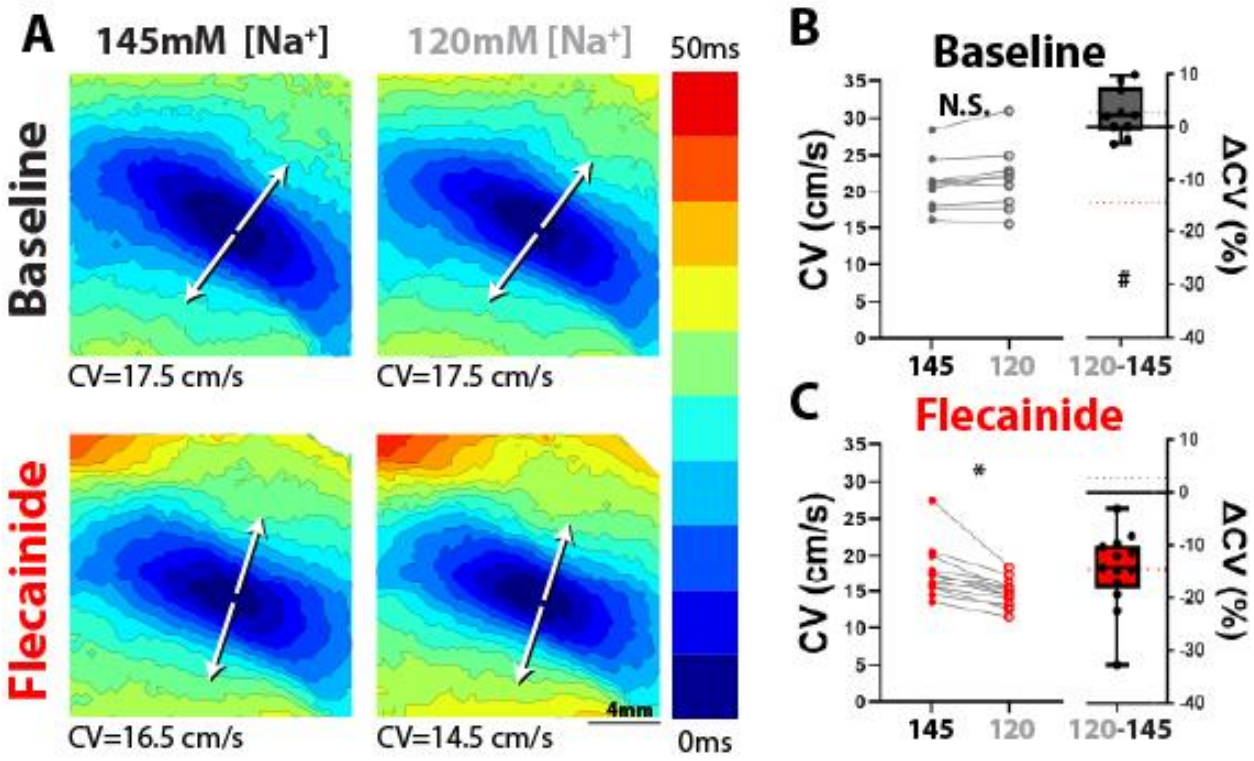

Figure 3. *Flecainide sensitizes CV to changes in [*Na^+*].* A) Isochrones showing the change in CV when [Na^+] is changed from 145 mM [Na^+] (left) to 120 mM [Na^+] (right) at baseline (top, n=10) or with 0.5 μM flecainide (bottom, n=13). B) Quantification of the changes represented in A. Raw CV values are plotted as paired data points on the left axis, and percent change is plotted as a bar graph on the right. Note that a dotted grey line marking the mean % change at baseline and dotted red line marking mean percent change with flecainide alone. *p<0.05 paired T-test, #p<0.05 relative to flecainide alone (one-way ANOVA).

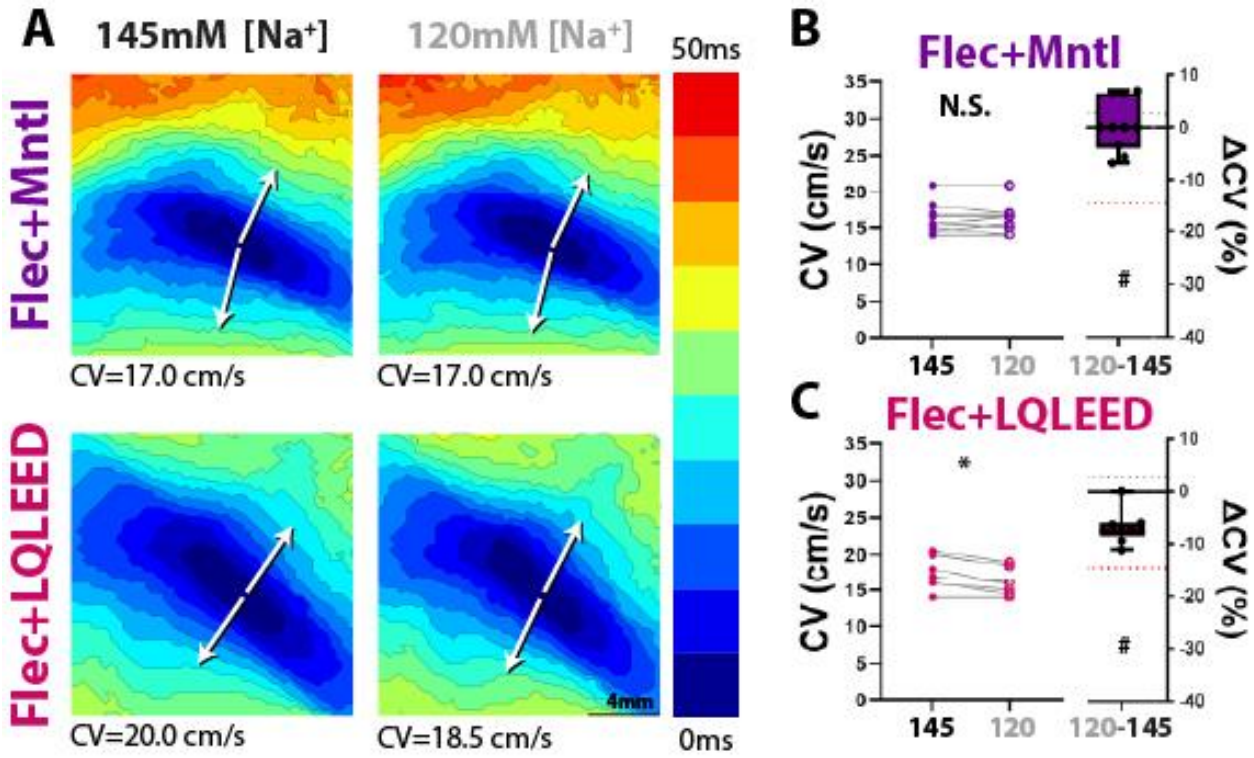

Figure 4. *Reducing ephaptic coupling attenuates the flecainide induced CV sensitivity to [*Na^+*].* A) Isochrones showing the change in CV when [Na^+] is changed from 145 mM [Na^+] (left) to 120 mM [Na^+] (right) during simultaneous treatment with both 0.5 μM flecainide and 26.1g/L Mannitol (top, n=10) or with 0.5 μM flecainide and 50 μM LQLEED peptide (bottom, n=9). B) Quantification of the changes represented in A. Raw CV values are plotted as paired data points on the left axis, and percent change is plotted as a bar graph on the right. Note that a dotted grey line marking the mean % change at baseline and dotted red line marking mean percent change with flecainide alone. *p<0.05 paired T-test, #p<0.05 relative to flecainide alone (one-way ANOVA).

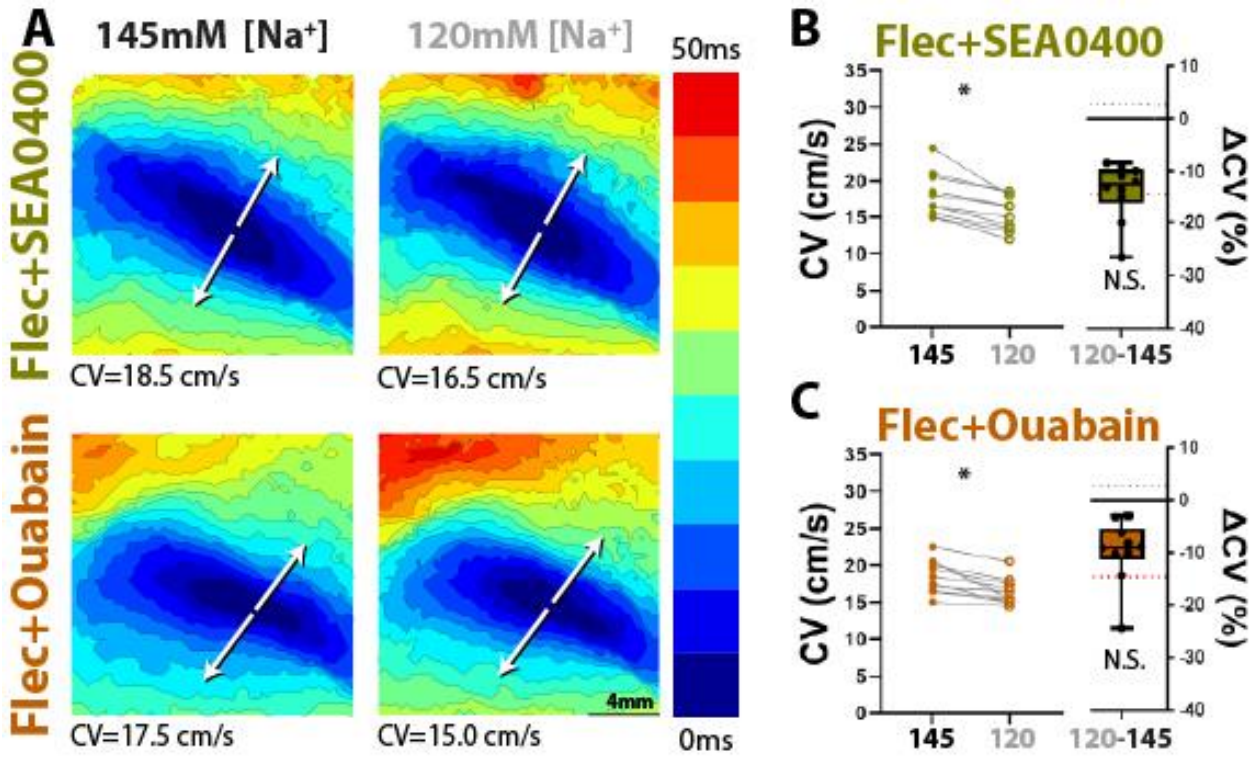

Figure 5. *Alterations in intracellular Ca^{2+} accumulation do not significantly impact the flecainide induced CV sensitivity to [*Na^+*].* A) Isochrones showing the change in CV when [Na^+] is changed from 145 mM [Na^+] (left) to 120 mM [Na^+] (right) during simultaneous treatment with both 0.5 μM flecainide and 1 μM SEA0400 (top, n=10) or with 0.5 μM flecainide and 1 μM ouabain (bottom, n=10). B) Quantification of the changes represented in A. Raw CV values are plotted as paired data points on the left axis, and percent change is plotted as a bar graph on the right. Note that a dotted grey line marking the mean % change at baseline and dotted red line marking mean percent change with flecainide alone. *p<0.05 paired T-test, #p<0.05 relative to flecainide alone (one-way ANOVA).

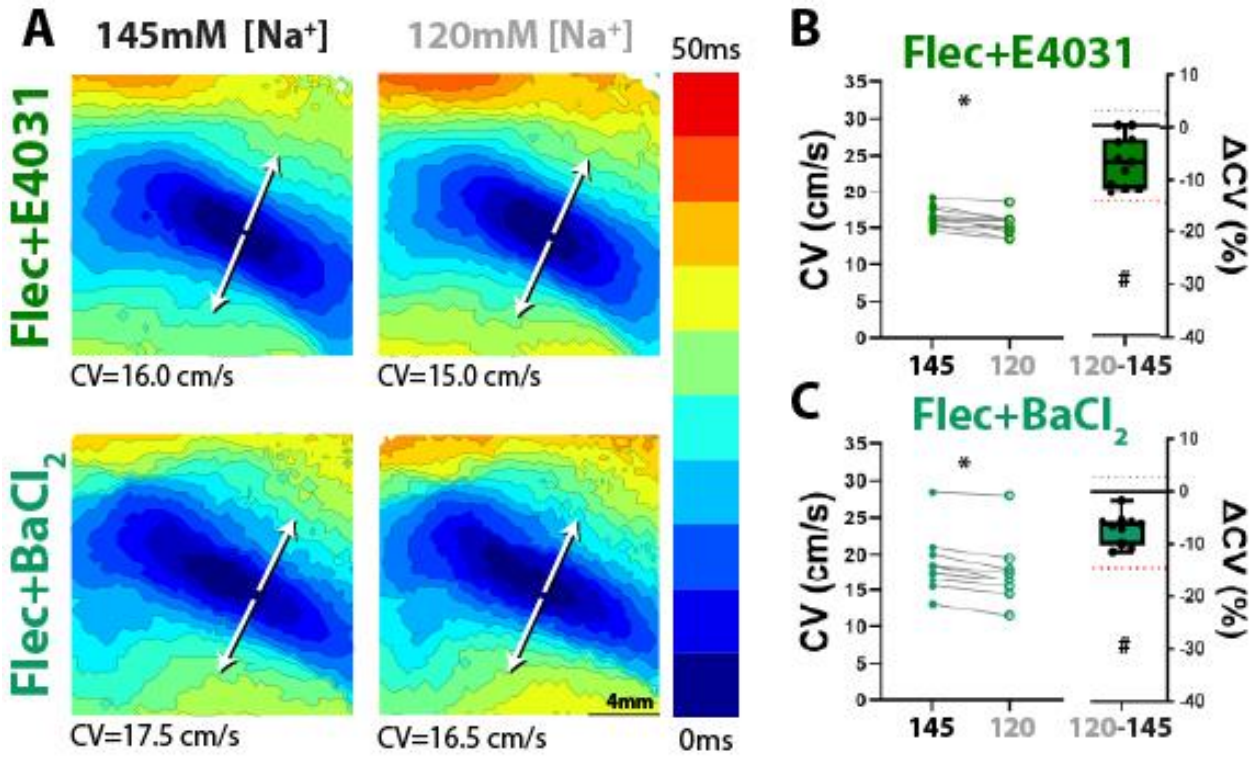

Figure 6. *Blocking repolarizing K^+ currents attenuates the flecainide induced CV sensitivity to [Na^+].* A) Isochrones showing the change in CV when [Na^+] is changed from 145 mM [Na^+] (left) to 120 mM [Na^+] (right) during simultaneous treatment with both 0.5 μM flecainide and 1 μM E4031 (top, n=11) or with 0.5 μM flecainide and 10 μM $BaCl_2$ (bottom, n=10). B) Quantification of the changes represented in A. Raw CV values are plotted as paired data points on the left axis, and percent change is plotted as a bar graph on the right. Note that a dotted grey line marking the mean % change at baseline and dotted red line marking mean percent change with flecainide alone. *p<0.05 paired T-test, #p<0.05 relative to flecainide alone (one-way ANOVA).

REFERENCES

1. Meert A, Vermeersch N, Beckers R, Hoste W, Brugada P, Hubloue I. Brugada-like ECG pattern induced by tricyclic antidepressants. Eur J Emerg Med. 2010;17(6):325-7. doi: 10.1097/MEJ.0b013e328334a98f. PubMed PMID: 19996975.

2. Zeppenfeld K, Tfelt-Hansen J, de Riva M, Winkel BG, Behr ER, Blom NA, Charron P, Corrado D, Dagres N, de Chillou C, Eckardt L, Friede T, Haugaa KH, Hocini M, Lambiase PD, Marijon E, Merino JL, Peichl P, Priori SG, Reichlin T, Schulz-Menger J, Sticherling C, Tzeis S, Verstrael A, Volterrani M. 2022 ESC Guidelines for the management of patients with ventricular arrhythmias and the prevention of sudden cardiac death. Eur Heart J. 2022;43(40):3997-4126. doi: 10.1093/eurheartj/ehac262. PubMed PMID: 36017572.

3. Preliminary report: effect of encainide and flecainide on mortality in a randomized trial of arrhythmia suppression after myocardial infarction. N Engl J Med. 1989;321(6):406-12. doi: 10.1056/nejm198908103210629. PubMed PMID: 2473403.

4. Coromilas J, Saltman AE, Waldecker B, Dillon SM, Wit AL. Electrophysiological effects of flecainide on anisotropic conduction and reentry in infarcted canine hearts. Circulation. 1995;91(8):2245-63. doi: 10.1161/01.cir.91.8.2245. PubMed PMID: 7697855.

5. Salerno DM, Granrud G, Sharkey P, Krejci J, Larson T, Erlien D, Berry D, Hodges M. Pharmacodynamics and side effects of flecainide acetate. Clin Pharmacol Ther. 1986;40(1):101-7. doi: 10.1038/clpt.1986.145. PubMed PMID: 3720173.

6. Kasia C, Henry C, Santucci P. A case of electrolyte disturbances leading to flecainide toxicity at normal serum levels and pacemaker malfunction. HeartRhythm Case Rep. 2019;5(9):448-51. Epub 20190612. doi: 10.1016/j.hrcr.2019.05.007. PubMed PMID: 31934538; PMCID: PMC6951303.

7. Khavandi A, Walker PR. Flecainide cardiotoxicity precipitated by electrolyte imbalance. Caution with thiazide diuretics. Emerg Med J. 2007;24(5):e26. doi: 10.1136/emj.2006.044362. PubMed PMID: 17452686; PMCID: PMC2658510.

8. Chan HY, Chan YC, Lau FL. Reversal of Brugada electrocardiographic pattern with sodium bicarbonate solution after amitriptyline overdose. Clin Toxicol (Phila). 2008;46(9):892-6. doi: 10.1080/15563650802293984. PubMed PMID: 18788005.

9. Di Grande A, Giuffrida C, Narbone G, Le Moli C, Nigro F, Di Mauro A, Pirrone G, Tabita V, Alongi B. Management of sodium-channel blocker poisoning: the role of hypertonic sodium salts. Eur Rev Med Pharmacol Sci. 2010;14(1):25-30. PubMed PMID: 20184086.

10. Ghataoura R, Patil S. Flecainide toxicity: a presentation to the emergency department with literature review. BMJ Case Rep. 2020;13(2). Epub 20200228. doi: 10.1136/bcr-2019-232691. PubMed PMID: 32114494; PMCID: PMC7050315.

11. Rognoni A, Bertolazzi M, Peron M, Macciò S, Cameroni GT, Gratarola A, Rognoni G. Electrocardiographic changes in a rare case of flecainide poisoning: a case report. Cases J. 2009;2:9137. Epub 20091203. doi: 10.1186/1757-1626-2-9137. PubMed PMID: 20062654; PMCID: PMC2803934.

12. Vu NM, Hill TE, Summers MR, Vranian MN, Faulx MD. Management of life-threatening flecainide overdose: A case report and review of the literature. HeartRhythm Case Rep. 2016;2(3):228-31. Epub 20151229. doi: 10.1016/j.hrcr.2015.12.013. PubMed PMID: 28491675; PMCID: PMC5419747.

13. Bellet S, Hamdan G, Somlyo A, Lara R. A reversal of the cardiotoxic effects of procaine amide by molar sodium lactate. Am J Med Sci. 1959;237(2):177-89. doi: 10.1097/00000441-195902000-00005. PubMed PMID: 13626960.

14. Bellet S, Hamdan G, Somlyo A, Lara R. The reversal of cardiotoxic effects of quinidine by molar sodium lactate: an experimental study. Am J Med Sci. 1959;237(2):165-76 passim. doi: 10.1097/00000441-195902000-00004. PubMed PMID: 13626959.

15. Bou-Abboud E, Nattel S. Relative role of alkalosis and sodium ions in reversal of class I antiarrhythmic drug-induced sodium channel blockade by sodium bicarbonate. Circulation. 1996;94(8):1954-61. doi: 10.1161/01.cir.94.8.1954. PubMed PMID: 8873674.

16. Ranger S, Sheldon R, Fermini B, Nattel S. Modulation of flecainide's cardiac sodium channel blocking actions by extracellular sodium: a possible cellular mechanism for the action of sodium salts in flecainide cardiotoxicity. J Pharmacol Exp Ther. 1993;264(3):1160-7. PubMed PMID: 8383739.

17. Blair GA, Wu X, Bain C, Warren M, Hoeker GS, Poelzing S. Mannitol and hyponatremia regulate cardiac ventricular conduction in the context of sodium channel loss of function. Am J Physiol Heart Circ Physiol. 2024;326(3):H724-h34. Epub 20240112. doi: 10.1152/ajpheart.00211.2023. PubMed PMID: 38214908.

18. Adams WP, Raisch TB, Zhao Y, Davalos R, Barrett S, King DR, Bain CB, Colucci-Chang K, Blair GA, Hanlon A, Lozano A, Veeraraghavan R, Wan X, Deschenes I, Smyth JW, Hoeker GS, Gourdie RG, Poelzing S. Extracellular Perinexal Separation Is a Principal Determinant of Cardiac Conduction. Circ Res. 2023;133(8):658-73. Epub 20230908. doi: 10.1161/circresaha.123.322567. PubMed PMID: 37681314; PMCID: PMC10561697.

19. Veeraraghavan R, Hoeker GS, Alvarez-Laviada A, Hoagland D, Wan X, King DR, Sanchez-Alonso J, Chen C, Jourdan J, Isom LL, Deschenes I, Smyth JW, Gorelik J, Poelzing S, Gourdie RG. The adhesion function of the sodium channel beta subunit (β1) contributes to cardiac action potential propagation. Elife. 2018;7. Epub 20180814. doi: 10.7554/eLife.37610. PubMed PMID: 30106376; PMCID: PMC6122953.

20. Luttgau HC, Niedergerke R. The antagonism between Ca and Na ions on the frog's heart. J Physiol. 1958;143(3):486-505. doi: 10.1113/jphysiol.1958.sp006073. PubMed PMID: 13588569; PMCID: PMC1356728.

21. Yabuuchi F, Beckmann R, Wettwer E, Hegele-Hartung C, Heubach JF. Reduction of hERG potassium currents by hyperosmolar solutions. Eur J Pharmacol. 2007;566(1-3):222-5. Epub 20070324. doi: 10.1016/j.ejphar.2007.03.028. PubMed PMID: 17477915.

22. El-Sherif N, Turitto G. Electrolyte disorders and arrhythmogenesis. Cardiol J. 2011;18(3):233-45. PubMed PMID: 21660912.

23. Rhett JM, Ongstad EL, Jourdan J, Gourdie RG. Cx43 associates with Na(v)1.5 in the cardiomyocyte perinexus. J Membr Biol. 2012;245(7):411-22. Epub 20120719. doi: 10.1007/s00232-012-9465-z. PubMed PMID: 22811280; PMCID: PMC4085045.

24. Weber CR, Ginsburg KS, Philipson KD, Shannon TR, Bers DM. Allosteric regulation of Na/Ca exchange current by cytosolic Ca in intact cardiac myocytes. J Gen Physiol. 2001;117(2):119-31. doi: 10.1085/jgp.117.2.119. PubMed PMID: 11158165; PMCID: PMC2217247.

25. Orrego F. Calcium and the mechanism of action of digitalis. Gen Pharmacol. 1984;15(4):273-80. doi: 10.1016/0306-3623(84)90001-6. PubMed PMID: 6092203.

26. Veeraraghavan R, Lin J, Keener JP, Gourdie R, Poelzing S. Potassium channels in the Cx43 gap junction perinexus modulate ephaptic coupling: an experimental and modeling study. Pflugers Arch. 2016;468(10):1651-61. Epub 20160811. doi: 10.1007/s00424-016-1861-2. PubMed PMID: 27510622; PMCID: PMC5131566.

27. Ponce-Balbuena D, Guerrero-Serna G, Valdivia CR, Caballero R, Diez-Guerra FJ, Jiménez-Vázquez EN, Ramírez RJ, Monteiro da Rocha A, Herron TJ, Campbell KF, Willis BC, Alvarado FJ, Zarzoso M, Kaur K, Pérez-Hernández M, Matamoros M, Valdivia HH, Delpón E, Jalife J. Cardiac Kir2.1 and Na(V)1.5 Channels Traffic Together to the Sarcolemma to Control Excitability. Circ Res. 2018;122(11):1501-16. Epub 20180307. doi: 10.1161/circresaha.117.311872. PubMed PMID: 29514831; PMCID: PMC5970051.

Chapter 4

Sudden Cardiac Death, Arrhythmia, and Sodium Channel Loss of Function

Summary and Future Directions

The study of cardiac conduction has come a long way since cable theory was first used to apply a mathematical and theoretical framework to the spread of electrical excitation through Purkinje fibers[1]. We have now identified gap junctions (or the nexus as it was originally called) as the low resistance conducting pathways between myocytes[2], and connexin 43 as the primary protein responsible for the formation of these junctions in working ventricular myocardium[3]. In the preceding chapters, I have described work and data that add yet another layer of complexity to our collective understanding of cardiac conduction and demonstrated the importance of futherr mechanisms beyond gap junctional coupling.

Extracellular Perinexal Separation Is a Principal Determinant of Cardiac Conduction

Although ephaptic coupling (EpC) as a theoretical mechanism of conduction had been openly discussed since the early 2000s[4], the reality and practical importance of such a mechanism was much disputed[5]. It was only with the discovery of the cardiac perinexus that a potential structural target for EpC was identified[6]. By correlating structural changes in the perinexal width (W_p) with the functional outcome of conduction velocity (CV) we could finally carry out experiments that would provide strong evidence for the existence of EpC, and by doing so with clinically relevant agents such as mannitol and albumin we were able to demonstrate both the existence of this conduction mechanism, and its physiologic relevance[7]. Of particular note, by demonstrating the biphasic nature CV–W_p relationship, and doing so with the combination of albumin and dextran (see figure 2.8), we were able to resolve an apparent contradiction in the literature. Specifically, in 1995 Fleischhauer showed that treating with dextran slowed CV[8], whereas in our hands we found the opposite, that dextran increased CV. The resolution of this apparent contradiction in results came when we realized that Fleischhauer's perfusate contained albumin as a base component, making it more akin to our albumin treatment condition than our baseline. From there, it was a simple experiment to see whether dextran in the presence of albumin narrowed

the perinexus sufficiently to get over the proverbial hump of the biphasic curve and show CV slowing instead of the CV speeding we saw with dextran in the absence of albumin.

As is only right with a paradigm shifting claim, we were challenged to rule out a wide array of alternatives that could have explained our results. Frustrating as it can be at times, that is what makes for good science. It's important to test whether we unknowingly changed gap junctional conductance (see figure 2.2) or peak sodium (Na^+) current (see figure 2.3). One novel challenge for me personally was working with our data on perinexal width (see figure 2.7). That type of data follows an inherently non-gaussian distribution and to address this I had to work with our university's center for biostatistics to develop the best way to hypothesis test those data while properly accounting for technical and biological replicates. Ultimately, we settled on using a generalized linear mixed effects model based on a gamma distribution. Working on this analysis, I gained a new appreciation for the input of statisticians and grew through the process of explaining our data to someone who thinks about experimental design and data collection in a fundamentally different way than I and most of my colleagues do.

Despite the thoroughness of this work, there is always more that can be done. There is one thing in particular that we could not accomplish: to show both slopes of the biphasic response curve of EpC with varying doses of a single intervention. We were only able to show the self-attenuation side of the biphasic curve using a combination of dextran and albumin (see figure 2.8). Although this experiment helped us resolve the apparent contradiction between our data and the earlier work by Fleischhauer *et al.*[8], being able to demonstrate first an increase and then a decrease in CV with increasing doses of a single intervention would be a gilding achievement to the study of EpC and conduction. We have shown that mannitol has a graded dose response[9], so it might be possible to start with a solution containing both albumin and dextran, or possibly a perfusate containing high calcium,[10] to have a very narrow perinexus as our starting condition and then use varying dosages of mannitol to show first speeding and then

slowing of CV. This would require the careful titration of the mannitol dosage, which would be difficult to do in the presence of albumin, as albumin causes the rapid degradation of optical signals, but might be more feasible with a high calcium perfusate.

Another area in which there is a great need for further study is that it seems to be much easier to disrupt EpC than to accentuate it. Widening the perinexus to a degree that slows conduction is as simple as using mannitol, a compound already in clinical use, but narrowing the perinexus to a degree that speeds conduction, or further to a degree that encourages self-attenuation (which may itself be therapeutic in some circumstances),[11] in a clinically viable manner is more complicated. We have some evidence that calcium mediated adhesion at the intercalated disc can narrow the perinexus.[10, 12] However, changes in serum calcium itself can have both contractile and electrical impacts on the heart that complicate its use as a therapy.[13] Peptides such as Badp1, and its derivative LQLEED have been designed to interfere with the adhesion domain of the sodium channel beta subunits located at and near the perinexus[14], but no peptides that facilitate this adhesion have yet been published on. It is also important to note that albumin is a native component of blood, and it may be that our perfusates themselves artificially widen the perinexus. It may be that *in vivo* the perinexus is already much narrower, and thus respond differently to interventions, than what we see in our experimental *ex vivo* models. Solving this problem, and understanding how our interventions behave under *in vivo* conditions, will be a key step in translating our understanding of EpC into usable therapies.

Flecainide Sensitizes Conduction to Hyponatremia Through an Ephaptic Mechanism

The paper presented in chapter 2 begins with a well described theoretical mechanism and we designed experiments to test if the predictions of that mechanism were borne out by the data. In contrast, the paper presented in chapter 3 comes at the process of scientific discovery from a different angle. In this paper, we begin with an observation: that CV is more sensitive to changes in Na^+ concentration during channel loss of function (LoF) than it is under baseline

conditions (see figure 3.1 and 3.3.). We do not have a mechanism that fully explains this observation, or a mathematical model that predicts this outcome. Lacking specific predictions to test, we have to step back and look at basic mechanisms that are already known to modulate conduction and explore how these mechanisms interact with this new observation. By understanding what does and does not modulate this newly observed phenomenon, we begin to build a mechanistic understanding of it from which we can develop a testable framework and understanding.

This study was largely inspired by work in mice that observed how low perfusate sodium concentration ([Na^+]) impaired conduction more in a genetic Na^+ channel LoF mutant mouse than it did in wild type littermates, and that this interaction between low [Na^+] and channel LoF might be mitigated by treatment with mannitol. The first step of investigating this phenomenon then, is to validate that a similar phenotype occurs in our pharmacologic guinea pig model, which was both in a different species and used a drug to induce LoF rather than a genetic technique.

This led to several interesting observations. The first and most important, was that flecainide induced channel LoF slows CV more at low [Na^+] than at nominal [Na^+] (see figure 3.1). If this had not been the case, then the entire finding of the genetic mouse study might have been written off as an oddity of mouse specific electrophysiology. Rather, this observation combined with Blair's work in mice[15] and the clinic studies highlight in chapter 3[16-21] suggests that more is happening than just a drug interaction. The totality of evidence suggests that there is a fundamental link between Na^+ concentration, channel loss of function, and CV.

Secondly, lowering [Na^+] with normal channel function had no measurable impact in the guinea pig model, even though lowering [Na^+] did slow conduction in the wild type mice. Although not explored in chapter 3, this difference suggests another direction for further investigation. Why does this difference occur? It is possible that the answer to this question lies in the result that

the induced [Na^+] sensitivity is modulated by potassium (K^+) currents (see figure 3.6). Unlike human and guinea pig, the mouse action potential is notable for the very large contribution of I_{to}, an early activating outward K^+ current[22]. It is possible that just as reduced K^+ currents attenuate CV sensitivity to [Na^+], increased K^+ current could accentuate it, and the balance of inward and outward currents in the mouse heart is such that the sensitivity appears at normal levels of Na^+ and K^+ channel function. The hypothesis that increased K^+ currents also sensitizes CV to changes in [Na^+] could be tested in guinea pig with drugs that agonize K^+ currents. In that case, we would expect to see a [Na^+] sensitivity with increased K^+ currents and normal Na^+ current similar to the [Na^+] sensitivity we otherwise see with normal K^+ currents and reduced Na^+ current. If that were to be shown, then this discovery would have implications for management of strong Na^+ channel blockers, K^+ channel agonists and patients with either gain of function or LoF mutations in both Na^+ and K^+ channels. Both of these drug classes are used in cardiac medicine, and often in combination with diuretics to manage hypertension. As thiazide diuretics are known to lead to hyponatremia[23], this work highlights that serum sodium is a critical marker to monitor for patients treated with any combination of these drugs.

Finally, in the mouse LoF model, lower [Na^+] induced what may have been a sort of unidirectional block in 4 out of 5 hearts. Mannitol rescued this so-called block without significantly improving CV in these mice. The CV result is consistent with the guinea pig experiments presented in chapter 3 (see figure 3.2), but no block was observed in the guinea pig model to allow for comparison. This difference could be a function of species-specific parameters or a function of the degree of Na^+ channel LoF. Regardless, one possible explanation for the resolution of apparent conduction block without a change in CV is that mannitol alters tissue excitability. Although this work has focused on CV, excitability is also an important parameter to consider in the study of arrhythmogenesis, and how channel LoF combined with hyponatremia interacts with changes in excitability is an open question ripe for

investigation. To explore whether this was a true unidirectional block or a local loss of tissue excitability, we could try pacing hearts that exhibit this apparent block from the other side of the region of impairment. If this is a loss of excitability, a similar impairment should be seen regardless of the direction of the incoming excitation wave front, while unidirectional block, by definition, would only occur with stimulation from the one side but not the other.

Final thoughts

This work has presented significant new data on the topic of conduction, but the effects of a mechanism like EpC go beyond just that one functional outcome. As we continue to explore the impact of electrogenic proteins localizing to restricted spaces and continue discovering a growing list of targets at the intercalated disc, we need to think beyond just conduction. Already some work has been done to characterize how this unique structural arrangement impacts repolarization[11, 24] and excitability,[25, 26] but there is still so much more to learn. If we only focus on one part of the equation of arrhythmogenesis, we risk repeating the failures of the CAST trials. So, perhaps the single most important piece of work moving forward from this is the actual exploration of how EpC modulate arrhythmias themselves as a distinct functional outcome; to test in disease specific models whether inhibiting or accentuating EpC increases or decrease arrhythmia susceptibility. Improving outcomes for human health and disease is the ultimate goal of all translational medical science, and I believe that step forward from tissue level functional measures to clinical outcome measures is how we can begin to translate EpC from the bench to the bedside.

References

1. Weidmann S. The electrical constants of Purkinje fibres. J Physiol. 1952;118(3):348-60. doi: 10.1113/jphysiol.1952.sp004799. PubMed PMID: 13000763; PMCID: PMC1392495.

2. Barr L, Dewey MM, Berger W. PROPAGATION OF ACTION POTENTIALS AND THE STRUCTURE OF THE NEXUS IN CARDIAC MUSCLE. J Gen Physiol. 1965;48(5):797-823. doi: 10.1085/jgp.48.5.797. PubMed PMID: 14324989; PMCID: PMC2213773.

3. Vozzi C, Dupont E, Coppen SR, Yeh HI, Severs NJ. Chamber-related differences in connexin expression in the human heart. J Mol Cell Cardiol. 1999;31(5):991-1003. doi: 10.1006/jmcc.1999.0937. PubMed PMID: 10336839.

4. Sperelakis N, McConnell K. Electric field interactions between closely abutting excitable cells. IEEE Eng Med Biol Mag. 2002;21(1):77-89. doi: 10.1109/51.993199. PubMed PMID: 11935993.

5. Roth BJ. Does ephaptic coupling contribute to propagation in cardiac tissue? Biophys J. 2014;106(4):774-5. doi: 10.1016/j.bpj.2014.01.011. PubMed PMID: 24559978; PMCID: PMC3944891.

6. Rhett JM, Gourdie RG. The perinexus: a new feature of Cx43 gap junction organization. Heart Rhythm. 2012;9(4):619-23. Epub 20111004. doi: 10.1016/j.hrthm.2011.10.003. PubMed PMID: 21978964; PMCID: PMC3266460.

7. Adams WP, Raisch TB, Zhao Y, Davalos R, Barrett S, King DR, Bain CB, Colucci-Chang K, Blair GA, Hanlon A, Lozano A, Veeraraghavan R, Wan X, Deschenes I, Smyth JW, Hoeker GS, Gourdie RG, Poelzing S. Extracellular Perinexal Separation Is a Principal Determinant of Cardiac Conduction. Circ Res. 2023;133(8):658-73. Epub 20230908. doi: 10.1161/circresaha.123.322567. PubMed PMID: 37681314; PMCID: PMC10561697.

8. Fleischhauer J, Lehmann L, Kléber AG. Electrical resistances of interstitial and microvascular space as determinants of the extracellular electrical field and velocity of propagation in ventricular myocardium. Circulation. 1995;92(3):587-94. doi: 10.1161/01.cir.92.3.587. PubMed PMID: 7634473.

9. Veeraraghavan R, Salama ME, Poelzing S. Interstitial volume modulates the conduction velocity-gap junction relationship. Am J Physiol Heart Circ Physiol. 2012;302(1):H278-86. Epub 20111021. doi: 10.1152/ajpheart.00868.2011. PubMed PMID: 22021331; PMCID: PMC3334234.

10. George SA, Hoeker G, Calhoun PJ, Entz M, 2nd, Raisch TB, King DR, Khan M, Baker C, Gourdie RG, Smyth JW, Nielsen MS, Poelzing S. Modulating cardiac conduction during metabolic ischemia with perfusate sodium and calcium in guinea pig hearts. Am J Physiol Heart Circ Physiol. 2019;316(4):H849-h61. Epub 20190201. doi: 10.1152/ajpheart.00083.2018. PubMed PMID: 30707595; PMCID: PMC6483020.

11. Wu X, Hoeker GS, Blair GA, King DR, Gourdie RG, Weinberg SH, Poelzing S. Hypernatremia and intercalated disc edema synergistically exacerbate long-QT syndrome type 3 phenotype. Am J Physiol Heart Circ Physiol. 2021;321(6):H1042-h55. Epub 20211008. doi: 10.1152/ajpheart.00366.2021. PubMed PMID: 34623182; PMCID: PMC8793943.

12. Hoeker GS, James CC, Tegge AN, Gourdie RG, Smyth JW, Poelzing S. Attenuating loss of cardiac conduction during no-flow ischemia through changes in perfusate sodium and calcium. Am J Physiol Heart Circ Physiol. 2020;319(2):H396-h409. Epub 20200717. doi: 10.1152/ajpheart.00112.2020. PubMed PMID: 32678707; PMCID: PMC7473923.

13. King DR, Padget RL, Perry J, Hoeker G, Smyth JW, Brown DA, Poelzing S. Elevated perfusate [Na(+)] increases contractile dysfunction during ischemia and reperfusion. Sci Rep. 2020;10(1):17289. Epub 20201014. doi: 10.1038/s41598-020-74069-x. PubMed PMID: 33057157; PMCID: PMC7560862.

14. Veeraraghavan R, Hoeker GS, Alvarez-Laviada A, Hoagland D, Wan X, King DR, Sanchez-Alonso J, Chen C, Jourdan J, Isom LL, Deschenes I, Smyth JW, Gorelik J, Poelzing S, Gourdie RG. The adhesion function of the sodium channel beta subunit (β1) contributes to cardiac action potential

propagation. Elife. 2018;7. Epub 20180814. doi: 10.7554/eLife.37610. PubMed PMID: 30106376; PMCID: PMC6122953.

15. Blair GA, Wu X, Bain C, Warren M, Hoeker GS, Poelzing S. Mannitol and hyponatremia regulate cardiac ventricular conduction in the context of sodium channel loss of function. Am J Physiol Heart Circ Physiol. 2024;326(3):H724-h34. Epub 20240112. doi: 10.1152/ajpheart.00211.2023. PubMed PMID: 38214908.

16. Kasia C, Henry C, Santucci P. A case of electrolyte disturbances leading to flecainide toxicity at normal serum levels and pacemaker malfunction. HeartRhythm Case Rep. 2019;5(9):448-51. Epub 20190612. doi: 10.1016/j.hrcr.2019.05.007. PubMed PMID: 31934538; PMCID: PMC6951303.

17. Khavandi A, Walker PR. Flecainide cardiotoxicity precipitated by electrolyte imbalance. Caution with thiazide diuretics. Emerg Med J. 2007;24(5):e26. doi: 10.1136/emj.2006.044362. PubMed PMID: 17452686; PMCID: PMC2658510.

18. Chan HY, Chan YC, Lau FL. Reversal of Brugada electrocardiographic pattern with sodium bicarbonate solution after amitriptyline overdose. Clin Toxicol (Phila). 2008;46(9):892-6. doi: 10.1080/15563650802293984. PubMed PMID: 18788005.

19. Di Grande A, Giuffrida C, Narbone G, Le Moli C, Nigro F, Di Mauro A, Pirrone G, Tabita V, Alongi B. Management of sodium-channel blocker poisoning: the role of hypertonic sodium salts. Eur Rev Med Pharmacol Sci. 2010;14(1):25-30. PubMed PMID: 20184086.

20. Ghataoura R, Patil S. Flecainide toxicity: a presentation to the emergency department with literature review. BMJ Case Rep. 2020;13(2). Epub 20200228. doi: 10.1136/bcr-2019-232691. PubMed PMID: 32114494; PMCID: PMC7050315.

21. Rognoni A, Bertolazzi M, Peron M, Macciò S, Cameroni GT, Gratarola A, Rognoni G. Electrocardiographic changes in a rare case of flecainide poisoning: a case report. Cases J.

2009;2:9137. Epub 20091203. doi: 10.1186/1757-1626-2-9137. PubMed PMID: 20062654; PMCID: PMC2803934.

22. Benndorf K, Nilius B. Properties of an early outward current in single cells of the mouse ventricle. Gen Physiol Biophys. 1988;7(5):449-66. PubMed PMID: 3234736.

23. Spital A. Diuretic-induced hyponatremia. Am J Nephrol. 1999;19(4):447-52. doi: 10.1159/000013496. PubMed PMID: 10460932.

24. Nowak MB, Greer-Short A, Wan X, Wu X, Deschênes I, Weinberg SH, Poelzing S. Intercellular Sodium Regulates Repolarization in Cardiac Tissue with Sodium Channel Gain of Function. Biophys J. 2020;118(11):2829-43. Epub 20200421. doi: 10.1016/j.bpj.2020.04.014. PubMed PMID: 32402243; PMCID: PMC7264809.

25. De Smet MA, Lissoni A, Nezlobinsky T, Wang N, Dries E, Pérez-Hernández M, Lin X, Amoni M, Vervliet T, Witschas K, Rothenberg E, Bultynck G, Schulz R, Panfilov AV, Delmar M, Sipido KR, Leybaert L. Cx43 hemichannel microdomain signaling at the intercalated disc enhances cardiac excitability. J Clin Invest. 2021;131(7). doi: 10.1172/jci137752. PubMed PMID: 33621213; PMCID: PMC8011902.

26. Leo-Macias A, Agullo-Pascual E, Sanchez-Alonso JL, Keegan S, Lin X, Arcos T, Feng Xia L, Korchev YE, Gorelik J, Fenyö D, Rothenberg E, Rothenberg E, Delmar M. Nanoscale visualization of functional adhesion/excitability nodes at the intercalated disc. Nat Commun. 2016;7:10342. Epub 20160120. doi: 10.1038/ncomms10342. PubMed PMID: 26787348; PMCID: PMC4735805.